166654

ISTANBUL TECHNICAL UNIVERSITY ★ INSTITUTE OF SCIENCE AND TECHNOLOGY

ASSESSMENT OF BIOGEOCHEMICAL INFLUENCE ON METAL SULFIDE AND FE (II) OXIDATION AS INFERRED FROM OXYGEN, SULFUR AND FE ISOTOPES.

Ph.D. Thesis by
Nurgül ÇELİK BALCI, M.Sc.

(505982108)

Date of submission : 28 March 2005

Date of defence examination: 4 July 2005

Supervisor (Chairman): Assoc. Prof. Dr. Fuat YAVUZ

Members of the Examining Committee Prof.Dr. Işık ÖZPEKER (İ.T.Ü.)

Prof.Dr. Atasever GEDİKOĞLU (İ.T.Ü.)

Prof.Dr. Selçuk TOKEL (K.Ü.)

Prof.Dr. Cahit HELVACI (D.Ü.)

JULY 2005

ACKNOWLEDGMENT

This thesis was funded by the National Science Foundation (NSF)–USA and TÜBITAK (The Scientific and Technical Research Council of Turkey)-Turkey. The laboratory work was completed in the Department of Chemistry and Geochemistry at Colorado School of Mines (CSM), Golden-Colorado-USA under the supervisor of Dr. Kevin Mandernack.

First of all, I would like to sincerely thank to my co-supervisor, Kevin W. Mandernack, Associate Professor who is thanked not only giving me the opportunity to be involved in this project, but more importantly for giving me a great support, motivation and encouragement all the time in the past four years. This thesis is the result of valuable discussions. Without his knowledge, this thesis would have been impossible to finish. I would like to express my thanks to my supervisor, Dr. Fuat Yavuz for lots of helpful advice and encouragements during this thesis.

I would like to thank my committee members for the unique contributions that they each provided–Professor Selçuk Tokel and Professor Işık Özpeker. I also would like to thank Professor Atasever Gedikoğlu, who served as project manager for TÜBITAK and supporting me over the period of the project.

I am grateful for all the help in the laboratory that I received from Dr. Bernhard Mayer and Dr. Tom Bullen, Pamela Gemery, and Dr. Rich Wanty. Dr. Pat Shanks provided significant assistance through academic discussions, and guidance.

Also many thanks to colleagues and Ph.D students at the department of Chemistry and Geochemistry, CSM. Thanks are especially extended to Chris Mills, Kerstin Lien, Chad Kinney and Roland Thurston and also to the rest of my friends. It has become a wonderful experience to study at the department. Also many thank to people at the division of Ore deposits and Geochemistry at İstanbul Technical University, Turkey.

Finally, I would like to thank my family and friends for their support and guidance over the years– my parents, my husband, and Dr. Yüksel Örgün. Thank you for your support and the enjoyable time you spend with me and interesting discussion about almost everything.

March 2005 **Nurgül ÇELİK BALCI**

TABLE OF CONTENTS

TABLE LISTS

Sayfa No

FIGURE LISTS

SYMBOL LISTS

ε	: Isotopic enrichment factor
ε_o	: Isotopic enrichment factor relative to molecular oxygen
ε_w	: Isotopic enrichment factor relative to water
$\delta^{18}O_{SO4}$	: Oxygen isotope value of sulfate
$\delta^{34}S_{SO4}$	: Sulfur isotope value of sulfate
σ	: Isotopic fractionation factor
‰	: Per mil
%	: Percentage
Δ	: Isotopic fractionation effect
A	: Matrix for least squares solution
$(A^TA)^{-1}$	: Inverse matrix
mg	: Milligram
g	: Gram
mL	: Milliliter
L	: Liter
mM	: Millimolar
aq	: Aqueous
µm	: Micrometer
$\delta^{56}Fe$	: Iron isotope value
$X_{Fe[II]aq}$	: Concentrations of $Fe[II]_{aq}$ and $Fe[III]_{aq}$
$X_{Fe[III]aq}$	: Concentrations of $Fe[III]_{aq}$
t	: Time
f	: Proportion of reactant remaining after time t
k	: Reaction rate constant
°C	: Centigrade
~	: Approximately

ABBREVIATIONS

NSF	: National Science Foundation -America
TÜBITAK	: The Scientific and Technical Research Council of Turkey
AMD	: Acid Mine Drainage Site
rpm	: Revolution per minute
CSM	: Colorado School of Mines
USGS	: United States Geological Survey
ATCC	: American Type Culture Collection
MPN	: Most probable number method
DI	: De-ionized water
SMOW	: Standard Mean Ocean Water
CDT	: Canyon Diablo Troilite
n.d	: Not determined
SPR	: Sulfate Production Rate
TIMS	: Thermal Ionization Mass Spectrometry
MC-ICPMS	: Multi-collector Inductively Coupled Plasma Mass Spectrometry
BIR-1	: Icelandic basalt
ETS	: Electron Transport System
ATP	: Adenosine Triphosphate
IC	: Ion Chromatography
MC-ICPMS	: Multi-Collector Inductively Coupled Plasma Mass Spectrometry
TIMS	: Thermal Ionization Mass Spectrometry

ASSESSMENT OF BIOGEOCHEMICAL INFLUENCE ON METAL SULFIDE AND FE (II) OXIDATION AS INFERRED FROM OXYGEN, SULFUR AND FE ISOTOPES

SUMMARY

Bacterially catalyzed reactions are important in geochemical cycling of large variety elements such as Fe, S, O and C. Sulfide mineral oxidation is widespread in many different environments and also regulates the global cycling of O, S and Fe. Furthermore, oxidation of metal sulfide minerals cause environmental problems known as acid mine drainage (AMD). Since AMD environments contain high concentration of metals and affect aquatic ecosystems, remediation of these environments is vital and requires an understanding of oxidation mechanism of sulfide minerals. It is widely accepted that oxidation of sulfide minerals is often mediated by bacterial reactions. The Fe(II) and sulfide oxidizing bacterium, *Acidithiobacillus ferrooxidans,* is commonly found in AMD sites. Understanding the mechanism and bacterial contribution to metal sulfide oxidation may assist with developing proper remediation strategies for AMD sites and contribute to our understanding of sulfur and oxygen cycle in ancient and modern environments.

My doctoral studies examined the bacterial influence on the oxidation of sulfide minerals at pH <3 from analyses of oxygen and sulfur isotopes of sulfate produced during aerobic and anaerobic laboratory experiments. Because most of metal sulfides contain Fe (II) and the oxidation of Fe (II) to Fe (III) is mediated by biological reactions at pH <3, investigation of oxidation pathway of Fe (II) may help to trace the biological signature. For this purpose, Fe (II) oxidation experiments were carried out by using *A. Ferrooxidans* bacteria and the δ^{56}Fe values of Fe-oxides were analyzed in order to elucidate the oxidation pathway.

Experimental methods for both metal sulfide and Fe (II) oxidation are described in detail in each chapter. Different type of sulfide minerals was used to investigate if sulfide mineralogy has effect on the $\delta^{18}O_{SO4}$ values. For this purpose, first set of experiments were carried out by using pyrite mineral. Pure sphalerite mineral (ZnS) was used for the second set of experiments. Since natural sphalerite usually contains significant amounts of Fe (II), a third set of sulfide oxidation experiments with sphalerite containing 12 % Fe were carried out. These experiments investigated if Fe (II) influences the oxidation mechanism of sphalerite and the resultant $\delta^{18}O_{SO4}$ values. Biotic and abiotic sulfide mineral oxidation experiments were carried out under aerobic and anaerobic conditions. Since Fe (III) concentration is usually high in AMD sites and Fe (III) is a strong oxidizer for sulfide minerals, anaerobic experiments were carried out by using Fe (III) as oxidizing agent. Also, short and long term aerobic experiments were designed to determine the integrity of the $\delta^{18}O_{SO4}$ values. Oxygen isotope exchange between water and sulfate is possible with decreasing pH and may complicate the interpretation of the $\delta^{18}O_{SO4}$ values. pH was used as a proxy for the short and long term experiments. The starting pH was 3 and the short and long term experiments were terminated at pH ~2.7 and pH 2.1, respectively. In the biological experiments, *A. ferrooxidans* were used. In addition, elemental sulfur oxidation experiments under the identical conditions with metal

sulfides minerals were carried out. These experimental results may help to determine if elemental sulfur forms as an intermediate of aerobic sphalerite oxidation and further influences the $\delta^{18}O_{SO4}$ values.

Chapter 2: Aerobic and anaerobic bacterial and abiotic pyrite experiments

Biological and abiotic pyrite experiments produced very similar $\delta^{18}O_{SO4}$ values under both aerobic and anaerobic conditions. Sulfate from the aerobic short term biological experiments (pH, 2.7; 20 days) derived 87 % oxygen from water and the correspondingly 13 % from molecular oxygen. Sulfate from the lower pH (2.1) long term experiments even show larger water –oxygen incorporation into sulfate (94 %). Aerobic abiotic-control pyrite experiments produce sulfate that has 89 % oxygen from water. Estimates of the kinetic oxygen isotopic fractionation effect with respect to H_2O and O_2 in the aerobic pyrite experiments revealed the very similar values. Kinetic oxygen isotope fractionation effect between sulfate and water ($\Delta^{18}O_{SO4-H2O}$) was estimated to be 5.3 ‰ and 3.8 ‰ for the aerobic biological short and long term experiments, respectively and 3.2 ‰ for the abiotic-control experiments. Sulfate - molecular oxygen fractionation effect ($\Delta^{18}O_{SO4-O2}$) was -21 ‰ and -29.7 ‰ for the biotic and abiotic experiments, respectively. The similarity between biotic and abiotic experiments may indicate the same oxidation mechanisms for pyrite. Data from aerobic pyrite experiments indicated that Fe (III) ions were the main oxidizing agent during pyrite oxidation and the role of bacteria was mainly to oxidize Fe (II) to Fe (III).

The $\delta^{18}O_{SO4}$ values from the anaerobic pyrite experiments show 100 % water oxygen in both biotic and abiotic experiments, indicating that chemical oxidation of pyrite by Fe (III) was dominant in both experiments. Kinetic oxygen isotope fractionation effect between sulfate and water ($\Delta^{18}O_{SO4-H2O}$) was estimated to be 4.2 ‰ and 3.5‰ for the biotic and abiotic experiments, respectively. It is interesting that kinetic oxygen isotope fractionation between sulfate and water ($\Delta^{18}O_{SO4-H2O}$) from the anaerobic experiments is similar to that from the aerobic long term pyrite experiments. The $\delta^{34}S_{SO4}$ values from aerobic experiments closely reflect the $\delta^{34}S$ composition of pyrite during both biotic and abiotic experiments in contrast to the anaerobic experiments which show ~-1 ‰ fractionation relative to the $\delta^{34}S_{FeS2}$ values during both biotic and abiotic oxidation.

Chapter 3: Aerobic and Anaerobic Bacterial and abiotic ZnS and 12 % Fe-bearing Sphalerite Experiments

The $\delta^{18}O_{SO4}$ values from both aerobic biological ZnS and Fe-containing sphalerite experiments indicated that all oxygen atoms in sulfate are derived from water during the short and long term experiments. In contrast to biological experiments, $\delta^{18}O_{SO4}$ values from abiotic ZnS experiments confirmed that a significant fraction of the oxygen in sulfate is derived from molecular oxygen (60 %). Differences in the percentage of molecular oxygen incorporated into sulfate between the biological and the abiotic experiments may imply different oxidation mechanism for each. The 100 % of water-oxygen into sulfate produced during biological experiments is in agreement with the theoretical sulfide oxidation pathway proposed by Kelly (1982). My experimental results showed that although the proposed pathway may explain the overall mass transformation during sphalerite oxidation, it does not explain the actual oxygen source to sulfate. The net stoichiometry of the proposed pathway suggests 100 % molecular oxygen incorporation into sulfate (reaction 16, chapter 3).

Oxygen isotope fractionation effect between sulfate and water ($\Delta^{18}O_{SO4-H2O}$) was estimated to be 9 ‰ for both short and long term pure sphalerite experiments and 8.2 and 7.2 ‰ for the short and long term Fe-bearing sphalerite experiments, respectively. Analogous between oxygen isotope fractionation effects during ZnS and Fe-bearing sphalerite oxidation may indicate the same reaction mechanism for each. Furthermore, the similar $\delta^{18}O_{SO4}$ values between ZnS and Fe-bearing sphalerite experiments suggest that Fe (II) in the crystal lattice of sphalerite mineral have no effect on the $\delta^{18}O_{SO4}$ values unless it is overprinted by other processes such as oxygen isotope exchange between water and sulfite.

Aerobic bacterial and abiotic elemental sulfur experiments

The $\delta^{18}O_{SO4}$ values produced from the biological elemental sulfur oxidation showed 100 % water-oxygen incorporation into sulfate as in sphalerite experiments. Oxygen isotope fractionation effect ($\Delta^{18}O_{SO4-H2O}$) was estimated to be 8 ‰ and 8.9 ‰ for the short and long term experiments, respectively.

The $\delta^{18}O_{SO4}$ values and the oxygen isotope fractionation effect from elemental sulfur experiments are very similar to those from aerobic sphalerite experiments. These results may indicate that elemental sulfur is the main sulfur intermediate during sphalerite oxidation (reaction 14) and subsequent oxidation is controlled by biological reactions since abiotic elemental sulfur experiments did not produce significant amount sulfate over the period of experiments. Consequently, these experimental results suggest that the actual sulfur moiety of sphalerite oxidized to sulfate is likely elemental sulfur. This explains why the $\delta^{18}O_{SO4}$ values from sphalerite experiments are almost identical to the $\delta^{18}O_{SO4}$ values from elemental sulfur experiments. These determinations are also consistent with the $\delta^{34}S_{SO4}$ values from anaerobic sphalerite experiments.

The sulfur isotope composition of elemental sulfur extracted from sphalerite surface at the end of the anaerobic oxidation experiments is identical to source of sphalerite, indicating that most of the sulfur moiety of sphalerite is oxidized to elemental sulfur under anaerobic conditions as well (reaction 18) and minor amount sulfate form.

Although the $\delta^{18}O_{SO4}$ values from ZnS and Fe-bearing sphalerite experiments are very similar under both aerobic and anaerobic conditions, these values are different from the $\delta^{18}O_{SO4}$ values produced during aerobic and anaerobic pyrite oxidation experiments.

Oxygen isotope fractionation effect ($\Delta^{18}O_{SO4-H2O}$) is also different for pyrite and sphalerite experiments. ~9 ‰ oxygen isotope fractionation effect between water and sulfate seems to be unique to sphalerite oxidation experiments since the same fractionation effect is ~ 4 ‰ for pyrite experiments.

Therefore, oxygen isotope fractionation effect between water and sulfate may be used to reveal the source of sulfide minerals.

Chapter 4: Iron isotope fractionation during microbially-stimulated Fe[II] oxidation and Fe[III] precipitation

Interpretation of the origins of iron-bearing minerals preserved in modern and ancient rocks based on measured $^{56}Fe/^{54}Fe$ ratios depends on our ability to distinguish between biological and non-biological iron isotope fractionation

processes. In this study, we compared $^{56}Fe/^{54}Fe$ ratios of coexisting aqueous iron ($Fe[II]_{aq}$, $Fe[III]_{aq}$) and iron oxyhydroxide precipitates ($Fe[III]_{ppt}$) resulting from the oxidation of ferrous iron under experimental conditions at low pH (<3). Experiments were carried out using both pure cultures of *A. ferrooxidans* and sterile controls to assess possible biological overprinting of non-biological fractionation, and both SO_4^{-2} and Cl^- salts as Fe[II] sources to determine possible ionic/speciation effects that may accompany oxidation/precipitation reactions. In addition, a series of ferric iron precipitation experiments were performed at pH ranging from 2 to 3.5 to determine if different precipitation rates impact the isotope composition of the iron oxyhydroxides. During microbially-stimulated Fe[II] oxidation in both the sulfate and chloride systems, $\delta^{56}Fe$ of residual $Fe[II]_{aq}$ sampled in a time series evolved along an apparent Rayleigh trend characterized by a fractionation factor $\alpha_{Fe[III]\text{-}Fe[II]aq}$ ~1.0022. This apparent fractionation factor was significantly less than that measured in our sterile control experiments (~1.0034) and predicted for equilibrium between $Fe[II]_{aq}$ and $Fe[III]_{aq}$, and might be interpreted to reflect a biological control. However, the measured difference in $\delta^{56}Fe$ between $Fe[II]_{aq}$ and $Fe[III]_{aq}$, isolated as a solid by the addition of NaOH to the final solution at each time point under N_2-atmosphere, was in most cases and on average close to 2.9‰, consistent with isotopic equilibrium between $Fe[II]_{aq}$ and $Fe[III]_{aq}$. The ferric iron precipitation experiments revealed that the $\delta^{56}Fe$ of $Fe[III]_{aq}$ is generally equal to or greater than the $\delta^{56}Fe$ of $Fe[III]_{ppt}$, and fractionation between these phases decreases with increasing precipitation rate and decreasing grain size. Considered together, the data confirm that the iron isotope variations observed in my microbial experiments are controlled by non-biological equilibrium and kinetic factors, a result that aids our ability to interpret present-day iron cycling processes but further complicates our ability to use iron isotopes alone to identify biological processing in the rock record.

FE(II) VE SÜLFÜRLÜ MİNERALLERİN OKSİDASYONU SIRASINDA BİYOJEOKİMYASAL ETKİLERİN OKSİJEN, KÜKÜRT VE FE İZOTOPLARI İLE TAYİN EDİLMESİ

ÖZET

Bakterilerin katalize ettiği reaksiyonlar Fe, S, O ve C gibi birçok elementin jeokimyasal döngüsünde önemli yer alır. Sülfürlü minerallerinin oksitlenmesi; değişik jeokimyasal ortamlarda yaygın bir işlem olup O, S ve Fe minerallerinin döngüsünü kontrol eder. Ayrıca, sülfürlü minerallerinin oksidasyonu asit maden sahaları (AMS) olarak ta bilinen çeşitli çevre problemlerine yol açmaktadır. Bu tür sahaların yüksek metal içeriğine sahip olması ve ekolojik hayatı uzun süre etkilemesinden dolayı iyileştirilmesi kaçınılmazdır. Bu amaçla, sülfürlü minerallerinin oksidasyon mekanizmalarının ortaya konması gerekir. Sülfürlü minerallerin bakteriler tarafından oksitlendiği yaygın bir şekilde kabul edilmektedir. Sülfür ve Fe (II) oksitleyen *A. Ferrooxidans* bakteri türü, asit maden sahalarında yaygın olarak bulunmaktadır. Bu nedenle, sülfürlü minerallerinin oksidasyon mekanizmasının ve bakterilerin buna katkısının ortaya konması güncel ve eski ortamlarda sülfür ve oksijen döngüsünün anlaşılmasına ve aynı zamanda da asit maden sahalarının iyileştirilmesi için alınacak tedbirlerin belirlenmesine yardımcı olacaktır.

Bu çalışmada, bakteriyel reaksiyonların asit koşullar (pH<3) altındaki sülfürlü minerallerinin oksitlenmesine olan etkisi, sülfatın oksijen ve kükürt izotop analizlerine dayanılarak araştırılmıştır. Bu amaçla, pirit ve sfalerit gibi sülfürlü mineraller biyolojik ve kimyasal olarak farklı deneysel koşullar (aerobik ve anaerobik) altında oksitlenmeye tabii tutulmuştur. Çoğu sülfür mineralinin Fe (II) içermesi ve asit koşullar (pH<3) altında Fe (II)'nin Fe (III)'e oksitlenmesi genellikle bakteriler tarafından kontrol edildiği için, Fe (II) oksidasyonu sonucunda oluşan Fe-oksitler, biyolojik izlerin ortaya konmasına yardımcı olabilir. Bu amaçla, Fe (II) oksidasyon deneyleri kimyasal ve *A. Ferrooxidans* bakteri türünün kullanımı ile biyojeokimyasal olarak gerçekleştirilmiş ve oksidasyon ürünü olan Fe-oksit ve Fe (III) oluşumlarının δ^{56}Fe izotop analizleri yapılarak, biyolojik izler araştırılmıştır. Sülfürlü minerallerin ve Fe(II) oksidasyonunda kullanılan deneysel metotlar, ilgili bölümlerde detayları ile açıklanmıştır. Deneylerde farklı mineraller kullanılarak, sülfür mineralojisinin sülfatın oksijen izotop bileşimi ($\delta^{18}O_{SO4}$) üzerine etkisi araştırılmıştır. Bu amaçla, ilk deney seti pirit kullanılarak gerçekleştirilmiştir. İkinci deney setinde ise saf sfalerit minerali kullanılmıştır. Doğal sfalerit minerali genellikle önemli derecede Fe (II) içerdiğinden, üçüncü deney setinde % 12 Fe(II) içeren sfalerit minerali kullanılarak, Fe (II)'nin sfaleritin oksidasyon mekanizmasına ve dolayısıyla oluşan sülfatın oksijen izotop değerine olan etkisi araştırılmıştır. Fe (III) iyonu konsantrasyonun asit koşullar altında yüksek ve aynı zamanda sülfür içeren mineralleri için de güçlü bir oksitleyici olmasından ötürü, anaerobik deneyler setlerinde Fe (III) oksitleyici olarak kullanılmıştır. Bu çalışmada, anaerobik deneylere ait sonuçlar aerobik deneylerle karşılaştırılmış ve moleküler oksijenin oksitlenmedeki rolü ortaya konmaya çalışılmıştır. Asit koşullar altında, sülfat ve su arasında oksijen izotop değişimi mümkün olduğundan ve $\delta^{18}O_{SO4}$ değerlerini

etkileyebileceğinden dolayı, aerobik deneyler pH'a bağlı olarak kısa ve uzun süreli deneyler olarak gerçekleştirilmiştir. Bu deneyler için başlangıç pH'ı 3 olarak seçilmiş; kısa sureli deneyler 20 gün sonra pH'2.7'de, uzun sureli deneyler ise 45 gün sonra pH' 2.1'de sona erdirilmiştir. Asit koşullar altında ($pH<3$) sfalerit ve galen gibi monosülfidlerin oksidasyonu sırasında sülfür (S^o) oluşumu yaygın olup bunların oksidasyonu biyolojik reaksiyonlar tarafından kontrol edilmektedir. Sfalerit deneylerinde sülfür oluşumunu ve bunun $\delta^{18}O_{SO4}$ değerlerine olan etkisini araştırmak amacıyla, sfalerit deneylerine ek olarak aerobik sülfür oksidasyon deneyleri de yapılmıştır. Bu deneyler, sfalerit deneyleri ile aynı koşullar altında gerçekleştirilmiştir.

Bölüm 2: Aerobik ve anaerobik biyolojik ve kimyasal pirit oksidasyon deneyleri.

Aerobik ve anaerobik koşullar altında biyolojik ve kimyasal pirit deneyleri sonucu oluşan sülfatın oksijen izotop değerleri oldukça benzerdir. Kısa süreli biyolojik pirit oksidasyon deneyleri sonucunda oluşan sülfat, oksijeninin % 87'sini sudan, % 13'nu moleküler oksijenden elde etmiştir. Düşük pH'li uzun süreli biyolojik deneyler sonucunda oluşan sülfat ise oksijeninin % 94'nu sudan elde etmiştir. Kimyasal deneyler sonucu oluşan sülfat, oksijenin % 89'nu sudan sağlamıştır. Sülfat ve su arasındaki oksijen izotopu ayrımlaşma değeri ($\Delta^{18}O_{SO4\text{-}H2O}$) biyolojik ve kimyasal deneylerde oldukça benzerdir. Benzer ilişki sülfat ve moleküler oksijen ($\Delta^{18}O_{SO4\text{-}O2}$) arasındaki oksijen izotopu değerleri içinde elde edilmiştir. Sülfat ve su arasındaki kinetik oksijen izotopu ayrımlaşma değeri ($\Delta^{18}O_{SO4\text{-}H2O}$); kısa süreli biyolojik deneyler için 5.3 ‰, uzun süreli ve düşük pH koşullarındaki biyolojik deneyler için 3.8 ‰ olarak hesaplanmıştır. Aynı değer kimyasal deneyler gerçekleştirildiğinde 3.2 ‰ elde edilmiştir. Sülfat ve moleküler oksijen arasındaki oksijen izotopu ayrımlaşması biyolojik deneyler için -21 ‰ , kimyasal deneyler için ise -29.7 ‰ olarak hesaplanmıştır. Bu veriler, piritin kimyasal ve biyolojik deneylerde benzer oksidasyon mekanizmasına sahip olduğuna işaret etmektedir.

Aerobik $\delta^{18}O_{SO4}$ değerleri ve yüksek Fe (III) iyon konsantrasyonu, moleküler oksijene oranla Fe(III) iyonunun pirit için ana oksitleyici olduğuna göstermektedir. Bu oksidasyonda bakterilerin ana rolü Fe (II)'yi Fe (III)'e oksitleyerek, piritin oksitlenmesi için gerekli olan Fe (III) iyonunu üretmektir.Biyolojik ve kimyasal karakterli anaerobik deneyler sonucunda oluşan sülfat, oksijeninin tamamını sudan elde etmiştir (% 100). Sülfat ve su arasındaki kinetik oksijen izotopu ayrımlaşma değeri biyolojik deneyler için 4.2 ‰, kimyasal deneyler için ise 3.5 ‰ olarak hesaplanmıştır. Biyolojik ve kimyasal deneylerden elde edilen benzer değerler, piritin Fe(III) tarafından kimyasal olarak oksitlenmesinin, biyolojik deneylere oranla daha baskın olduğunu önermektedir. Öte taraftan, aerobik koşullarda oluşan sülfatın kükürt izotop değerleri ($\delta^{34}S_{SO4}$), piritin kükürt izotop değeri ile uyum içersindedir. Ancak, anaerobik koşullar altında oluşan sülfatın kükürt izotop değerleri, piritin kükürt izotop değerine oranla 1‰ oranında ^{32}S açısından zenginleşmiştir.

Bölüm 3: Aerobik ve anaerobik biyolojik ve kimyasal saf ve % 12 Fe içeren sfalerit oksidasyon deneyleri:

Aerobik koşullar altında, saf ve Fe (II) içeren sfaleritlerin biyolojik oksidasyonu sonucu oluşan $\delta^{18}O_{SO4}$ değerler,i sülfatın oksijeninin tamamının sudan elde edildiğini ortaya koymaktadır. Biyolojik deneylere karşılık, saf sfalerit örnekleri üzerindeki yürütülen kimyasal deneyler, sülfatın oksijeninin % 60'nin moleküler oksijenden sağlandığını göstermektedir. Sülfatın oksijen kaynağındaki farklılık, sfaleritin biyolojik ve kimyasal olarak farklı şekilde oksitlendiğini ön plana çıkarmaktadır. Biyolojik deneylerin sonuçları, Kelly (1982) tarafından sülfür mineralleri için önerilen teorik oksidasyon mekanizması ile uyumlu olup elde edilen sonuçlar aynı zamanda bu teorik çalışmayı da desteklemektedir. Herne kadar deney sonuçları, önerilen reaksiyon stokiyometrisinin sfalerit oksidasyonu sırasındaki kütle dönüşümünü açıklamasa da, aslında sülfatın oksijen kaynağını yansıtmadığını göstermiştir (reaksiyon 16, bolum 4). Önerilen reaksiyon stokiyometrisine göre sülfat; oksijeninin tamamını moleküler oksijenden elde ederken, deneyler oksijen kaynağını su olarak yansıtmaktadır. Sülfat ve su arasındaki oksijen izotopu ayrımlaşma değeri ($\Delta^{18}O_{SO4-H2O}$) kısa ve uzun süreli biyolojik saf sfalerit deneyleri için 9 ‰ ve 9 ‰, demir içeren sfalerit deneyleri için aynı değerler sırasıyla 8.2 ve 7.2 ‰ olarak hesaplanmıştır. Deney sonuçları arasındaki benzer değerler, her iki sfalerit örneği için aynı oksidasyon mekanizmasını ön plana çıkarmakta ve aynı zamanda sfaleritin kristal yapısında bulunan Fe(II)'nin, oksijen izotopu üzerinde önemli bir etkisinin olmadığını yansıtmaktadır. Sfaleritin (saf ve %12 Fe içeren) anaerobik koşullar altında oksitlenmesi sonucu oluşan sülfat, oksijeninin tamamını sudan elde etmiştir. Anaerobik koşullar altında yapılan deneyler sonucunda her iki sfalerit örneği için hesaplanan ($\Delta^{18}O_{SO4-H2O}$) değerleri hem kendi içerisinde hem de aerobik deneylerle benzerlik göstermektedir. Bu sonuçlar, oksijen izotopu ayrımlaşma değerinin, sülfit ve su arasındaki oksijen izotopu değişimi nedeniyle oluştuğunu belirtmektedir. Oksijen izotopu ayrımlaşma değeri kimyasal saf sfalerit deneyleri için veri eksikliği nedeni ile hesaplanamamıştır. Bununla beraber, biyolojik deneylere oranla sülfatın farklı miktarda moleküler oksijen içermesi, en azından farklı oksidasyon mekanizmasının varlığını ortaya koymaktadır.

Aerobik biyolojik ve kimyasal sülfür (kükürt) oksidasyon deneyleri:

Biyolojik sülfür oksidasyonu sonucu oluşan sülfatın oksijen izotop değerleri, sfalerit deneylerinde olduğu gibi oksijenin kaynağını su olarak göstermiştir (100 %). Sülfat ve su arasındaki oksijen izotopu ayrımlaşma değeri ($\Delta^{18}O_{SO4-H2O}$) kısa süreli deneyler için 8 ‰, uzun sureli deneyler için 8.9 ‰ olarak hesaplanmıştır. Bu değerler, aerobik sfalerit deneyleri ile oldukça benzerlik içersindedir. Bu sonuçlar, sülfürün sfalerit oksidasyonu sırasında oluştuğunu ve daha sonraki oksitlenme işlemlerinin biyolojik reaksiyonlar tarafından kontrol edildiğini göstermektedir. Kimyasal sülfür oksidasyon deneylerinin sülfat üretmemesi bu sonuçla uyum içersindedir. Sonuç olarak sülfür oksidasyon deneyleri, sfalerit oksidasyonu sırasında oksitlenen asıl bileşimin sfaleritin bileşimindeki sülfid iyonundan ziyade, sfaleritin yüzeyinde oluşan sülfürden kaynaklandığını desteklemektedir. Bu sonuç, sfalerit ve sülfür deneyleri arasındaki benzer oksijen izotop değerlerini de açıklamaktadır. Ayrıca, elde edilen veriler anaerobik sfalerit oksidasyonu sonucu oluşan sülfatın sülfür izotop değerleriyle de uyumludur. Sfaleritin yüzeyinden elde edilen kükürdün $\delta^{34}S$ değerinin, sfaleritin $\delta^{34}S$ değeri ile aynı olması, sfaleritin anaerobik oksidasyonu sırasında ana oluşumun kükürt olduğuna işaret etmektedir. Saf ve Fe içeren sfaleritin biyolojik oksidasyonu sonucu oluşan $\delta^{18}O_{SO4}$ değerleri birbiri ile benzerlik göstermesine rağmen, piritin oksidasyonu sonucu oluşan $\delta^{18}O_{SO4}$ değerlerinden farklıdır. Aynı zamanda, oksijen izotopu ayrımlaşma değeri pirit ve sfalerit deneyleri için farklı değerler ortaya koymuştur. Sfalerit deneyleri için, sülfat ve su arasındaki oksijen izotopu ayrımlaşma değeri ~9 ‰ olarak hesaplanmışken, aynı değer pirit deneyleri için ~4 ‰ olarak elde edilmiştir. Bu farklılık, sülfat oluşumuna neden olan sülfürün kaynağını tayin etmekte kullanılabileceğini göstermektedir.

Bölüm 4: Mikrobiyolojik Fe (II) oksidasyonu ve Fe(III) çökelmesi sırasında oluşan Fe izotop ayrımlaşması.

Güncel ve eski kayaçlar içerisindeki Fe'li minerallerin kökeninin, Fe izotop değerlerine bağlı olarak yorumlanması, Fe izotoplarının biyolojik ve kimyasal reaksiyonlar sırasında nasıl ayrımlaştığını anlamamıza bağlıdır. Bu çalışmada, Fe(II)'nin asit koşullar (pH <3) altında oksitlenmesi sonucu oluşan çözünmüş Fe bileşiklerinin ($Fe[II]_{aq}$, $Fe[III]_{aq}$) ve aynı çözeltide çökelmiş halde bulunan Fe-oksitlerin ($Fe[III]_{ppt}$) Fe izotop değerleri karşılaştırılmıştır. Deneyler biyolojik ve kimyasal olarak gerçekleştirilmiştir. *A. Ferrooxidans* bakteri türü biyolojik deneylerde kullanılmış, kimyasal deneyler ise sisteme bakteri eklenmeksizin steril ortamda gerçekleştirilmiştir. Deneylerde SO_4^{2-}ve Cl^- tuzları Fe(II) kaynağı olarak kullanılarak, oksitlenme ve çökelme sırasında farklı Fe bileşiklerinin izotoplar üzerine olan etkisi araştırılmıştır. Bu deneylere ek olarak, 2 ve 3 pH aralıklarında Fe(III) çökelme deneyleri de yapılmıştır. Bu deneyler, çökelme hızının Fe-oksitlerin izotop bileşimine olan etkisini ortaya koymak amacıyla gerçekleştirilmiştir. Mikrobiyolojik Fe(II) oksidasyonu suresince, çözeltide kalan Fe(II)'nin δ^{56}Fe değeri periyodik olarak ölçülmüştür. δ^{56}Fe(II) değerleri, Rayleigh tipi bir davranış ortaya koymuş ve Fe(II) ve Fe(III) arasındaki izotopik ayrımlaşma faktörü ($\alpha_{Fe[III]-Fe[II]aq}$) ~1.0022 olarak hesaplanmıştır. Bu değer, hem kimyasal kontrol deneylerinden elde edilen değerden ($\alpha_{Fe[III]-Fe[II]aq}$ ~1.0034), hem de Fe(II) ve Fe(III) arasındaki izotopik değişim nedeniyle oluşan α değerinden farklıdır. Bu nedenle, ~1.0022 değerinin biyolojik reaksiyonları temsil ettiği düşünülebilir. Ancak, Fe(II) ve N_2 atmosferi altında NaOH eklenerek elde edilen Fe(III)'un δ^{56}Fe değerleri arasındaki farkın ortalaması 2.9 ‰ dir, ve bu değer Fe(II) ve Fe(III) arasındaki izotopik değişim nedeniyle oluşan α değeriyle uyumludur. Fe(III) çökelme deneylerinde çözünmüş halde bulunan Fe(III)' ün δ^{56}Fe değeri genellikle Fe-oksidin δ^{56}Fe değerine eşit ya da daha büyüktür. Bu fazlar arasındaki izotopik ayrımlaşma ise artan çökelme hızıyla ve düşen tane boyuyla birlikte azalma seyri içersindedir.

Bütün deney sonuçları birlikte dikkate alındığında, biyolojik deneylerde gözlenen Fe izotop değişimlerinin denge ve kinetik gibi kimyasal faktörler tarafından kontrol edildiğini ortaya çıkmaktadır. Sonuç olarak, güncel Fe döngüsünü yorumlamaya yardımcı olacak bu veriler, kayaçlarda kayıtlı biyolojik işlemlerin tek başına Fe izotoplarına dayanarak ortaya koyma yeteneğimizi de bir ölçüde kısıtlamaktadır.

1 INTRODUCTION

Sulfide mineral oxidation is a common chemical process in many environments, including fresh and marine water, and soil, and is often related to biogeochemical cycles, such as C, O and Fe. Sulfide mineral oxidation is also widespread and one of the main processes in mine waste sites because mining activities expose sulfide mineral deposits to the atmosphere and facilitate oxidation processes. As a result of these oxidation process a common environmental problem known as acid mine drainage (AMD) occurs. These environmental problems have received increasing attention due to their long-term environmental effects and high cost of remediation efforts. In addition to the acid contribution to surface waters, AMD may contain metals such as arsenic, cadmium, copper, silver, and zinc. The metal load causes environmental damage, and is of great concern due to its ecological effects. Another important characteristic of AMD sites is the widespread formation of iron oxides due to excess biological Fe (II) oxidation following dissolution of pyrite or other metal sulfides containing Fe (II). Fe oxides can scavenge metals and play a significant role in the cycling of these metals in watersheds. Furthermore, as strong oxidizers, Fe (III) and Fe-oxides play significant roles in the oxidation of metal sulfides (Moses et al., 1987; Luther, 1987; Schippers et al., 1999, 1996). Therefore, understanding of iron oxides formation and the iron cycle are important for revealing metal sulfides oxidation pathways in AMD sites. A sulfur and Fe(II) oxidizing bacterium, *Acidothiobacillus ferrooxidans,* is commonly found in AMD. The assessment of biological influences on sulfide mineral oxidation is not only important for environmental aspects but also for understanding the sulfur cycle in modern and ancient environments.

Despite increasing attention on the subject due to environmental concerns, oxidation mechanisms of sulfide minerals are poorly understood. Most of the studies on metal sulfides oxidation and the stable isotopes of sulfate focus on pyrite. There has been no detailed study about the isotope composition of sulfate produced during oxidation of the other metal sulfide minerals, such as sphalerite. To elucidate the oxidation mechanisms of pyrite and other metal sulfide minerals from sulfate isotopes, the possible effects of sulfide mineralogy on the sulfate isotopic composition and biological influences must be examined.

This chapter explains the objectives of the study and provides an overview of the stable isotope composition of sulfate (oxygen and sulfur isotopes) and Fe- oxides (Fe isotopes).

Several broad questions for each chapter are summarized as follows along with the objectives of the presented research.

Chapter 2:

1-What is the microbial influence on pyrite oxidation? Do oxygen and sulfur isotopes in sulfate ($\delta^{18}O_{SO4}$ and $\delta^{34}S_{SO4}$) reflect the oxidation pathway (biotic vs. abiotic) ?

Chapter 3:

1- Do $\delta^{18}O_{SO4}$ and $\delta^{34}S_{SO4}$ values reveal microbial influence on sphalerite and elemental sulfur oxidation?

2- Do comparisons between the $\delta^{18}O_{SO4}$ and $\delta^{34}S_{SO4}$ values of sphalerite and elemental sulfur oxidation and those of pyrite oxidation, show the effect of sulfide mineralogy on $\delta^{18}O_{SO4}$ and $\delta^{34}S_{SO4}$ values?

Chapter 4:

1-What is the microbial influence on Fe (II) oxidation and do the $\delta^{56}Fe$ values of different Fe forms ($_{Fe\,(III),\,FeOx}$) reflect this influence?

1.2 The Oxygen and Sulfur isotope composition of sulfate

The applicability of stable isotopes to understanding and revealing the geochemistry of metal sulfide oxidation arises from the fact that oxidation involves the interaction of sulfide minerals with water and atmospheric oxygen. The stable isotopes of oxygen and sulfur provide the most direct record of this interaction through their fractionation processes. Isotopic fractionation is a result of variations in the thermodynamic properties of molecules that depend on mass and of the related equilibrium and kinetically controlled chemical and physical processes. Equilibrium processes include isotopic exchange reactions, which redistributes isotopes among molecules of different substances. Equilibrium isotope effects result from the affect of atomic mass on bonding; molecules containing a heavier isotope are more stable than those containing a lighter isotope. Kinetic processes include irreversible chemical reactions and physical processes such as evaporation and diffusion (O'Neil, 1986). Kinetic isotope effects are related to vibrational velocities associated with lighter isotopes. It is easier to break bonds between elements with lighter isotopes compared with heavier isotopes (Bachinski, 1969). For example, heavier isotopes of oxygen (^{18}O) will be more abundant in a solid than in a liquid of the same molecular mass. Likewise, it is generally believed that biological processes will preferentially use the nutrients with light isotopes (^{16}O) because of weaker bonds (Taylor, et al., 1984). Therefore, biological reactions may produce different isotope signature than abiotic reactions and this signature could be a useful diagnostic tool to trace the oxidation pathways (biotic vs. abiotic).

Stable isotope fractionation associated with the oxidation of metal sulfide minerals occurs due to various reactions involved in the oxidation processes (Figure 1.1). Nordstrom (1982) provided an extensive review about biotic and abiotic oxidation of pyrite oxidation. Furthermore, Goldhaber (1983), Wiersma and Rimstidt (1984), McKibben and Barnes (1996), Luther (1987), Moses et al. (1987), Moses and Herman (1991), and Rimstidt and Vaughan (2003) have made additional contributions. All of these studies suggest that metal sulfide oxidation can be mediated by biotic and abiotic reactions.

Although metal sulfide minerals can be oxidized by different reaction pathways (biotic vs. abiotic), sulfate will be the dominant sulfoxyanoins at pH<3 (Mckibben and Barnes, 1986; Moses et al., 1987, Goldhaber, 1983). Therefore, if oxygen isotopes can be differently fractionated during oxidation processes and if the $\delta^{18}O_{SO4}$ values preserves the identity of its original source of oxygen (water and/or molecular oxygen), the $\delta^{18}O_{SO4}$ value can be used to elucidate reaction pathways (Taylor et al., 1984; Taylor and Wheeler, 1994, Van Stempvoort and Krouse, H., 1994).

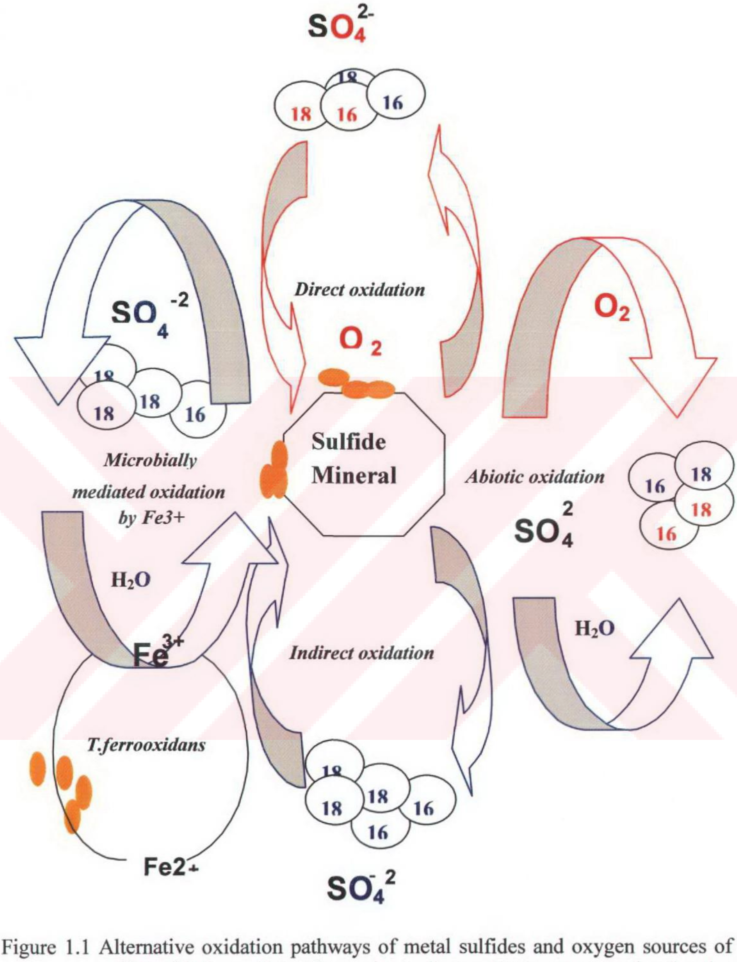

Figure 1.1 Alternative oxidation pathways of metal sulfides and oxygen sources of sulfate (H_2O vs. O_2). Blue color indicates H_2O-oxygen and red color indicates molecular oxygen-O_2 incorporated into sulfate- oxygen through different oxidation pathways

Interpretation of oxygen and sulfur isotopes of sulfate requires an understanding how oxygen and sulfur isotopes of sulfate are fractionated during the different reaction pathways. Therefore, a controlled and detailed experimental investigation of different oxidation pathways under different environmental conditions is necessary. These detailed experimental studies, presented in chapters 2 and 3, may permit us to determine whether the isotopic signatures of sulfate could be used to infer mechanisms of metal sulfide oxidation (biotic vs. abiotic).

1.3 Fe(II) oxidation and $Fe(III)_{aq}$ precipitation

Iron (Fe) is one of the most common metals in the earth's crust and plays an active role in many biogeochemical processes. The Fe isotope composition of Fe-oxides may be used as diagnostic tool to understand bacterial influence on the Fe cycle. The common source of Fe (II) in many environments is sulfide minerals, such as pyrite. Fe (II) and metal sulfide oxidation at pH <3 can often co-occur.

In low pH environments, Fe (II) oxidation is largely driven by bacteria because of the slower kinetics associated with chemical reactions (Savic et al., 1998; Stumm and Morgan et al., 1998; Nordstrom et al.,1997; Lizama et al., 1989).

Clarification of the biological influence on Fe (II) oxidation may also help to trace the biological signature during metal sulfide oxidation. Furthermore, ferric oxides serve as important electron acceptors for metal sulfide oxidation in many aquatic and terrestrial environments increasing the importance of understanding Fe (II) oxidation and formation of Fe-oxides (Kappler, et al., 2004; Glasauer, et al., 2003; Lovely, et al., 1987; 1986a and b).

Biological and non-biological Fe(II) oxidation produce Fe(III)aq and Fe-oxides. The amount and type of these Fe compounds is controlled by the pH of the solution and the anion type in the environment. For example, at pH <3 , Fe(III)aq dominates over the Fe-oxides, whereas Fe-oxides dominates at pH >4.

In addition to the biological effect, geochemical conditions may also influence the type of Fe compounds. If the Fe isotope composition of Fe compounds such as Fe-oxides, Fe (II) and Fe (III) can preserve these effects, then the δ^{56}Fe values can be used to reveal these effects and their biological signatures. The research presented in chapter 4 seeks to document the role of microorganisms during Fe (II) oxidation by means of Fe isotopes. The results of this research may provide information needed to trace biological signatures in the rock record.

2 OXYGEN AND SULFUR ISOTOPE SYSTEMATICS OF SULFATE PRODUCED BY BACTERIAL AND ABIOTIC OXIDATION OF PYRITE

2.1 Introduction

Iron and sulfur are redox active elements and participate in a variety of geochemical and biogeochemical processes. Pyrite, FeS_2, is the most abundant metal sulfide and therefore, its oxidation can regulate the biogeochemical iron, sulfur and oxygen cycle. In addition to its role in the cycling of these elements in ancient and modern environments, pyrite oxidation has received significant attention because of its environmental impact in the formation of acid mine drainage sites (AMD). Consequently, the understanding of oxidation pathways of pyrite (biotic and abiotic) may help to minimize the formation of AMD and reveal sulfur, iron and oxygen cycling in modern and ancient environments.

In AMD systems, oxidation of pyrite to sulfate is described by the following two end-member reactions (Garrels and Thompson, 1960; Simmer and Stumm, 1970; Taylor and Wheeler, 1994; Nordstrom and Alpers, 1999a); which differ in oxidizing agents (molecular oxygen and ferric iron) and in their inferred oxygen sources (O_2 and H_2O) to the sulfate product.

$$FeS_2 + 7/2O_2 + H_2O \rightarrow Fe^{2+} + 2SO_4^{2-} + 2H^+ \tag{2.1}$$

$$FeS_2 + 14Fe^{3+} + 8H_2O \rightarrow 15Fe^{2+} + 2SO_4^{2-} + 16H^+ \tag{2.2}$$

Reaction 1 and 2 are termed the direct and indirect oxidation mechanisms, respectively. The rate of Reaction 1 is enhanced by the bacterium *Acidothiobacillus ferrooxidans*. The rate of reaction 1 is limited by the availability of dissolved oxygen and therefore it could be the common reaction for pyrite oxidation under O_2 saturation conditions. Compared to direct oxidation, Fe^{3+} can rapidly oxidize pyrite abiotically and anaerobically via reaction 2. To maintain reaction 2, however, Fe^{3+} must be regenerated by the following reaction.

$$Fe^{2+} + 1/4O_2 + H^+ \rightarrow Fe^{3+} + 1/2H_2O \quad (2.3)$$

Under acidic conditions (pH<3), reaction 3 is the rate limiting step for reaction 2 and bacterial oxidation of Fe^{2+} is several orders of magnitude faster relative to abiotic oxidation (Schippers, et al. 1996,1999; Nordstrom et al., 1999, Stumm and Morgan, 1968). In addition to direct oxidation of pyrite, re-generation of ferric iron via reaction 3 is generally mediated by bacteria in AMD sites. Consequently, the role of iron and sulfur oxidizing bacteria are both very important in the oxidation of pyrite.

Oxygen of sulfate may come from either atmospheric oxygen or water during pyrite oxidation. The large contrast in the oxygen isotope composition of molecular oxygen ($\delta^{18}O = +23.5$ ‰) and water ($\delta^{18}O < 0.0$ ‰) may provide an opportunity to reveal the reaction pathways of pyrite by determining the relative source of oxygen in sulfate based on its measured $\delta^{18}O_{SO4}$ value (Taylor, 1984). The $\delta^{18}O$ value of the sulfate produced during abiotic and biotic pyrite oxidation may vary depending on reactions pathways and due to differences in the relative amount of molecular oxygen that becomes incorporated into sulfate (Lloyd 1968; Taylor et al. 1984; Van Everdingen and Krouse 1985; Toran and Harris 1989). For example, according to the stoichiometry of reaction 1, it can be predicted that the amount of oxygen in sulfate derived from H_2O would be 12.5% and the remaining 87.5% coming from molecular O_2 (Taylor et al., 1984; Van Everdingen and Krouse, 1985; Taylor and Wheeler,1994).

Despite extensive studies, the key mechanisms which control the oxidation pathways and rates of pyrite are poorly understood. This is partly because of the complexity of the Fe-O-S redox systems and biogeochemical cycling of these elements. However, most studies suggest that it is the Fe-S bond in pyrite that weakens during oxidation rather than the S-S bond (Moses and Herman, 1991; Sato , 1992, Rimsdit et al., 2003). According to this oxidation pathway, the first step in the oxidation of pyrite is release of Fe (II) to solution which leaves a S rich surface. Under acidic conditions, surface studies have confirmed a sulfur rich layer on pyrite containing disulfides, monosulfides and polysulfides (Sasaki,1994; Nesbit and Muir, 1994; Sasaki et al., 1995). It is also suggested that this sulfur rich layer gradually undergoes oxidation to thiosulfate and sulfate (Nesbit and Muir, 1994; Schippers et al., 1996; Guevremont et al., 1998). Although molecular oxygen is needed for the release of iron from the pyrite lattice to initiate the reaction, most studies indicated that ferric iron is the primary oxidant for pyrite in both biotic and abiotic systems (Moses and Herman,1991; Wiersma and Rimstidt, 1984; Mackibben and Barnes, 1986; Moses et al., 1987; Brown and Jurinack, 1989).

The greater reaction rate of Fe (III) with pyrite relative to O_2 has been explained by Moses et al. (1987) and Luther (1987). They indicated that relative to dissolved ferric iron, oxidation is less likely between paramagnetic O_2 and diamagnetic FeS_2. Luther (1987) explained that the faster rate of pyrite oxidation by Fe^{3+} was the result of Fe^{3+} binding directly to the pyrite surface via formation of a transition intermediate oxidant (i.e. persulfido bridge), which facilitates the electron transfer from highest occupied molecular orbital of S_2^{-2} to the lowest unoccupied molecular orbital of Fe^{3+}.

Although pyrite can be oxidized by different reaction pathways (Reaction 1 and 2; biotic vs. abiotic), sulfate will be the dominant sulfoxyanion product at pH<3 (Mckibben and Barnes, 1986; Moses et al., 1987, Goldhaber, 1983, Schippers et al., 1996, 1999). Therefore, if the $\delta^{18}O_{SO4}$ sulfate preserves the identity of its original source of oxygen (water and/or molecular oxygen), the $\delta^{18}O_{SO4}$ value can be used to elucidate reaction pathways which in turn could assist with the design of proper remediation strategies for AMD sites (Taylor et al., 1984; Taylor and Wheeler, 1994, Van Stempvoort and Krouse, 1994). Schwartz et al. (1974) presented the first study that illustrated a correlation between $\delta^{18}O_{SO4}$ and $\delta^{18}O_{H2O}$ during pyrite oxidation experiments at pH ~7. They suggested that this correlation is due to rapid oxygen isotope exchange between water and intermediate sulfite. Taylor et al. (1984) measured $\delta^{18}O_{SO4}$ values from AMD systems at pH <3 and determined the kinetic oxygen isotope fractionations for the incorporation of water and O_2 into sulfate during biotic and abiotic oxidation of pyrite. They performed the experiments under submerged and wet/dry conditions. According to these studies, biologically–mediated reactions of pyrite produced sulfate enriched in ^{18}O by ~3‰ under submerged and ~6‰ under wet/dry conditions, respectively relative to abiotic reactions. They attributed this enrichment to the incorporation of molecular oxygen to sulfate as a result of bacterial metabolic activity. Krouse et al (1991) later demonstrated the incorporation of ^{18}O-labelled O_2 into sulfate and water during biologically mediated pentlandite oxidation by *A. ferrooxidans*. They also concluded that the $\delta^{18}O_{SO4}$ values from bacterial oxidation were higher than those produced by abiologic reactions.

Because the oxidation of pyrite to produce sulfate requires the transfer of an average of 7 electrons per sulfur atom to an aqueous oxidant, a number of intermediate sulfur oxyanion species can be produced at various steps in the system (Basolo and Pearson, 1967). Each step may affect the isotopic composition of sulfate, such as by oxygen isotopic exchange of oxyanion intermediates with water which would increase the apparent contribution of H_2O-derived oxygen to the sulfate product (Taylor and Wheeler, 1994; Krouse et al., 1991; Van Stempvoort and Krouse, 1994). Rimsdit and Vanguah (2003) suggested that molecular oxygen probably interacts with Fe^{2+} sites on the pyrite surface, but not directly with sulfur atoms. According to this model, pyrite oxidation is electrochemical in nature and consists of three different steps: 1) a cathodic reaction, 2) an electron transport and 3) an anodic reaction. Although the nature of the cathodic reaction is not well understood, there is evidence that electrons from metal rather than sulfur in the mineral are transferred to the oxidant at the cathodic sites. At anodic sites, the oxygen atom of a water molecule interacts with a sulfur atom to produce a sulfoxy species. As a result, oxidation occurs at the anodic site. However, to initiate this oxidation, it is necessary to remove the electron from cathodic sites. Therefore, the cathodic reaction is thought to be the rate limiting step for oxidation. According to these reaction mechanisms, water molecules seem to be the only source of oxygen for sulfate during pyrite oxidation. Therefore, Rimsdit and Vanguah (2003) indicated that reaction 1 does not accurately describe the mechanistic role of molecular oxygen in the formation of sulfate from pyrite even though the reaction can describe the overall mass transformation. In reaction 2, all oxygen atoms of sulfate are derived from water (100 %) and the oxygen source is consistent with the electron transfer pathways proposed in the literature (Moses et al., 1987, 1991). Consequently, reaction (1) and (2) may only represent the net stoichiometry for overall mass transformation and may not describe the actual source of oxygen atoms of sulfate.

The $\delta^{18}O$ value of sulfate may also be influenced by the isotopic enrichment factor with respect to O_2 (ε_o) and water (ε_w). The isotopic enrichment may vary depending on the reaction pathways. In general, ε_o appears to be more negative for bacterial reactions (-11.4 ‰) than for abiotic oxidation of sulfide (–4.3 to –8.7 ‰). Compared to ε_o, the value for ε_w is less variable and generally falls between 0 and 4 ‰ (Lloyd 1968; Taylor et al. 1984; Van Everdingen and Krouse 1985; Taylor and Wheeler, 1994; Van Stempvoort and Krouse, 1994).

With respect to the sulfur isotope composition of sulfate, the oxidation of sulfide to sulfate produces small or negligible sulfur isotope fractionation at low pH(<3) (Taylor et al., 1984). Sulfur isotope enrichment factors (ε_s) ranging from +2 ‰ to -5 ‰ have been reported for abiotic and bacterial oxidation of HS^- (Fry et al. 1984; 1988). However, ε_s is generally considered to be 0 ‰ (i.e., no isotopic fractionation) during bacterial and abiotic oxidation of solid phase metal sulfides as the mineral surface becomes oxidized and dissolved "layer by layer" (Nakai and Jensen 1964; McCready and Krouse 1982; Taylor et al. 1984; Taylor and Wheeler, 1994).Therefore, the $\delta^{34}S$ values of sulfate are generally indistinguishable from that of the parent sulfide mineral (Taylor and Wheeler, 1994., Seal and Wandless, 1997). However, experiments that involve aqueous sulfide oxidation to sulfate under neutral and alkaline conditions produced a negative kinetic isotopic effect (0 to 5 ‰) between sulfate and sulfide (Toran and Harris , 1989). Consequently, interpretation of oxygen and sulfur isotopes of sulfate is not straightforward. In order to distinguish the reaction pathways of sulfide oxidation based on the $\delta^{34}S$ and $\delta^{18}O$ composition of sulfate requires carefully controlled laboratory investigations where the $\delta^{18}O$ of H_2O, O_2, and sulfate, and the $\delta^{34}S$ of sulfide and sulfate are all measured under different experimental conditions.

To date, there has been no systematic and detailed experimental study of the $\delta^{34}S$ and $\delta^{18}O$ of sulfate produced during biotic and abiotic pyrite oxidation. In this study, I investigated oxygen and sulfur isotope composition of sulfate produced abiotically and by *A. ferrooxidans* during aerobic and anaerobic pyrite oxidation. These experiments were designed to mimic two common oxidation pathways (reaction 1 and 2) and as well as to determine other environmental effects on oxygen isotope composition of sulfate. Consequently, these detailed experimental studies may permit us to re-assess whether $\delta^{34}S_{SO4}$ and $\delta^{18}O_{SO4}$ values can be reliably used to infer mechanisms of pyrite oxidation (biotic vs. abiotic) and/or oxidation environments (aerobic vs. anaerobic).

2.2 Experimental Methods

2.2.1 Pyrite preparation

Pyrite samples used in the current study were obtained from the Geology Museum of the Colorado School of Mines, Golden, Colorado. The purity of the pyrite was checked (~99%) by analyzing the elemental composition by ICP analysis at the United States Geological Survey (USGS), in Denver, Colorado. Prior to use in all of the experiments, the pyrite was ground and sieved. A grain size of < 63 μm was used for the experiments. Iron and sulfur coatings on the pyrite surface were first cleaned by boiling 10 g of the pyrite in 100 ml of 6 M HCI for approximately 15 minutes. The pyrite was then subsequently rinsed three times with deionized water, followed by rinses with acetone, and then dried under nitrogen atmosphere at room temperature (Moses et al., 1987). For sterilization, the pyrite samples were soaked with 70 % ethanol and spread in a thin even layer under UV radiation (germicidal) in a sterile hood for~30 minutes to decontaminate the surface. These sterilization methods were effective since contamination effects were not observed in the abiotic control experiments. Following these treatments, the pyrite was immediately placed in sterile experimental containers.

2.2.2 Bacterial culture preparation

The acidophilic Fe (II)- and sulfur oxidizing bacteri, *Acidithiobacillus ferrooxidans* (23270) (formerly, Thiobacillus ferrooxidans) was obtained from the American Type Culture Collection (ATCC) and used in all the biological experiments. Bacteria were maintained in a modified 2039-ATCC medium which contains the following per liter: 0.6 g NH_4CI, 0.2 g $MgCI_2.6H_2O$, 0.1 g K_2HPO_4; 7.1 g $FeCI_2$ and 1.5 g FeSO4 and 5 ml Wolfe's mineral solution (1.5 g nitrilotriacetic acid , 3 g $MgSO_4.7H_2O$, 0.5 g $MnSO_4.7H_2O$, 1 g NaCI, 100 mg $FeSO_4.7H_20$, 100 mg $CoCI_2.6H_2O$, 100 mg $CaCI_2$, 100 mg $ZnSO_4.7H_2O$, 100 mg $CuSO_4.7H_2O$, 10 mg $AlK(SO_4)_2$. $12H_2O$, 10mg H_3BO_3, 10mg $Na_2MoO_4.2H_2O$ per liter) (ATCC web site). The medium was prepared by adding the above to 800 ml of de-ionized (DI) water which contain 5 ml of sulfate free Wolfe's mineral solution. The medium used for growing bacteria was adjusted to pH 2.3 with trace-metal grade HCI and autoclaved for 25 minutes. $FeCl_2$ (7.1 g) and $FeSO_4$ (1.35 g) salts were added as energy substrates to 200 ml acidified DI water and immediately filter sterilized.

The salt medium and the Fe (II) solution were aseptically combined. *A. ferrooxidans* was subcultured three times before being used in the final biological pyrite experiments.

In order to prepare cell cultures for the experiments, 3 liters of 12 day old cultures were first filtered using whatman #1 filter paper to retain the iron oxides and the supernatant then centrifuged at 12000 rpm for 10 min to concentrate the cell pellet.

The resulting supernatant was washed twice with sterile-acidified DI water (pH 2) and resuspended in a small volume of DI water. The cell suspensions were used as inoculums the same day they were prepared.

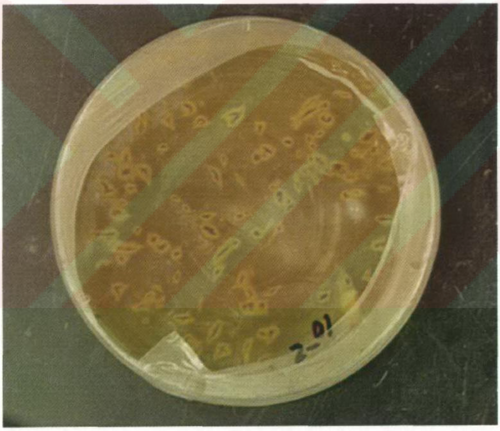

Figure 2.1 Bacterial culture (*A. ferrooxidans*) used in the biological experiments

In order to determine the actual cell densities in the biological experiments, cell numbers were estimated by the Most Probable Number Method (MPN) using the ferrous sulfate medium previously described.

Five milliliters of the cell suspension which contain (~2.7×10^7cell) was used for 250 ml medium in the biological experiments.

2.2.3 Aerobic experiments

In order to elucidate the reaction pathway of pyrite and the relative contribution of molecular oxygen to sulfate, biotic and abiotic experiments were performed under O_2 saturated conditions with continuous sparging with air.An initial pH of 3 was used for all experiments. The biological aerobic experiments were designed both as short and long-termto assess the integrity of the oxygen isotope composition of sulfate with the extent of the reaction and decreasing pH with time. Oxygen isotope exchange between water and intermediate sulfur species is possible over time and will increase at lower pH (Llyod, 1968; Pearson et al., Holt et al., 1981; Fritz et al., 1973). Short- term biological experiments were ended at pH ~2.7 (~20 days) while long-termexperiments were ended at pH 2.1 (~44 days). These pH values mimic the range observed in many AMD sites. Abiotic oxidation experiments were carried out under identical conditions as the biological experiments except without addition of the bacterial culture.

2.2.3.1 Aerobic biological experiments

For the bacterial experiments, sulfate and Fe(II)-free medium was used as the experimental solution (NH_4CI, 0.6 g; $MgCI_2.6H_2O$, 0.2 g ; K_2HPO_4, 0.1 g ; Wolfe's mineral solution, 5 ml) and pH was adjusted to 3 with HCl at 25 °C. Wolfe's mineral solution was prepared with CI salt instead of SO_4 salt to prevent sulfate contamination to the final experimental solution (1.5 g nitrilotriacetic acid , 3 g $MgSO_4.7H_2O$, 0.5 g $MnSO_4.7H_2O$, 1 g NaCI, 100 mg $FeSO_4.7H_20$, 100 mg $CoCI_2.6H_2O$, 100 mg $CaCI_2$, 100 mg $ZnSO_4.7H_2O$, 100 mg $CuSO_4.7H_2O$, 10 mg $AlK(SO_4)_2$. $12H_2O$, 10mg H_3BO_3, 10mg $Na_2MoO_4.2H_2O$ per liter. The salts and 5 ml of sulfate-free sterile Wolfe's mineral solution were added to DI water. Trace metal grade HCI was subsequently added to the medium to a pH of 3. The 250 ml of medium was placed into acid washed 500 ml Erlenmeyer flasks and autoclaved at 121 °C for 20 minutes.

After autoclaving, the flasks were kept in the sterile hood under the UV for 25 minutes to decontaminate the surfaces of the flasks. Five hundred milligrams of pyrite sample was sterilized and cleaned by the methods described previously and 5 ml (~2.7 x 10^7 cell/ml) of the *A. Ferrooxidans* cell suspension was added to 250 ml of medium.

To determine the kinetic oxygen isotopic fractionation effect (ε_o) during pyrite oxidation and the relative contribution of water and molecular oxygen to the oxygen of the sulfate product, four different bacterial incubations were made with waters having different $\delta^{18}O$ values of -15.3 ‰, -2.5 ‰, 1.8 ‰ and 13‰. The experiments were performed as duplicates for each given water. Therefore, 8 flasks for the short-term and 8 flasks for the long-termbiological experiments were incubated in the environmental room at 25 °C and continuously shaken (150 rpm) over the entire period of the incubations. The flasks were covered with rubber stoppers fitted with inflow and outflow tubes for aeration. Sterile air filters (0.2 μm, whatman) were connected to the inflow and exit ports to prevent microbial contamination and to minimize evaporation. The flasks were continuously bubbled with compressed air (General Air Company) and several tanks were used during these experiments. During each set of incubations, additional biotic and abiotic laboratory experiments with normal laboratory water (-15.3 ‰) were also performed under identical experimental conditions in order to monitor pH and the solution chemistry of the solutions. Aliquots from these experiments were taken periodically to measure the concentration of sulfate, Fe(III)aq, Fe(II)aq and pH.

At the end of the short and long-termpyrite oxidation experiments, the solutions were filtered (0.1 μm,Milipore) to remove iron oxides that may interfere with oxygen isotope measurements of sulfate. Some portion of the filtrate was reserved for oxygen isotope measurement of water and for sulfate concentration measurements by ion chromatography. The water samples were kept frozen until oxygen isotope measurements. To the remainder of the filtrate (~200 ml), a small amount of concentrated HCI and 10 ml of 10 % $BaCl_2$ solution were added to precipitate SO_4 as $BaSO_4$ and the precipitate was allowed to settle overnight. The barium sulfate was filtered and collected on a 0.2 μm Millipore filter, washed first with 100 ml of 1N HCI, then rinsed 3 times with total 500 ml of DI water and dried for 24 h at 100 °C. As a final purification step, all of the $BaSO_4$ powders were baked under an air atmosphere at 500 °C for 2 h. This treatment was previously shown to effectively remove any possible organic material and not interfere with $\delta^{18}O$ measurements (Mandernack et al., 2000).

Air samples from both biotic and abiotic experiments were collected in an evacuated 200 ml collection vessel at the end of the experiments and isotopically analyzed for the ^{18}O isotopic composition of O_2 in the air. Prior to sampling the gas headspace, the air source and exit port of the flask were closed and the air in the head space allowed to mix a few minutes before drawing the gas sample. The air sample was collected with a gas-tight syringe which was flushed twice before taking the final sample.

Figure 2.2 Experiments set up under aerobic conditions

2.2.3.2 Aerobic abiotic experiments

In order to accurately interpret whether bacterial mediation of pyrite oxidation can produce sulfate with a $\delta^{18}O_{SO4}$ value that has a distinct biological signature, abiotic control experiments were performed under identical conditions as the biological experiments.

To obtain enough SO_4 for isotope analysis, abiotic experiments were carried out in 500 ml of medium in 1 liter Erlenmeyer flasks. All experimental conditions and surface cleaning methods were identical to the biological experiments, except that 1 g pyrite sample was used for 500 ml medium in order to keep the ratio of mineral mass to solution volume (1g/500ml) the same as the biological experiments (500 mg/250 ml). Although the abiotic experiments were incubated for the same time period as the long-termbiological experiments (44 days), due to slower rates of oxidation the pH only dropped slightly to pH 2.8. This pH matched the short- term biological experiments. The pH, sulfate, Fe(III)aq and Fe(II)aq concentration were also monitored (Table 2.1).

2.2.4 Bacterial and abiotic anaerobic experiments

In order to determine the oxygen isotope composition of sulfate produced anaerobically by ferric iron oxidation of pyrite (reaction 2), biotic and abiotic experiments were carried out. For these experiments, 100 ml of the microbiological medium, as described previously, was placed into 200 ml serum bottles and the pH adjusted to ~2 with trace metal grade HCI. Lower pH was necessary to keep aqueous Fe (III) in solution. The serum bottles were then autoclaved for 20 minutes. Afterwards, serum bottles were aseptically purged with nitrogen for 30 minutes by using pre-sterilized inline gas filters (0.2 μm, whatman) at the both the inlet and outlet in order to keep the medium sterile. After purging, serum bottles were kept overnight in the anaerobic microbiological glove box to equilibrate with the anaerobic atmosphere before starting the experiments. The atmosphere in the glove box consisted of 5 % CO_2, 5 % H_2, and 90 % N_2. For the anaerobic experiments, ~200 mg of pyrite was cleaned and sterilized according to the methods described above. The ferric iron used in these experiments was prepared by dissolving ferric chloride ($FeCl_3$) into acidified DI water (pH 2), then filter sterilized (0.2 μm, whatman) and aseptically purged with nitrogen for ~25 min. The ferric iron stock solution (1M) was kept inside the anaerobic chamber until used. To 100 ml of microbiological medium, 200 mg of pyrite, 1 ml of the cell culture (2.7×10^7 cells/ml) and the $FeCl_3$ solution (10mM final) were added to each 200 ml vial and then sealed with a gas headspace inside the anaerobic chamber. As a final step, the serum bottles were covered with aluminum foil to prevent iron photo oxidation/ reduction and placed in an environmental room at 25° C. The vials were shaken continuously at 150 rpm during the entire incubation period (35 days). Abiotic experiments were prepared under identical conditions except that no bacterial culture was added. Biotic and Abiotic experiments were performed in duplicate and concentrations of Fe(II) and sulfate were monitored during the course of the experiments (Table 2.2).

Three different $\delta^{18}O$ value waters (-15.3 ‰, -2.5 ‰, 1.8 ‰) were used for the biological and abiotic anaerobic experiments in order to determine the kinetic isotopic fractionation effect between water and sulfate during pyrite oxidation.

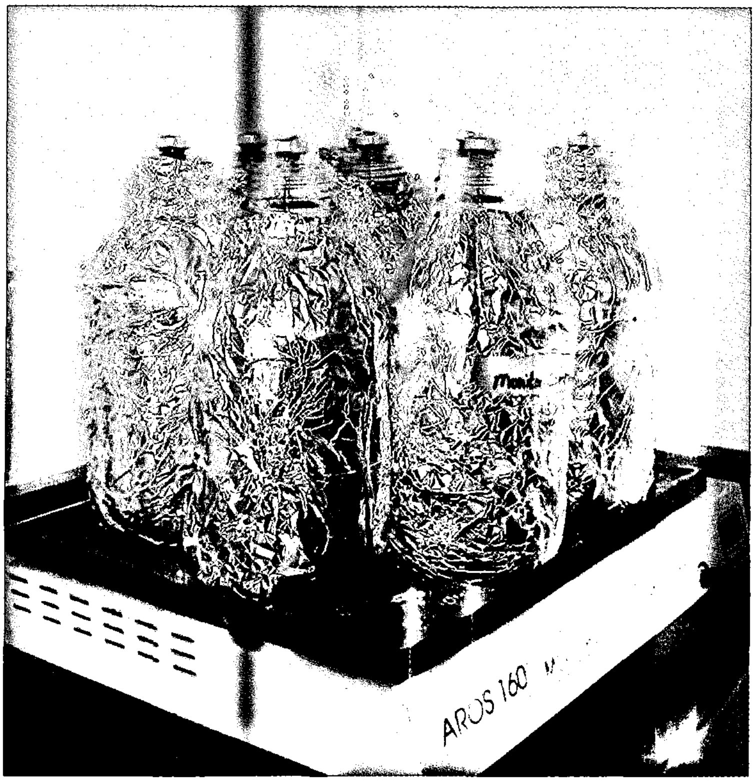

Figure 2.3 Experiments set up under anaerobic conditions

2.2.5 Oxygen and sulfur isotope analyses of SO_4 from AMD sites

In order to determine whether the results from the laboratory experiments could be used to predict the oxygen isotope composition of natural sulfate and to characterize the biotic or abiotic oxidation pathways of pyrite in AMD environments, sulfate samples were collected from drainage waters of the Quartz-Hill and Argo tunnel AMD sites in Colorado. Quartz-Hill and Argo tunnel are part of the same mining sites and are connected with the each other. The Quartz-Hill mining district, near Central City, exploited veins of gold, silver, uranium and base metals. In 1893, the Argo tunnel, located in Gilpin, was constructed to drain ground water from the mine workings in Central City. Sulfide minerals in 26 veins intersect the Argo Tunnel and include pyrite, chalcopyrite, tennantite ($Cu_3AsS_{3.25}$), enargite (Cu_3AsS_4), sphalerite and galena (Wentz, 1975; Simms et al., 1963). It was reported that the acid waters draining from the Argo tunnel in the period January 1976 to March 1977 had a relatively constant pH of 3.0 and temperature of 16 ^{o}C (Wentz,1975). Water samples from Quartz-Hill pond and Argo Tunnel were collected from 2000 to 2003 (Table 6). Due to freezing, only a couple of winter samples were collected. Water samples were filtered (0.1μm, Millipore) in the field, and the filtrate reserved for sulfate concentration measurements. Water was also collected in 12 ml glass vials for $\delta^{18}O_{H2O}$ analysis. In addition to pH, aqueous Fe (II) and Fe (III) were measured in the field using a DR/700 Hach colorimeter.

2.2.6 Isotopes analysis of sulfate

For all the incubation experiments and field samples described above, sulfate for isotopic analyses was collected by precipitation as $BaSO_4$ by addition of a few ml of a 10% solution (wt/wt) of $BaCl_2$. The $BaSO_4$ samples were dried and homogenized by grinding. As a final purification, prior to $\delta^{34}S$ and $\delta^{18}O$ analysis the samples were baked at 500° C for two hours to remove possible organic contaminants as described elsewhere (Mandernack et al., 2000). Sulfur and oxygen isotope ratios of samples were determined by continuous flow isotope ratio mass spectrometry (CF-IRMS) using an elemental analyzer ($\delta^{34}S$) or a Thermo-Finnigan TC/EA at 1450°C ($\delta^{18}O$) coupled to a gas source mass spectrometer. Reproducibility of the $\delta^{34}S$ and $\delta^{18}O$ values for sulfate were generally better than ± 0.5 ‰. The oxygen and sulfur isotope results of this study are referred to in the standard δ notation, an expression of the per mil deviation of the sample with respect to a given standard. For $\delta^{18}O$ and $\delta^{34}S$, Standard Mean Ocean Water (SMOW) and Canyon Diablo Troilite (CDT) are the respective standards. For $\delta^{18}O$ the δ notation is expressed as follows:

$$\delta^{18}O_{(SMOW)}\text{sample} = [(^{18}O/^{16}O\text{sample})/(^{18}O/^{16}O_{(SMOW)} - 1] \times 10^3$$

2.2.7 Analytical approach for oxygen isotope composition of sulfate

Analyses of the oxygen isotope composition of sulfate produced during the aerobic biotic and abiotic pyrite oxidation experiments revealed that oxygen atoms of sulfate are derived both from water and molecular oxygen. Furthermore, kinetic oxygen isotopic fractionation effects are expressed for both sources of oxygen. Therefore, interpretation of $\delta^{18}O_{SO4}$ values are not straight forward and determination of the percent oxygen in the sulfate derived from H_2O and O_2 is necessary. The linear relationship observed between $\delta^{18}O_{SO4}$ and $\delta^{18}O_{H2O}$ (for 3 different $\delta^{18}O$ waters) was used to estimate % oxygen incorporation to sulfate from H_2O and O_2. The slope (m) of this line estimates the % contribution of oxygen to sulfate from water and 1-m represents the % contribution of oxygen to sulfate from O_2. Based on the values of the % oxygen contribution to the sulfate from H_2O and O_2, the fractionation of oxygen isotopes between SO_4 and H_2O and between SO_4 and O_2 can then be estimated by a least squares method (Mandernack et al., 1995). The measured $\delta^{18}O_{SO4}$ value is defined by the following equation:

$$\delta^{18}O_{SO4} = X.(\delta^{18}O_{SO4\text{-}O2}) + (1-X).(\varepsilon_{SO4\text{-}H2O} + \delta^{18}O_{H2O}) \tag{2.4}$$

In equation (4), X represents the fraction of oxygen in sulfate derived from O_2 and (1-X) the remaining fraction from H_2O. $\varepsilon_{SO4\text{-}H2O}$ is the kinetic isotope fractionation effect between SO_4 and H_2O and $\delta^{18}O_{SO4\text{-}O2}$ is the isotopic value of SO_4 derived from O_2 (i.e., the isotopic value of sulfate if all of its oxygen atoms came from O_2). The estimated value of $\delta^{18}O_{SO4\text{-}O2}$ minus the measured $\delta^{18}O$ value of the O2 gas yields $\varepsilon_{SO4\text{-}O2}$, the isotopic fractionation between O_2 gas and sulfate. Therefore, equation 4 can be re-arranged by multiplying the terms in the second parameter of equation 4: which rearranges to

$$\delta^{18}O_{SO4} = X.(\delta^{18}O_{SO4\text{-}O2}) + \varepsilon_{SO4\text{-}H2O} + \delta^{18}O_{H2O} - X\,\varepsilon_{SO4\text{-}H2O} - X\,\delta^{18}O_{H2O} \tag{2.5}$$

$$\delta^{18}O_{SO4} - \delta^{18}O_{H2O} + X\,\delta^{18}O_{H2O} = X.(\delta^{18}O_{SO4\text{-}O2}) + (1-X)\,\varepsilon_{SO4\text{-}H2O} \tag{2.6}$$

Equation 6 can then be rearranged in order that the unknown values, $\delta^{18}O_{SO4\text{-}O2}$ and $\varepsilon_{SO4\text{-}H2O}$, are expressed as multiples of the known or measured values ($\delta^{18}O_{SO4}$, $\delta^{18}O_{H2O}$, and X), in the following mass balance equation

$$1 = \{X/\delta^{18}O_{SO4} + (X-1)\,\delta^{18}O_{H2O}\}\,\delta^{18}O_{SO4\text{-}O2} + \{(1-X)/\delta^{18}O_{SO4} + (X-1)\,\delta^{18}O_{H2O}\}\,\varepsilon_{SO4\text{-}H2O} \tag{2.7}$$

$$\underbrace{\begin{bmatrix} \{X/\delta^{18}O^1_{SO4} + (X-1)\,\delta^{18}O^1_{H2O}\} & \{(1-X)/\delta^{18}O^1_{SO4} + (X-1)\,\delta^{18}O^1_{H2O}\} \\ \{X/\delta^{18}O^2_{SO4} + (X-1)\,\delta^{18}O^2_{H2O}\} & \{(1-X)/\delta^{18}O^2_{SO4} + (X-1)\,\delta^{18}O^2_{H2O}\} \\ \{X/\delta^{18}O^3_{SO4} + (X-1)\,\delta^{18}O^3_{H2O}\} & \{(1-X)/\delta^{18}O^3_{SO4} + (X-1)\,\delta^{18}O^3_{H2O}\} \\ \{X/\delta^{18}O^4_{SO4} + (X-1)\,\delta^{18}O^4_{H2O}\} & \{(1-X)/\delta^{18}O^4_{SO4} + (X-1)\,\delta^{18}O^4_{H2O}\} \\ \{X/\delta^{18}O^5_{SO4} + (X-1)\,\delta^{18}O^5_{H2O}\} & \{(1-X)/\delta^{18}O^5_{SO4} + (X-1)\,\delta^{18}O^5_{H2O}\} \\ \{X/\delta^{18}O^6_{SO4} + (X-1)\,\delta^{18}O^6_{H2O}\} & \{(1-X)/\delta^{18}O^6_{SO4} + (X-1)\,\delta^{18}O^6_{H2O} \end{bmatrix}}_{\mathbf{A}} \times \underbrace{\begin{bmatrix} 1 \\ 1 \\ 1 \\ 1 \\ 1 \\ 1 \end{bmatrix}}_{\overrightarrow{\mathbf{Y}}} = \underbrace{\begin{bmatrix} \delta^{18}O_{SO4\text{-}O2} \\ \\ \\ \\ \varepsilon_{SO4\text{-}H2O} \\ \\ \end{bmatrix}}_{\overrightarrow{\mathbf{X}}}$$

The least squares solution is then:

$$\vec{X} = (A^T A)^{-1} A^T * \vec{Y}$$

2.3 Results

2.3.1 Aerobic experiments

According to the rates of sulfate and Fe(III) $_{aq}$ production under the aerobic experimental conditions, *A. ferrooxidans* oxidized pyrite at faster rates relative to the abiotic experiments (Table 2.1, Figs.2.4a and b). Sulfate production in the abiotic incubations (44 days-0.87×10^{-3} mg/FeS_2-day) was significantly less than in the biotic experiments (44-days 0.051 mg/FeS_2-day) (Table 2.1).

In the biological experiments, sulfate concentration consistently increased until day 27 when the pH had dropped to 2.5 (Fig. 2.4a.). Although pH continued to drop to 2.1 at day 44, the sulfate concentration decreased relative to day 27. This decrease in the sulfate concentration could be due to the precipitation of ferric iron sulfate mineral such as jarosite (Blowes et al., 2003, Jambor et al., 2003).

At this point, there was also a decrease in the ferric iron concentration (Fig. 2.4a). Although the solid phase formed during the oxidation experiments was not determined by X-ray diffraction, after filtration the filter was red indicating the presence of solid iron oxides.

X-ray diffraction analyses of iron oxides precipitated during oxidation of Fe(II) by replicate cultures of *A. ferrooxidans* have indicated the presence of sulfate-bearing schwertmannite and jarosite (unpublished results), consistent with *A.ferrooxidans* being able to oxidize $Fe(II)_{aq}$ faster relative to chemical oxidation of Fe(II)aq at pH <3.0 (Nordstrom and Southam, 1997).

Table 2.1. Solution chemistry during short and long-term aerobic bacterial and abiotic pyrite oxidation experiments

	Biological							Abiotic					
	Days	pH	SO_4 (mg/L)	SO4 production Rate (mg/FeS2-mg*day)	Fe_t (mg/L)	Fe(II) (mg/L)	Fe(III) (mg/L)	pH	SO_4 (mg/L)	SO4 production Rate (mg/FeS2-mg*day)	Fe_t (mg/L)	Fe(II) (mg/L)	Fe(III) (mg/L)
	0	2.91	14	0	32.6	20.4	20.4	3.0	3.7	0	3.6	2.9	0.8
	3	2.84	n.d.	n.d.	29.8	2.4	27.4	n.d.	n.d.	n.d.	n.d.	n.d.	n.d.
	5	2.78	35	0.008	37.2	12.9	24.3	2.9	14.1	2.09×10^{-3}	4.8	3.6	1.2
	7	2.90	n.d.	n.d.	29.2	9.2	20.8	n.d.	n.d.	n.d.	n.d.	n.d.	n.d.
	11	2.90	55	0.007	72.5	50.7	21.8	2.9	14.5	0.9×10^{-3}	6.4	4.8	1.6
	16	2.81	n.d.	n.d.	138.5	19.1	119	n.d.	n.d.	n.d.	n.d.	n.d.	n.d.
Short term	20	2.65	597	0.058	437	19.0	418	2.9	16.3	0.6×10^{-3}	n.d.	n.d.	n.d.
	27	2.50	2000	0.147	482	24.0	458	n.d.	24.0	0.7×10^{-3}	7.2	5.1	2.1
	35	2.45	n.d.	n.d.	660	28.2	631	2.8	35.0	0.8×10^{-3}	n.d.	n.d.	n.d.
Long term	44	2.20	1149	0.051	305	34.0	271	2.8	42.0	0.87×10^{-3}	16.7	14.8	2.0

n.d = Not Determined

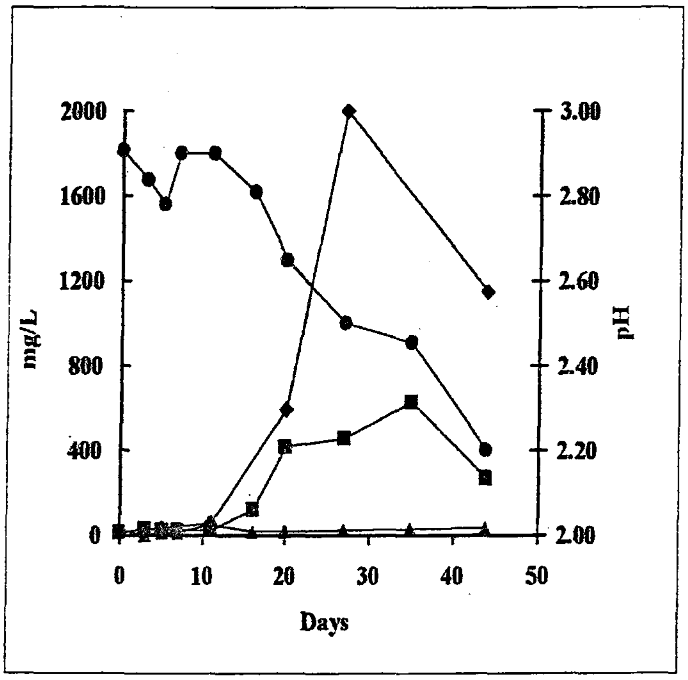

Figure 2.4a. Solution chemistry during aerobic bacterial pyrite oxidation experiments. Sulfate concentration, ◆. Fe(III) concentration, ■. Fe(II) concentration, ▲. pH of the solution, ●.

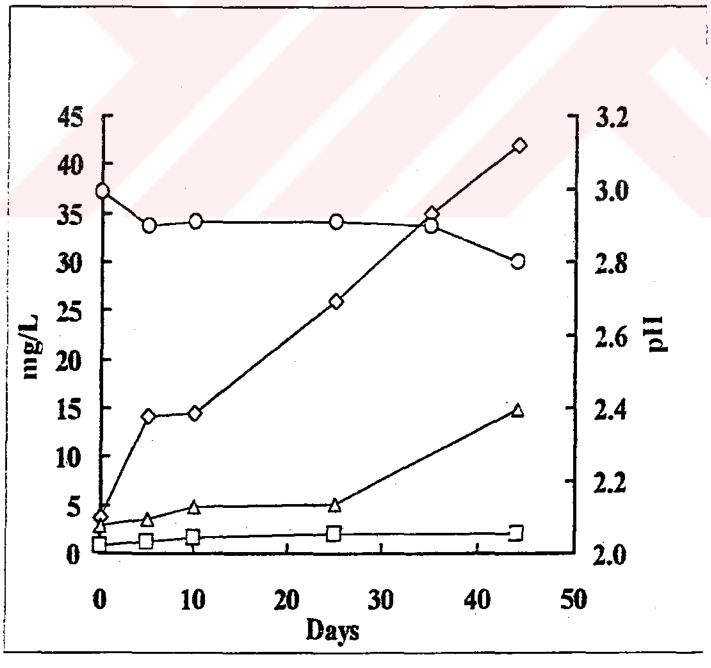

Figure 2.4b. Solution chemistry during aerobic abiotic pyrite oxidation experiments Sulfate concentration, ◇. Fe(III) concentration, □. Fe(II) concentration, . △. pH of the solution, ○ .

The short-term biological experiments were terminated when pH reached ~2.7 after 20 days. Sulfate and ferric iron concentrations were measured as 597 mg/L and 437 mg/L, respectively (Table 2.1).

The Fe (III) aq concentration was also higher in the biological experiments compared to abiotic experiments (Figs. 2.4a and b). The long-termbiological experiments were ended at pH 2.1 after 44 days. Although abiotic experiments were maintained for the same time period as the long-termbiological experiments (44 days), the pH only dropped slightly to 2.8 which approximated the final pH of the short-term biological experiments (Fig.2.4b).

2.3.2 Anaerobic experiments

The chemical and isotopic results of sulfate from the biotic and abiotic anaerobic experiments are provided in Tables 2.2 and 2.4. The increase in sulfate concentration during both 35 day incubations was very similar.

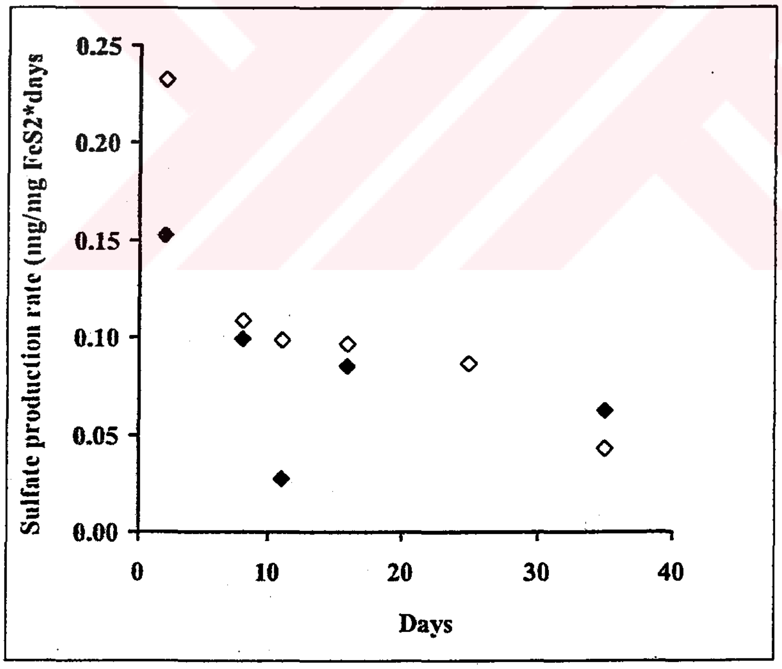

Figure 2.5 Sulfate production rate during anaerobic pyrite oxidation. Bacterial experiments, ◆. Abiotic-control experiments, ◇.

These results suggest that chemical oxidation may have been dominant in both experiments. In the biotic and abiotic anaerobic experiments, the rate of sulfate production generally decreased with time (Table 2.2).

Table 2.2 Solution chemistry during bacterial and abiotic anaerobic pyrite oxidation experiments

	Biotic					Abiotic				
Days	pH	Fe(II) mg/L	SO4[a] mg/L	SO4[b] mg/L	SPR (mg SO4/(mg FeS2* days)[c]	pH	Fe(II) mg/L	SO4[a] mg/L	SO4[b] mg/L	SPR(mg SO4/(mg FeS2* days)[c]
0	1.90	100	23	18	0.000	1.98	140	32	24	0.000
2		740	84	96	0.153		460	125	109	0.232
8	1.85	1120	182	215	0.099	1.83	770	206	156	0.108
11		420	83	96	0.027		940	249	212	0.099
16	1.87	1340	296	306	0.085	1.86	1280	342	322	0.097
25		n.d.	n.d.	n.d.	n.d.		2040	466	402	0.087
35	1.88	1800	462	411	0.062	1.87	1450	331	412	0.043

[a] sulfate concentration measured directly by IC
[b] sulfate concentration based on mass balance calculation
[c] SPR (Sulfate production rate)

This decreasing trend could be indicative of formation of different S-oxyanions and thus incomplete oxidation to sulfate.Precipitation of sulfate-bearing minerals (e.g. jarosite) might also contribute to this decrease. These observations appear to be consistent with an increase in the Fe (II) aq concentration which was produced as a result of pyrite oxidation by ferric iron.

2.3.3 Oxygen and sulfur isotopic composition of sulfate produced under aerobic conditions

Table 2.3 shows the $\delta^{18}O$ and $\delta^{34}S$ values of sulfate formed during the biotic and abiotic pyrite oxidation experiments. Both experiments indicated that the $\delta^{18}O_{SO4}$ values show a strong linear dependence ($r^2 \geq 0.99$) on the $\delta^{18}O$ of water (Fig. 2.6). In the short-term biological experiments, the linear regression between $\delta^{18}O_{SO4}$ and $\delta^{18}O_{H2O}$ has a slope of 0.87±0.06, indicating that 87 % of the sulfate-oxygen is derived from H_2O and the remaining 13 % from O_2 (Fig. 2.6). The incorporation of water-oxygen into sulfate increased with the extent of the reaction as inferred from a greater slope of 0.94±0.09 in the long-term biological experiments (Fig.2.6). The aerobic abiotic-control experiments produced sulfate that had similar $\delta^{18}O_{SO4}$ values as the short-term biological experiments, the $\delta^{18}O_{SO4}$ versus $\delta^{18}O_{H2O}$ plotting with a slope of 0.89. These results suggest that approximately 11 % of the oxygen atoms in sulfate are derived from O_2. Standard deviations were generally low for the slope and the intercept of all plots: ±0.06, ±0.09, ±0.38 for the slopes of the short-term biological experiments, the long-term biological experiments; and the abiotic experiments, respectively. The respective values for the y intercept of each plot were ± 0.6, ± 0.5, ± 3.8. In the biological experiments, there were small increases in the $\delta^{18}O_{H2O}$ during the incubations which was attributed to the evaporation. Most of these increases were ~ 1‰ or less, with the exception of one long-term bacterial experiments that showed a 2 ‰ increase (Table 2.3).

The kinetic oxygen isotope fractionation effect between sulfate and water ($\Delta^{18}O_{SO4-H2O}$) and between sulfate and O_2 ($\Delta^{18}O_{SO4-O2}$) was calculated for the short and long-term biological and abiotic experiments. Using the least squares and matrix analysis, the fractionation effect of oxygen isotopes between sulfate and water was estimated to be 5.3, 3.8 ‰ for the short and long-term biological experiments, respectively and 3.2 ‰ for the aerobic-abiotic-control experiments (Table 2.5).

Table 2.3 Oxygen and sulfur isotope composition of sulfate from bacterial and abiotic aerobic pyrite oxidation experiments.

Biological		$\delta^{18}O_{H2Oinitial}$ (‰)	$\delta^{18}O_{H2Ofinal}$ (‰)	Avg.$\delta^{18}O_{SO4}$ (‰)	Avg.$\delta^{34}S_{SO4}$[b] (‰)
	Short-term	-15.3	-14.8	-7.5	2.3
		-15.3	-14.2	-8.4	2.4
		-2.5	-1.8	3.2	2.3
		-2.5	-2.4	2.5	2.4
		1.8	1.7	6.3	2.4
		1.8	1.6	6.0	2.4
		13.2	12.5	15.5	2.3
	Long-term				
		-15.3	-14.3	-9.9	2.2
		-15.3	-14.0	-9.4	2.5
		-2.5	-1.4	3.5	2.5
		-2.5	-1.5	2.1	2.4
		1.8	3.7[a]	6.9	2.3
		1.8	2.9	6.2	2.4
		13.2	13.0	15.6	2.4
Abiotic	Long-term	-15.3	-14.7	-8.6	2.1
		-2.5	-1.6	3	2.1
		1.8	1.4	3.2	2.5
		13.2	12.5	16	2.1

[a] sample with highest evaporation effect
b $\delta^{34}S_{SO4}$ of pyrite used in experiments was 2.3±0.5 ‰

The $\delta^{34}S_{SO4}$ values showed insignificant fractionation (<0.2 ‰) compared to the sulfur isotope value of pyrite (Table 2.3). Sulfur isotope fractionation was determined as the difference between the $\delta^{34}S_{SO4}$ and $\delta^{34}S_{FeS2}$ ($\Delta^{34}S_{SO4-FeS2}$).

2.3.4 Oxygen and sulfur isotopes of sulfate produced under anaerobic conditions

The $\delta^{18}O_{SO4}$ values from both biotic and abiotic anaerobic experiments when plotted relative to $\delta^{18}O_{H2O}$ yielded slopes of 0.99 and 0.97, respectively and suggest that most of the oxygen in sulfate is derived from H_2O (Fig. 2.7). These results are consistent with the fact that only water was available as an oxygen source to sulfate under anaerobic conditions.

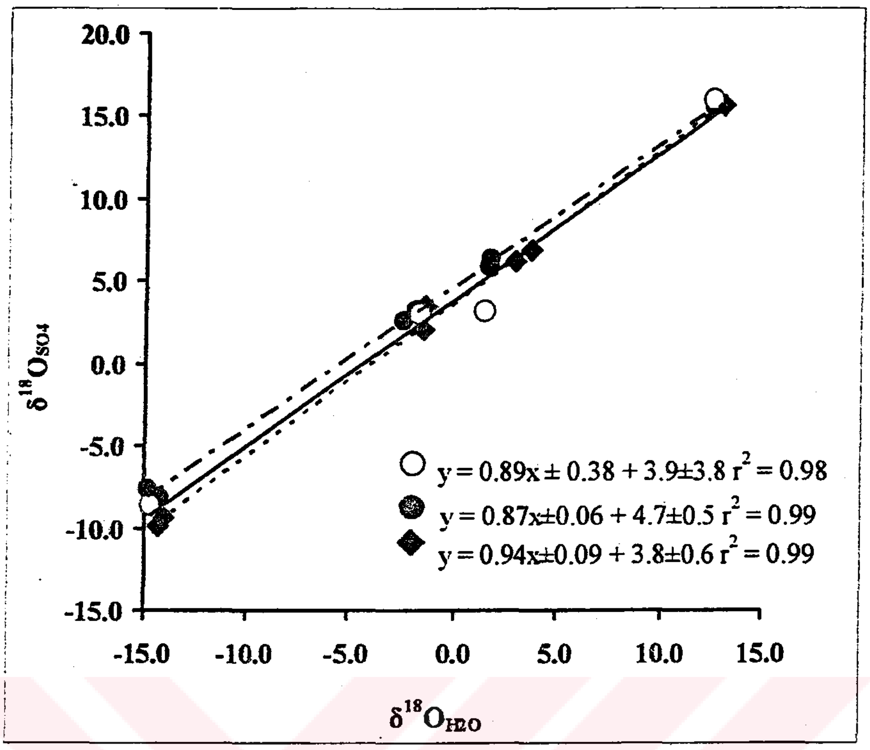

Figure 2.6 Relationship of the $\delta^{18}O$ of the SO_4 produced during aerobic pyrite oxidation experiments relative to the $\delta^{18}O$ of the experimental H_2O. Abiotic-control experiments (pH 2.8, 44 days), ○. Short term bacterial experiments (pH 2.8, 20 days), ●. Long term bacterial experiments (pH 2.1, 44 days), ◆

The standard deviations for the slope and y intercept were small, respective values for the biotic experiments were ±0.2 and ± 1.1 and ± 0.02 and ± 0.2 for the abiotic control experiments. The determination of the kinetic oxygen isotope fractionation effect between sulfate and water ($\Delta^{18}O_{SO4-H2O}$) from the anaerobic experiments was straightforward. Because all oxygen atoms to sulfate are derived from water, the y-intercept obtained from the linear relationship between $\delta^{18}O_{SO4}$ and $\delta^{18}O_{H2O}$ approximates the kinetic oxygen isotope fractionation between sulfate and water. The fractionation was determined as 4.2 ‰ and 3.5 ‰ for the biotic and abiotic experiments, respectively (Table 2.5). In general, these values are in good agreement with those estimated from the aerobic experiments. These results suggest that both the biotic and abiotic systems fractionate the oxygen isotopes similarly. Therefore the $\delta^{18}O_{SO4}$ values produced biotically and abiotically under anaerobic conditions by biotic and abiotic reactions may reflect the same $\delta^{18}O_{SO4}$ value.

Table 2.4 Oxygen and sulfur isotope composition of sulfate from bacterial and abiotic anaerobic pyrite oxidation experiments

Biological	$\delta^{18}O_{H2Oinitial}$ (‰)	$\delta^{18}O_{H2Ofinal}$ (‰)	$\delta^{18}O_{SO4}$ (‰)	$\delta^{34}S_{SO4}$ [a] (‰)
	-15.4	-14.0	-9.2	1.6
	-15.4	-15.4	-11.1	1.6
	-15.4	-15.3	-11.3	1.7
	-3.2	-4.9	-0.2	1.6
	3.2	2.2	6.1	1.0
				Avg. 1.5
Abiotic	-15.4	-15.4	-11.6	1.6
	-15.4	-15.4	-11.4	1.7
	-3.2	-4.2	-0.6	1.7
	-3.4	-5.1	-1.7	1.5
	3.4	2.7	6.2	1.5
				Avg. 1.4

[a] $\delta^{34}S_{SO4}$ of pyrite used in experiments was 2.3±0.5 ‰

The $\delta^{34}S_{SO4}$ values from the anaerobic experiments showed significant sulfur isotope fractionation (~-1 ‰) compared to aerobic experiments (~0 per mil). This fractionation was observed in both the biotic and abiotic –control experiments (Table 2.4).

2.3.5 Natural sulfate samples

Chemistry, $\delta^{34}S_{SO4}$ and $\delta^{18}O_{SO4}$ values for waters collected from the Argo Tunnel and QHill AMD sites are reported in Table 6. The range of pH measured was 2.3-3.0.

Sulfate concentrations varied from ~300 mg to 4000 mg at QHill and from 2700 mg to 3800 mg at Argo Tunnel. Fe (III) aq concentration is always higher than Fe (II) aq at both sites. The highest $\delta^{18}O_{SO4}$ values were observed during winter and spring times at both sites (Table 2.6). The range of $\Delta^{18}O_{SO4\text{-}H2O}$ is 3.5-8 ‰ for QHill and 4.5-6.8 ‰ for Argo Tunnel. The larger values of $\Delta^{18}O_{SO4\text{-}H2O}$ are consistent with the kinetic isotopic effects observed in the aerobic short-term biological experiments ($\Delta_{SO4-H2O}$ = 5.3‰) (Table 2.5).

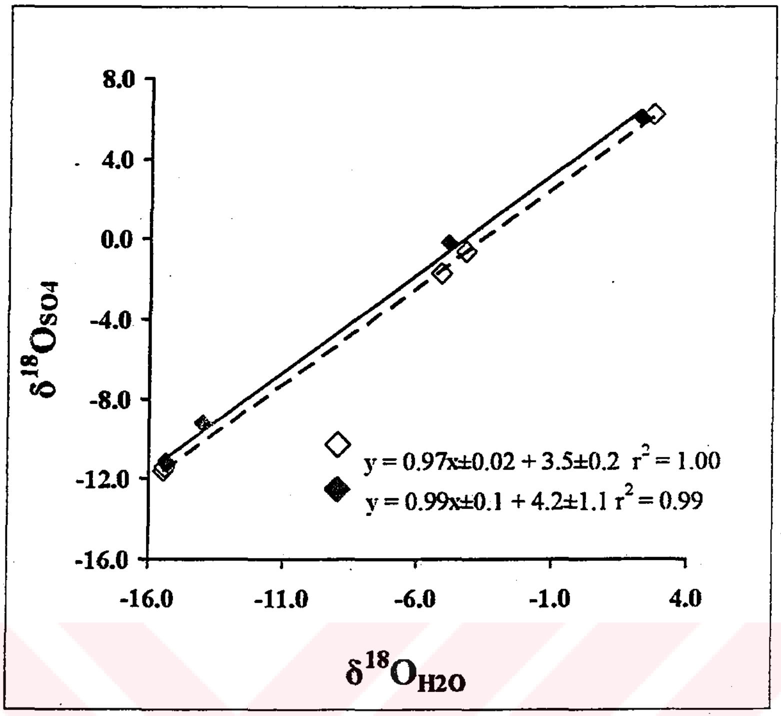

Figure 2.7 Relationship of the $\delta^{18}O$ of the SO_4 produced during anaerobic experiments (pH: ~2 35 days) relative to the $\delta^{18}O$ of the experimental H_2O. Bacterial experiments, ◆. Abiotic experiments, ◇

Based on the kinetic oxygen isotopic effect between SO_4 and O_2 and SO_4 and H_2O determined from the laboratory experiments (Table 2.5) and measured $\delta^{18}O_{SO4}$ values from the field sites, the percentage of water-oxygen incorporated into sulfate was estimated to vary from 88- 117 %. These results indicate that the oxygen isotope composition of sulfate is largely controlled by the isotopic composition of water.

The $\delta^{34}S_{SO4}$ values varied from 0 to -1.4 ‰ at the QHill site and -0.5 to -2.3 ‰ at Argo Tunnel. The higher Fe concentration compared to other metals at QHill may suggest that pyrite is the main sulfur source for sulfate.

The $\delta^{34}S$ values of five pyrite sample from Quartz Hill were 0.72±0.1 ‰ and -1.2±0.1‰ for Argo Tunnel (n=3)

Table 2.5 Summary of oxygen isotope fractionation during aerobic and anaerobic pyrite oxidation experiments.

Sample	% oxygen from H_2O[a]	Isotopic Fractionation Δ_{SO4-O2}[b]	Δ_{SO4-O2}[e]	$\Delta_{SO4-H2O}$	$\Delta_{SO4-H2O}$[f]	References
Aerobic Exps.						
			-22.0[g]			Mandernack et al[g].,
Short Term Biotic	87	-20.8	-11.4[e]	5.3[c]		Taylor et al[e]., 1984b
			-4.3[e]			Taylor et al[e]., 1984b,
Abiotic	89	-29.7	-8.7[e]	3.2[c]	0.0[f]	Lloyd, [ef] 1968
Long Term Biotic	94	-21.0		3.8		
Anaerobic Exps.						
Biotic	99	n.a		4.2[d]		
Abiotic	97	n.a		3.5[d]	2.6[f] 4.1[f]	Van everdingen[f] et al., 1988
						Taylor[f] et al., 1984b,

% estimated from linear regressions between SO_4 and H_2O. see figures 2.6, 2.7
[b] $\Delta_{SO4-O2} = (\delta^{18}O_{SO4-O2})$.(measured $\delta^{18}O_{O2}$): $\delta^{18}O_{O2}$=~21 ‰ and 29.7 ‰ for short term biotic and abiotic, respectively.
[c] calculated by least squares and matrix analysis based on % oxygen value from linear regression.
[d] obtained from the intercept calculated from linear regressions, see figure 2.7
[e,f]. previous studies see references
[g]. for Mn^{2+} oxidation reported by Mandernack et al., 1995.

2.4 Discussion

2.4.1 Pyrite oxidation

Sulfate Production Rates (SPR) from my experiments can be used to estimate the rates of pyrite oxidation under aerobic and anaerobic conditions. Although these estimates carry some uncertainty because other sulfur species, such as elemental sulfur, could also form in the system as products (Schippers, et al., 1999,1996). However, Schippers et al., (1996) reported less than 1 % of the total sulfur was elemental sulfur with pure cultures of *A. ferrooxidans* grown under aerobic conditions. It would be expected that under aerobic conditions, pyrite can be oxidized by $Fe(III)_{aq}$ and O_2. Since bacteria would catalyze oxidation of Fe(II) to Fe(III) and in turn Fe(III) oxidizes pyrite, sulfate production rate was higher compared to aerobic abiotic control experiments. Although both Fe(III) and O_2 may also contribute to oxidation of pyrite in the abiotic experiments, pyrite oxidation by .ferric iron was probably insignificant since chemical oxidation of Fe (II) is very slow at pH <3. Although both Fe(III) and O_2 may also contribute to oxidation of pyrite in the abiotic experiments, pyrite oxidation by ferric iron was probably insignificant since chemical oxidation of Fe (II) is very slow at pH <3. Therefore, aerobic abiotic reactions showed the lowest SPR (44 days-0.87×10^{-3} mg/FeS_2-day) of all the pyrite oxidation experiments and may represent the lower limit for SPR at pH < 3 (Table 2.1).

At low pH pyrite oxidation appears to be primarily controlled by biological reactions. Sulfate production rate is generally similar in the anaerobic biotic and abiotic experiments (Fig. 2.5, Table 2.2), suggesting that chemical oxidation of pyrite by ferric iron dominated in both. The sulfate production rate from the anaerobic experiments is lower than the aerobic biotic but higher than the aerobic abiotic control experiments.

The decreasing trend in the rate of sulfate production under anaerobic conditions could be related to formation of other non-sulfate sulfur species such as elemental sulfur. Based on the $Fe(II)_{aq}$ concentration and the stoichiometry of the reaction 2, the concentration of sulfate was calculated and compared to sulfate concentrations measured directly by IC (Table 2.2).

Table 2.6 Isotopic, chemical data for field samples

Sample /date	pH	T (°C)	SO4 mg/L	$\delta^{18}O_{SO4}$	$\delta^{18}O_{H2O}$	$\Delta^{18}O_{(SO4-H2O)}$	% H2O[a] Aerobic Biotic	% H2O[a] Aerobic Abiotic	% H2O[b] Anaerobic Biotic	% H2O[b] Anaerobic Abiotic	$\delta^{34}S_{SO4}$	$\Delta^{34}S_{(SO4-FeS2)}$	Fe_{tot} mg/L	Fe(II) mg/L	Fe(III) mg/L
Argo Tunnel AMD sites, Colorado															
Summer															
8.11.02	n.d.	n.d.	n.d.	-10.6	-15.9	5.3	100	68	96	85	-0.5	-0.6	n.d.	n.d.	n.d.
8.20.02	n.d.	21.0	n.d.	-10.8	-16.0	5.2	102	70	97	87	-1.6	-1.7	n.d.	n.d.	n.d.
6.29.03	2.5	18.0	2688	-17.4	-15.4	-2.0	287	187	165	146	-1.2	-1.3	134	23	111
7.28.03	2.5	18.1	2675	-16.4	-15.6	-0.8	249	165	153	135	-1.5	-1.6	214	61	153
Winter															
12.03.02	n.d.	n.d.	n.d.	-9.2	-15.7	6.5	71	48	85	75	-1.9	-2.0	n.d.	n.d.	n.d.
1.19.03	2.8	17.0	n.d.	-9.7	-15.4	5.7	90	58	92	81	-1.9	-2.0	172	44	128
Spring															
04.11.03	2.9	n.d.	3800	-10.5	-15.2	4.7	116	74	101	90	n.d.	n.d.	618	41	127
05.29.03	2.8	17.4	n.d.	-9.6	-14.4	4.8	117	68	101	88	-2.3	-2.4	187	64	123

Quartz-Hill, $\delta^{34}S_{FeS2}$ 0.7±0.2‰, average of five pyrites isotopic composition.
Argo Tunnel, $\delta^{34}S_{FeS2}$ -0.1±0.2‰, average of four pyrites isotopic composition.
[a], estimation of percent of water-oxygen incorporated into sulfate based on oxygen isotope fractionation calculated from aerobic bacterial &abiotic experiments.
[b], estimation of percent of water-oxygen incorporated into sulfate based on oxygen isotope fractionation calculated from anaerobic bacterial &abiotic experiments.

Table 2.6 Isotopic, chemical data for field samples (continue from Table 2.6)

Sample/date	pH	T (oC)	SO4 mg/L	$\delta^{18}O_{SO4}$	$\delta^{18}O_{H2O}$	$\Delta^{18}O$ $_{(SO4-H2O)}$	% $_{H2O}$ [a] Aerobic Biotic	Abiotic	% $_{H2O}$ [b] Anaerobic Biotic	Abiotic	$\delta^{34}S_{SO4}$	$\Delta^{34}S$ $_{(SO4-FeS2)}$	Fe_t (mg/L)	Fe(II mg/L	Fe(III) mg/L
Quartz-Hill AMD sites, Colorado															
Summer															
7.12.00	2.9	17.5	298	n.d.	n.d.	n.d.	n.d.	n.d.	n.d.	n.d.	n.d.	n.d.	499	10	490
7.21.00	3.1	24.5	311	n.d.	n.d.	n.d.	n.d.	n.d.	n.d.	n.d.	n.d.	n.d.	463	24	440
8.02.00	3.1	24.5	336	n.d.	n.d.	n.d.	n.d.	n.d.	n.d.	n.d.	n.d.	n.d.	481	22	456
8.16.00	7.4	16.0	420	n.d.	n.d.	n.d.	n.d.	n.d.	n.d.	n.d.	n.d.	n.d.	440	9.2	431
9.22.00	2.6	9.4	396	n.d.	n.d.	n.d.	n.d.	n.d.	n.d.	n.d.	n.d.	n.d.	396	5.0	391
8.27.01	2.6	17.3	2390	-10.6	-15.7	5.1	101	70	98	87	0.0	-0.7	610	70	540
8.11.02			2454	-11.1	-15.3	4.2	108	83	106	94	-0.1	-0.8	n.d.	n.d.	n.d.
7.20.02	2.6	24.8	2380	-10.6	-15.3	4.7	104	75	98	87	-0.3	-1.0	960	242	718
6.02.02	2.5		n.d.	-9.0	-14.7	5.7	97	53	92	80	0.1	-0.6			
6.29.03	2.5		n.d.	-17.7	-15.2	-2.5	162	198	171	151	0.2	-0.5	116	224	941
7.28.03	2.6		3450	-17.2	-15.0	-2.2					0.5	-0.2	148	182	1298
Fall															
9.12.01	2.3	21.4	3463	-10.2	-15.7	5.5	98	63	95	84	0.5	-0.2	910	60	850
10.26.01	2.5	14.1	2722	-11.7	-15.6	3.9	110	88	97	109	0.0	-0.7	440	250	190
10.13.02	2.4		2530	-11.7	-15.6	3.9	110	88	97	109	0.2	-0.5	n.d.	n.d.	n.d.
Winter															
12.03.02	2.5		3890	-10.3	-15.4	5.1	101	68	87	98	-0.9	-1.6	n.d.	n.d.	n.d.
1.19.03	2.6		3760	-9.0	-15.4	6.4	91	47	76	86	-1.0	-1.7	752	122	630
Spring															
4.14.01	n.d.		3393	n.d.	n.d.	n.d.	n.d.	n.d.	n.d.	n.d.	n.d.	n.d.	n.d.	n.d.	n.d.
4.20.01	n.d.		3180	n.d.	n.d.	n.d.	n.d.	n.d.	n.d.	n.d.	n.d.	n.d.	438	6.2	431
4.13.02	2.8		2780	-10.3	-16.9	6.6	90	55	77	86	0.2	-0.5	395	110	285
4.30.02	n.d.		n.d.	-11.9	-15.4	3.5	114	95	100	113	0.7	-0.0	637	137	500
5.29.03	2.6		3450	-7.1	-15.1	8.0	78	16	61	70	-1.4	-2.1	1360	226	1134

The difference in the measured and estimated concentrations of sulfate for the anaerobic experiments indicated that ~10 % of the pyritic sulfur consisted of a different, non-sulfate sulfur species. This determination appears to be consistent with results of Schippers et al. (1999) who reported the elemental sulfur formation during chemical oxidation of pyrite by Fe(III)aq but not in the experiments carried out with pure cultures of *A. ferrooxidans* under atmospheric conditions. This suggests that elemental sulfur most likely occur during chemical oxidation of pyrite but not during biological oxidation. These results may also explain why there was ~ -1 ‰ sulfur isotope fractionation during anaerobic oxidation but not during aerobic biological oxidation. Consequently, the rate of pyrite oxidation under anaerobic conditions can be underestimated based on the sulfate production rate, but this does not invalidate comparisons between the various experiments.

2.4.2 Reaction mechanisms of pyrite oxidation under anaerobic conditions

Reaction 2 (see page #7) should be the sole reaction mechanism for anaerobic pyrite oxidation since ferric iron is the only oxidizing agent. In reaction 2, all oxygen atoms of sulfate are derived from water (100 %) and the oxygen source is consistent with the electron transfer pathways (Moses et al., 1987, 1991). The anaerobic biotic and abiotic experiments produced very similar $\delta^{18}O_{SO4}$ values that indeed reflect the 100 % water-oxygen (Fig. 2.7). The interaction between pyrite and water occurs through the formation of an aqua-Fe(III) complex (Moses et al., 1991). In this model, the aqua-Fe(III) complex can react with pyrite by transferring a hydroxyl radical from its water molecules to the sulfur side of pyrite. This explains why water is the oxygen source for sulfate during oxidation of pyrite by Fe (III) complexes and is consistent with my experimental results.

The kinetic oxygen isotope fractionation ($\Delta^{18}O_{SO4-H2O}$) is estimated to be 4.2 ‰ and 3.5 ‰ for the biotic and abiotic experiments, respectively (Table 2.5). These results are consistent with the range measured by previous studies (0-4.1‰) (see Table 2.5) (Lloyd, 1968, Van Everdingen, 1985, Taylor, et al., 1984,).

Although it is reported that *A. ferrooxidans* is able to grow under anaerobic conditions by using Fe (III) as an electron acceptor (Suzuki et al., 1990; Pronk et al., 1990; Sugio et al., 1985), the similar $\delta^{18}O_{SO4}$ values from the biotic and abiotic experiments may suggest that abiotic oxidation of pyrite by $Fe(III)_{aq}$ was rate controlling and faster when compared to bacterial reactions. Therefore, bacteria may not be able to compete with Fe(III) driven abiotic oxidation. The similar kinetic oxygen isotope fractionation effects between the biological and abiotic control experiments are consistent with this idea.

Kinetic oxygen isotope fractionation effect (~4‰) between sulfate and water obtained from the anaerobic experiments show the similarity to that from the aerobic long-term biological experiments (3.8 ‰) (Table 2.5). When the similar percentage of water–oxygen incorporation into sulfate during both experiments are considered, this fractionation effect may represent pyrite oxidation which produced sulfate that has ~100 % water-oxygen at pH ~2. Water-oxygen incorporation into sulfate is generally attributed to chemical oxidation of pyrite by Fe(III)aq (reaction 2) which required acidic conditions (pH <3).

Because the solubility of Fe (III)-oxides is very low and the concentration of soluble Fe (III) could be too low for FeS_2 oxidation at higher pH values, pyrite oxidation by Fe(III) can be dominant in acidic environments (pH<3). Schippers and Jorgensen (2001) investigated pyrite and iron monosulfides (FeS) oxidation in marine sediments by using NO_3^-, Fe(III) oxide and MnO_2 as electron acceptor. In chemical experiments, they reported that FeS_2 and FeS was oxidized by MnO_2 but not with NO_3^- and Fe(III) oxide. In a different study, they carried out tracer experiments with labeled $^{55}FeS_2$ by using NO_3^{2-}, Fe(III) oxide and MnO_2 as electron acceptor to investigate FeS_2 and FeS oxidation in anoxic marine sediments (Schippers and Jorgensen, 2002).

They showed that in experiments with anoxic sediments slurries, dissolution of tracer–marked $^{55}FeS_2$ occurred only with MnO_2, consistent with the results of the earlier study. They concluded that MnO_2 and O_2, but not NO_3^- and Fe(III) oxide are chemical oxidants for FeS_2 and FeS. Although their experimental studies contradict with my study here, it suggest that pyrite oxidation by Fe(III) is likely dominant at low pH conditions. Therefore, ~ 4‰ kinetic oxygen isotope fractionation effect between sulfate and water estimated in this study could be a good indicative of chemical pyrite oxidation by Fe(III) for terrestrial environment at pH <3.

2.4.3 Reaction mechanisms of pyrite oxidation under aerobic conditions

Aerobic experiments may give an opportunity to reveal the role and the relative contribution of O_2 into sulfate during pyrite oxidation.

Although reaction 1 and 2 (see page 7) are commonly used to describe pyrite oxidation, the real oxidation mechanisms are much more complex due to the high number of electron transfers to produce sulfate (Seal, 2003; Rimstidt et al., 2003).

Both the biotic and the abiotic experiments showed that most of the sulfate oxygen is derived from water. The range of water-oxygen (87-95%) incorporated into sulfate in my experiments are consistent with previous studies (Taylor et al., 1984ab; Krouse et al., 1991, Van Stempvoort, 1994). Based on Fig. 2.6 it appears that SO_4 produced via bacterial or abiotic reactions has indistinguishable $\delta^{18}O$ values and similar percentage of water-oxygen (Table 2.3). The similar percentage of water-oxygen incorporation into sulfate between bacterial and abiotic control reactions in my experiments are consistent with aerobic submerged pyrite oxidation experiments performed by Taylor et al. (1984). Taylor et al. (1984) investigated $\delta^{18}O_{SO4}$ and $\delta^{34}S_{SO4}$ values produced during biological and abiotic pyrite oxidation at pH 2 under submerged and wet/dry conditions. They reported that in abiotic control experiments water-oxygen incorporation into sulfate was 83 % and 70-75 % for biological experiments under submerged conditions in contrast to wet/dry experiments which biologically produced sulfate enriched in ^{18}O and thus showed 50 % water-oxygen incorporation. However, my results contrast with those from wet-dry experiments of Taylor et al. (1984) where pyrite samples were periodically submerged in water and then exposed to air. In Taylor et al.'s (1984) wet-dry experiments biotic reactions produced SO_4 enriched in ^{18}O compared to abiotic reactions. They attributed the enrichment in ^{18}O to bacterial influence and more availability of O_2. The contrast between the results of Taylor et al. (1984) and my experiments may stem from different experimental conditions. Taylor et al. (1984) carried out their wet-dry experiments in a way that pyrite was periodically exposed to air and was allowed to air-dry between leaching events. However, my aerobic experiments were carried out as solutions in sealed flasks which were continuously purged with air and did not experience significant evaporation effect. The heavy $\delta^{18}O_{SO4}$ values reported by Taylor et al. (1984) could also be due to evaporation and enrichment in ^{18}O of water between the pyrite/solution boundary layer since pyrite oxidation is largely controlled by surface reaction prior to desorption of sulfur oxyanions (Alpers et al., 1994). Alternatively, it is also possible that Fe(III) oxidation was dominant in my experiments compared to their wet-dry experiments where pyrite oxidation by Fe(III) may have been limited by reduced contact between pyrite and the solution. Because sulfate produced by Fe(III) oxidation derives all of its oxygen atoms from water, which is less enriched in ^{18}O (<0 ‰) relative to O_2 (23.5 ‰), $\delta^{18}O_{SO4}$ values from Fe(III) oxidation will be more depleted in ^{18}O relative to sulfate that derives oxygen atoms from O_2.

During the short-term (20 days) and the long-termexperiments (45 days), percent of oxygen atoms incorporated into sulfate from water and O_2 indicate that neither reaction 1 nor 2 represent the stoichiometry of pyrite oxidation under O_2 saturated conditions (Fig. 2.3). Also, a larger incorporation of oxygen from water into sulfate was observed with increasing extent of the reaction as inferred from the long-termexperiments (Fig.2.6, Table 2.3). Based on the percent of oxygen incorporated into sulfate during the short-term biotic and abiotic aerobic experiments, the reaction pathway presented by Schippers et al., (1996) is proposed here for pyrite oxidation under O_2 saturated conditions at pH 2.7 (Fig. 2.8). According to this pathway, two steps (9 and 11) produce sulfate (Schippers et al., 1996).

$$2FeS_2 + 12Fe(H_2O)_6^{+3} + 18H_2O \rightarrow 2S_2\cancel{O}_3^{-2} + 14Fe(H_2O)_6^{+2} + 12H^+ \qquad (2.7)$$

$$2S_2\cancel{O}_3^{-2} + 2Fe^{3+} \rightarrow S_4\cancel{O}_6^{-2} + 2Fe^{2+} \qquad (2.8)$$

$$S_4\cancel{O}_6^{-2} + H_2O \rightarrow SO_4^{-2} + S_3\cancel{O}_3^{-2} + 2H^+ \qquad (2.9)$$

$$S_3\cancel{O}_3^{-2} \rightarrow 0.25S_8 + S\cancel{O}_3^{-} \qquad (2.10)$$

$$S\cancel{O}_3^{-2} + 1/2O^*_2 \rightarrow SO^*{}_4^{-2} \qquad (2.11)$$

$$2FeS_2 + 12Fe(H_2O)_6^{3+} + 19H_2O + 2Fe^{3-} + 1/2O_2 \rightarrow 14Fe(H_2O)_6^{2+} + 2Fe^{2-} + 14H^+ + 2SO_4^{2-} + 0.25S_8 \qquad (2.12)$$

These results are in good agreement with my short-term experiments (Fig. 2.6) and suggest that pyrite may have been oxidized according to the stoichiometry of this proposed pathway (reaction 12). When the net stoichiometry (reaction 10) is taken into account, 87.5 % of sulfate oxygen comes from water and correspondingly 12.5 % from O_2. Sulfate produced by reaction 9 derives all oxygen atoms from water (100 %) whereas sulfate from reaction 11 derives 75 % of oxygen atoms from water and 25 % from O_2.

In the proposed pathway, the first intermediate oxidation product is thiosulfate ($S_2O_3^{2-}$) (reaction 7) (Moses, et al., 1987; Xu et al., 1995; Schippers, et al., 1999). The pyrite surface catalyzes the oxidation of thiosulfate to tetrathionate (reaction 8) (Xu et al., 1995; Schippers et al., 1999). Tetrathionate is then hydrolyzed to form sulfate and disulfane-monosulfonic acid (reaction 9).

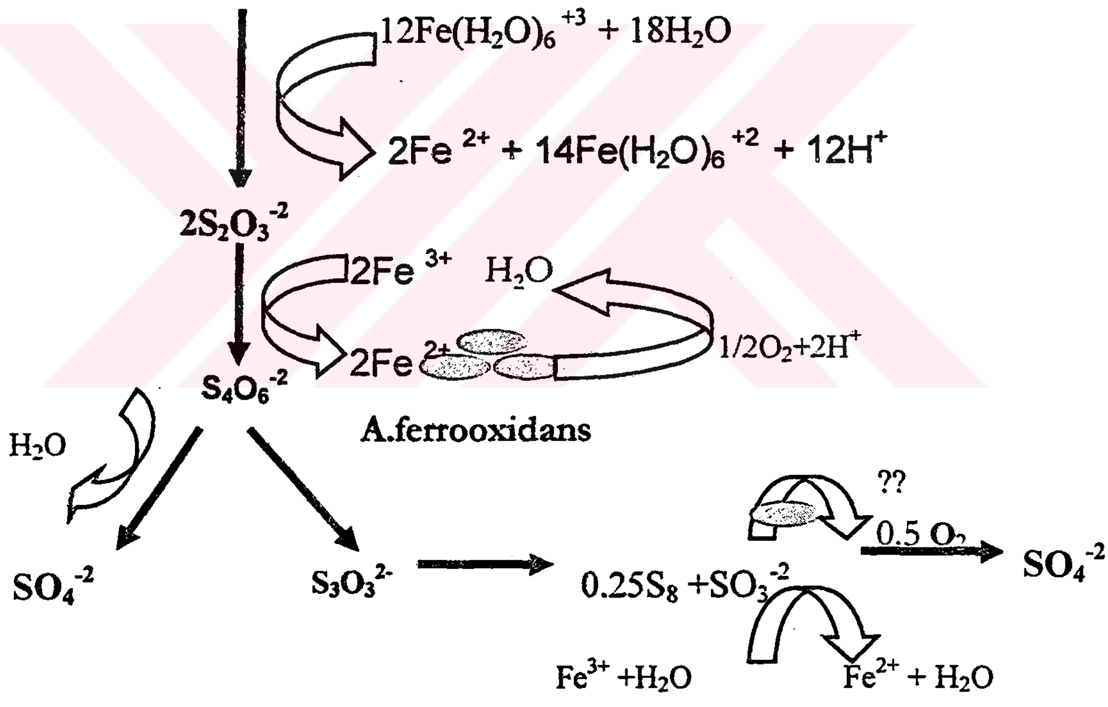

Figure.2.8 Proposed pyrite oxidation pathways for the short-term biological (pH 2.7) experiments under aerated conditions, as originally proposed by A. Schippers et al., (1996).

Different reactions could start from disulfane-monosulfonic acids which finally give rise to elemental sulfur, thiosulfate and the other sulfoxyanoins at pH <3 (Schippers, et al., 1996, 1999; Descostes, et al., 2004). Thiosulfate is then re-oxidized to tetrathionate as in reaction 9. Sulfite is unstable in the acidic solution and is chemically oxidized to sulfate by incorporating O_2 into sulfate (reaction 11).

Because Fe(III) is still the main oxidizing agent for pyrite in the proposed pathway and the chemical oxidation of $Fe(II)_{aq}$ to $Fe(III)_{aq}$ is very slow at pH <3, the dominant role of the bacteria is likely to oxidize ferrous iron to ferric iron and thus catalyze reaction 3. The similar kinetic oxygen isotope fractionation effect ($\Delta^{18}O_{SO4-H2O}$) and the similar $\delta^{18}O_{SO4}$ values between aerobic abiotic and biotic experiments may suggest that the proposed reaction mechanism (reactions 7 – 11) also applies to abiotic pyrite oxidation (Table 2.3, Fig.2.6). This is in agreement with previous studies that indicate ferric iron is the dominant oxidizing agent for abiotic and biotic experiments at pH <3 (Taylor et al., 1984; Moses, et al., 1984, Schippers et al., 1996, 1999).

2.4.4 Changes in δ_{SO4} as a result of prolonged incubation and/or lower pH

The $\delta^{18}O_{SO4}$ values from the lower pH long-termexperiments at 45 days showed larger oxygen incorporation from water into sulfate (94 %) compared to the short-term experiments and do not follow the stoichiometry of the proposed pathway. There are several possible explanations for increasing water-oxygen incorporation into sulfate during long-termexperiments: 1) slower rate of reaction 11 relative to reaction 9 with decreasing pH, 2) increased oxygen isotopic exchange between a sulfite intermediate and H_2O, and 3) oxidation by Fe(III) was dominant due to increasing Fe(III) concentration where reaction 2 became dominant.

The following figure summarizes the main reaction steps of the proposed pathway. Sulfate can be produced by sulfite oxidation (step 11) and hydrolysis of tetrathionate (step 9). Therefore, the final $^{18}O_{SO4}$ values could depend on the competing rate of these two steps since each step has a different oxygen source. If at lower pH the hydrolysis of tetrathionate is dominant over sulfite oxidation for sulfate production, then $^{18}O_{SO4}$ values should reflect more incorporation of water-oxygen. Disulfane-monosulfonic ($S_3O_3^{2-}$) which is also produced during reaction 9 decomposes elemental sulfur and sulfite (reaction 10). Because intermediate sulfoxyanoins and sulfite are more common at higher pH values (Goldhaber, 1983), the relative contribution of sulfite oxidation to sulfate may decrease with decreasing pH. This would result in less O_2 incorporation into sulfate and $\Delta^{18}O_{SO4-H2O}$ values should decrease with decreasing pH.

$$\begin{array}{ccccccccc}
 & 7 & & 8 & & 9\,\&\,10 & & 11 & \\
\mathrm{FeS_2} & \rightarrow & \mathrm{S_2O_3^{-2}} & \rightarrow & \mathrm{S_4O_6^{-2}} & \rightarrow & \mathrm{SO_3^{-2}} & \rightarrow & \mathrm{SO_4^{-2}} \\
 & & & & \downarrow\;| & & \downarrow\uparrow & & || \\
 & & & & \mathrm{SO_4^{2-}} & & & & \mathrm{H_2O}
\end{array} \qquad (2.13)$$

$\Delta^{18}O_{SO4-H2O}$ values of 5.3 ‰ and 3.8 ‰ were obtained for the short and long-termexperiments, respectively. The smaller $\Delta^{18}O_{SO4-H2O}$ value during the long-termlower pH experiments may have resulted from less sulfite oxidation and is in general agreement with previous studies that reported higher O_2 incorporation into sulfate during sulfide oxidation at neutral pH (Lloyd, 1968). Although my experimental conditions were different than Lloyd (1968), an increase in O_2 incorporation into sulfate with increasing pH is consistent with my results.

Alternatively, the variations in oxygen contribution by water may also occur because of several different pathways of sulfite oxidation, which may involve disulfate ($S_2O_7^{2-}$) or other intermediates (Chang, 1987). These sulfo-oxyanion intermediates could undergo oxygen isotopic exchange with H_2O and thus increase the percentage of water-oxygen incorporated into sulfate. The oxygen isotope exchange between sulfite and water was demonstrated to be on the order of nanoseconds at pH <3 by previous studies (Lloyd, 1968; Pearson et al. 1980; Holt et al., 1981). Therefore, if sulfite is present in the system, oxygen isotope exchange between sulfite and water may occur. Llyod (1968) estimated the time required for equilibration of ocean water and sulfate–oxygen exchange (pH 8.2, 4 °C) to be on the order of 250,000 yr based on laboratory experiments at pH 7 and 25 °C. Further, Chiba and Sakai (1985) extrapolated their laboratory studies for conditions of 100 to 300 °C and pH 2 to 7 and reported that half–life for ocean water-sulfate exchange is 10^9 year. Chiba and Sakai's results are in agreement with the earlier studies by Hoering and Kennedy (1957) who reported experimentally water-sulfate exchange at low pH (<0). Based on these studies, it appears that in most Earth surface including the experimental conditions of this study, the oxygen exchange between water and sulfate is extremely slow. Therefore, under the experimental conditions of the current study, this process can not be the reason for larger water–oxygen incorporation into sulfate.

Alternatively, Mizutani et al. (1969,1973) and Fritz, et al. (1973) indicated oxygen isotope exchange between sulfate and water proceeds through enzyme-bound intermediates during the bacterial reduction of sulfate. Similar oxygen isotope exchange processes may also occur during sulfide oxidation.

The incorporation of oxygen into sulfate exclusively from water is generally attributed to the ferric iron oxidation pathway by previous studies (Taylor, et al., 1984 a,b). Reaction 2 (page 7) represents the stoichiometry of this reaction and indicates 100 % water-oxygen incorporation into sulfate. Since long-termexperiments showed ~94 % water-oxygen incorporation into sulfate, pyrite oxidation by ferric iron may have become increasingly dominant during the long-termpyrite experiments. Almost identical oxygen isotope fractionation between sulfate and water ($\Delta^{18}O_{(SO4-H2O)}$) was measured for the aerobic long-term(3.8 ‰) and anaerobic experiments (3.5 ‰), which would be consistent with ferric iron as the sole or dominant oxidant.

2.4.5 Oxygen isotope fractionation

Using the calculated values for the percentage of oxygen contribution by O_2 and H_2O, fractionation with respect to both O_2 and H_2O were made for the aerobic biotic and abiotic experiments by a least squares and matrix analysis (Table 2.5).The kinetic oxygen isotope fractionation effect between sulfate and O_2 ($\Delta^{18}O_{SO4-O2}$) is estimated as ~-21 ‰ during the short and long-termaerobic biological experiments. This compares to an estimate of -29.7 ‰ for the abiotic experiment, values of -10 to -29 ‰ for biological respiration (Guy et al., 1987; Kroopnick and Craig, 1976; Lane and Dole, 1956), -22.0 ‰ for Mn(II) oxidation to Mn(IV) oxides (Mandernack et al., 1995) and -11.4 ‰ previously measured for bacterial oxidation of pyrite (Taylor, et al., 1984). All of these previous studies and my own here indicate that $^{16}O_2$ is favored when it oxidizes organics, sulfide, and Mn(II). The similarity in $\Delta^{18}O_{SO4-O2}$ and $\Delta^{18}O_{Mn(IV)oxide-O2}$ suggest that the reaction mechanism of pyrite oxidation and Mn(II) oxidation may be the same.

Pyrite oxidation is generally considered to be initiated by reaction with molecular oxygen (Sasaki, 1994; Nesbitt and Muir, 1994; Sasaki et al., 1995, Moses and Herman, 1991; Sato, 1992). Molecular oxygen is reduced through the oxidation of

$Fe(II)(H_2O)_6$ complexes on the surface of pyrite. Fe(III)aq form and oxidize pyrite by producing thiosulfate (Luther, 1987; Descostes et al., 2001; Rimstidt and Vaughan, 2003; Moses et al. 1987; Moses and Herman,1991). Because there is not a direct attack of sulfur atoms by O_2 during formation of thiosulfate, it is unlikely that oxygen atoms from O_2 are incorporated into thiosulfate. Therefore, molecular oxygen incorporation into sulfate may occur during subsequent oxidation of thiosulfate to sulfate. Because thiosulfate is commonly oxidized to sulfite prior to oxidation to sulfate by both biotic and abiotic pathways (Williamson and Rimstidt, 1992; Suzuki et al., 1994), O_2 incorporation into sulfate may occur during sulfite oxidation as suggested in the proposed pyrite oxidation pathway (Fig. 2.8). Therefore, oxygen isotope fractionation between sulfate and O_2 may have occurred at this stage. Because the concentration of sulfite is pH dependent (e.g. increase at higher pH, the $\delta^{18}O_{SO4}$ values would show less O_2 incorporation into sulfate with decreasing pH (Goldhaber, 1983; McKibben and Barnes, 1986; Moses et al., 1987; Llyod, 1968). My aerobic long-termlower pH experiments is consistent with this, indicating that O_2 incorporation into sulfate may have been controlled by sulfite oxidation and oxygen isotope fractionation may have occurred at this step. Although *A. ferrooxidans* has ability to oxidize sulfite (Kelly, 1982), the similar percent O_2 incorporation into sulfate and the similar kinetic oxygen isotope fractionation effect between sulfate and O_2 ($\Delta^{18}O_{SO4-O2}$) during both biotic and abiotic experiments indicate that sulfite oxidation to sulfate may have been mediated by chemical reactions rather than biological reactions. This determination is also consistent with the result of Krouse's et al. (1991) who indicated sulfite oxidation by O_2 during both biological and abiotic sulfite oxidation.

The oxygen isotope fractionation effect between sulfate and water estimated from both aerobic and anaerobic experiments display resemblance (Table 2.5). The similar $\Delta^{18}O_{SO4-H2O}$ values between aerobic and anaerobic experiments suggest that oxygen isotopes may have been fractionated by the same mechanism during oxidation of pyrite under both experimental conditions.

Water-oxygen incorporation into sulfate occurs during oxidation of pyrite by aqua-Fe (III) complexes (Moses et al., 1987, 1991; Luther, 1987). Three primary steps are involved to the oxidation processes (Luther, 1987; Moses et al., 1987). The first step is the formation of aqua Fe(III) complexes through the oxidation of adsorbed Fe(II) by O_2 (Mckibben and Barnes, 1986; Moses et al., 1987; Singer and Stumm, 1970; Wiersma and Rimstidt, 1984). The next step involves the binding of $Fe(III)(H_2O)_6$ complexes to the pyrite surface. The remaining step is the electron transfer between sulfur side of pyrite and aqua Fe(III) complexes, involving removing of an oxygen atoms from water to sulfur side of pyrite (Luther, 1987, Rimstidt, 2003). Based on these processes, it could be predicted that there may be two steps which cause oxygen isotope fractionation between sulfate and water. First step is binding of $Fe(III)(H_2O)_6{}^{3+}$ complexes to the pyrite surface and the second one is during transfer of an oxygen atom from hydroxyl radical from aqua-Fe (III) complexes to the sulfur side of pyrite. The latter determination is consistent with the results of Biegler and Swift (1979) who reported that pyrite oxidation is controlled by the attachment of an oxygen atom from water to a sulfur atom at the mineral surface.

2.4.6 Sulfur isotope fractionation associated with aerobic and anaerobic pyrite oxidation

In general, sulfur isotope effect associated with solid phase metal sulfide oxidation is insignificant compared to aqueous phase of sulfide oxidation (Nakai and Jensen, 1964; Taylor et al., 1984; Fry et al., 1986, McCready and Krouse, 1982). Low temperature oxidation of sulfide minerals to sulfate seems to be quantitative, unidirectional process that produces negligible sulfur-isotope fractionation; the $\delta^{34}S$ of sulfate is indistinguishable from that of the parent sulfide minerals (Gavelin et al., 1960; Field, 1966; Rye et al., 1992). Sulfur isotope fractionation during sulfide oxidation under different conditions such as bacterial catalyses (Kaplan and Rafter, 1958; Kaplan and Rittenberg, 1958; Fry et al. 1988) dissolved sulfide as a source (Sakai, 1957; Fry et al. 1986, 1988) and low (Taylor, et al. 1984b; Seal and Wandless, 1997) and high pH (Toran and Harris, 1989) have been suggested in the previous studies. The largest sulfur isotope fractionation was reported by Kaplan and Rittenberg, (1964) during oxidation of dissolved Na_2S in experiments inoculated with *T. thiooxidans*. They measured heavy sulfur isotopes in an intermediate sulfur species and attributed this fractionation to exchange between intermediate sulfur species and sulfate. Toran and Harris (1989) measured -2 to -5.5‰ fractionation for FeS_2 and ZnS oxidation experiments that inoculated with a mixture of *T. neopolitanus*, *T. intermedius*, and *T. ferrooxidans* and run at a pH of 5 to 6. -4.7 ‰ fractionation was reported by Chamber and Trudinger (1978) during oxidizing thiosulfate by *T. intermedius.* Fry et al. (1988) reported -5.2 ‰ fractionation during oxidation of Na_2S in aqueous solution at pH 11. Sulfur isotope fractionation was reported for high pH conditions seem to be related to formation of intermediate sulfoxyanoins which is controlled by pH (Goldhaber, 1983).

Low pH environments (<3) produce sulfate that show no sulfur isotope fractionation. Taylor and Wheeler (1984b) did not obtained a significant sulfur isotope fractionation between sulfide mineral and sulfate at low pH (<3). Fry et al. (1986) reported no fractionation during oxidation of thiosulfate by *T. versutus.*

The $\delta^{34}S_{SO4}$ values from the aerobic biological and abiotic-control experiments in this study closely reflect the $\delta^{34}S$ value of pyrite (Table 2.3). Lack of sulfur isotope fractionation in my aerobic experiments is consistent with the previous studies and indicates the quantitative oxidation of pyritic sulfur to sulfate under the experimental conditions. The $\delta^{34}S_{SO4}$ values from anaerobic experiments are enriched in $^{32}S \sim 1$ ‰ compared to $\delta^{34}S_{FeS2}$ (Table 2.4). This fractionation seems to be significant compared to aerobic experiments which show approximately ±0.1‰ fractionation relative to $\delta^{34}S_{FeS2}$ values. The main difference between aerobic and anaerobic experiments is the oxidizing agent and pH. $Fe(III)_{aq}$ was used as oxidizing agent and pH was ~2. It is most likely that the oxidation of pyrite by $Fe(III)_{aq}$ results in intermediate sulfur species between pyritic sulfur and sulfate (Moses, et al.,1987; Goldhaber, 1983, Schippers et al., 1996, 1999). Increasing concentration of intermediate sulfur species, possible elemental sulfur, due to the lack of bacterial activity and low pH conditions (Schippers et al. 1999, Descostes et al., 2004; McGuirre M. M. et al., 2001;) may have caused the measurable sulfur isotope fractionation under anaerobic conditions in contrast to aerobic biological experiments.

Previous studies and my own work here indicate that in addition to bacterial activity, pH of the solution which sulfide oxidation take place may be a factor whether fractionation occurs during sulfide oxidation.

2.4.7 Interpretation of natural sulfate samples

The isotopic composition of sulfate may provide usefully insights into the oxidation processes in the formation of AMD sites. However, to proper interpretation of the $\delta^{18}O_{SO4}$ values, one should need to know how each oxidation process fractionates oxygen isotopes and the interpretation of the $\delta^{18}O_{SO4}$ values without taking into account this fractionation effects may cause errors. In this study, it was possible to estimate oxygen isotope fractionation effect between sulfate and water and between sulfate and molecular oxygen under different experimental conditions (Table 2.5).

Based on isotopic mass balance (see pg. 20, equation 4), kinetic oxygen isotope fractionation from my experimental results (Table 2.5) and the $^{18}O_{SO4}$ values measured from the field, the oxygen source of sulfate was calculated. These calculations were made by using kinetic oxygen isotope fractionation effect determined under different experimental conditions such as biotic vs. abiotic, aerobic vs. anaerobic. According to these calculations, SO_4 derived large portion of oxygen from water. The percent of water-oxygen incorporated into sulfate ranges between 88 % and 100 % (Table 2.6). However, some of the samples showed an unrealistically high percent of water-oxygen incorporation into sulfate (165-287 %) as one may predict the maximum oxygen incorporation into sulfate should be 100 %. Most of the calculated data however, fall into 100 % range and provide confidence to my kinetic oxygen isotope fractionation effect used for the calculation.

The range of water-oxygen incorporated into sulfate and the sulfate-water oxygen fractionation from the field samples are similar to the range of experimentally determined (3.2 to 5.3 ‰) under aerobic and anaerobic conditions. The similarity between experimental and the field samples may indicate that natural sulfate samples may have been produced by the same reaction pathway as proposed for pyrite oxidation (Figure 2.8). Large water-oxygen incorporation into sulfate is generally attributed to oxidation of pyrite by Fe(III) (Taylor, et al., 1984:). The high Fe (III) concentration measured in the AMD water may imply that Fe(III) could be an oxidizing agent for pyrite (Table 2.6). Alternatively, as my long-term lower pH biological experiments show, the pathways for derivation from water-oxygen may be a different than the commonly reported in the literature; oxygen isotope exchange between intermediate sulfur species and water may increase the percent of oxygen atoms from water into sulfate. Whatever the real mechanism behind water-oxygen incorporation into sulfate is, my experimental results showed that the $\delta^{18}O_{SO4}$ values may reflect the $\delta^{18}O_{H2O}$ values which sulfate formed when appropriate oxygen isotope fractionation effect is applied. When the slow oxygen isotope exchange rate between sulfate and water is taken into account, $\delta^{18}O_{SO4}$ values may hold promises for paleo temperature studies.

My experimental results showed that sulfate produced during biological and abiotic pyrite oxidation exhibit the similar $\delta^{18}O_{SO4}$ values and percent of water-oxygen. The high Fe(III) and sulfate concentration in the field samples indicate the presence of bacteria as my experimental results demonstrated (Figs. 2.4a, b). However, the percent of water-oxygen incorporated into sulfate from the field samples fall into the range which is produced by both biological and abiotic pyrite oxidation reactions. These results suggest that the $^{18}O_{SO4}$ values can not be used to assess the involvement of *A. ferrooxidans* into pyrite oxidation in contrast to the previous studies which the heavy $^{18}O_{SO4}$ values were generally attributed to the indication of bacterial activity (Taylor et al., 1984; Wheeler and Taylor, 1982,1994; Krouse et al., 1991). Formation of sulfate from water enriched in ^{18}O by evaporation may be responsible for the heavy values.

Sulfate production rate from the biological experiments is significantly higher than the abiotic experiments under aerobic conditions. Because sulfate production rate can not be easily determined in a natural environment, this parameter can not be used to assess the bacterial activity during pyrite oxidation either.

The percent of molecular oxygen incorporated into sulfate vary between 10 % and 40 % and the highest values were obtained from winter and spring samples which consistent with the fact that dissolution of molecular oxygen into water would be expectedly higher during these seasons. These results indicate the significance of the environmental conditions on the $^{18}O_{SO4}$ values. The $^{34}S_{SO4}$ values from Q-hill sites shows sulfur isotope fractionation effect varied from 0 to -1.0 ‰ relative to pyrite except the winter samples. These results may suggest that the source of sulfate could be pyrite since insignificant sulfur isotope fractionation would be expected between sulfur source and sulfate (Taylor et al., 1984). However, the winter samples show larger range and this may be due to dissolution of secondary sulfate minerals during flushing. The average of sulfur isotope composition of pyrite from Argo Tunnel is -0.1± 0.2. The general trend is often larger than the expected sulfur fractionation. This may be due to the fact that pyrite may not be the only sulfur source for sulfate. Pyrite oxidation experiments conducted here indicated that bacteria controls the pyrite oxidation at low pH (<3) but the $\delta^{18}O_{SO4}$ values may not represent this. Therefore, the $\delta^{18}O_{SO4}$ values can not be used to assess the bacterial activity during pyrite oxidation in natural environments. It is also shown here that oxygen isotope exchange between water and intermediate sulfur species may occur with decreasing pH and may mask the original $^{18}O_{SO4}$ values. Therefore, geochemical condition seems to be a controlling factor whether bacterial activity can impart a unique isotope signature. In contrast to $\delta^{18}O_{SO4}$ values, high sulfate and Fe(III) concentration in sulfide mineral rich environment at low pH (<3) can be attributed to bacterial activity. Overall results indicate that a better assessment of the extend of biological involvement in oxidation processes of pyrite in any natural setting require the combination of isotopic, chemical and microbiologic data.

3. OXYGEN AND SULFUR ISOTOPES SYSTEMATIC OF SULFATE PRODUCED BACTERIAL AND ABIOTIC OXIDATION OF SPHALERITE AND ELEMENTAL SULFUR

3.1 Introduction

The oxidation chemistry of sulfide minerals and subsequent generation of acid mine drainage (AMD) has been extensively studied. In particular, pyrite has been the subject of several studies due to the fact that pyrite is the most abundant metal sulfide mineral and initiates the formation of AMD (Evangelou and Zhang, 1995; Lowson, 1982; Nordstrom, 1982; Nordstrom and Alpers, 1999; Nordstrom and Southam, 1997; Moses et al. 1987; Luther ,1987; Descostes et al. 2001). Despite the extensive studies to understand the specific chemical reactions that control the formation of AMD, there are still issues regarding the mechanism and kinetics of the oxidation process at the mineral surface and the extent of the microbial contribution to these processes. One of the main questions related to oxidative dissolution of sulfide minerals is the speciation of sulfur during oxidation. The most commonly accepted model is based on pyrite studies and according to the model; all of the oxidized sulfur is released as thiosulfate (Moses et al. 1987; Luther, G 1987). In contrast, other studies demonstrated that elemental sulfur forms at the surface of pyrite and other sulfide minerals (Turcotte, et al. 1993; McGuire et al. 2001; Sasaki, et al. 1995, 1997; Mycroft, et al. 1990; Sand et al. 2001; Schippers et al. 1999, 1996). Because most oxidation models for sulfide minerals only accounts for sulfoxy anions and do not account for insoluble sulfur species, it is important to understand the formation of elemental sulfur as an intermediate to decipher the actual oxidation mechanisms of sulfide minerals. Because elemental sulfur is insoluble under most conditions (Curutchet, et al. 1996; Garcia, et al. 1995), the amount of sulfur formed at the surface may have important implications for oxidation of sulfide minerals by controlling the passage of oxidants to the surface.

The oxidation mechanisms and the formation of oxidation products from sulfide minerals may depend on the type and composition of the mineral (Schippers et al. 1999; Nordstrom and Goutham, 1997). The first simple distinction is the oxidation state of sulfur in parent minerals between minerals such as monosulfides (sphalerite, galena, covellite, pyrrhotite) that contain S^{-2} versus disulfides (pyrite) that contain sulfur with an average oxidation state of -1 due to contribution from S (-II) and S (o). Because of the difference in oxidation state of sulfur, monosulfides (sphalerite, galena) can be oxidized by different mechanisms compared to disulfides (pyrite) (Sand et al. 2001; Schippers, et al.1999).

Sand et al. (2001) investigated oxidation pathways of monosulfides in the example of sphalerite and galena minerals and disulfides (pyrite) at pH ~ 2 in pure chemical bases. They suggested different oxidation mechanisms for each group: thiosulfate intermediates forming from disulfides and polysulfides forming from monosulfides. According to their studies, disulfides can only be degraded by an attack from an oxidant such as Fe (III) and which forms sulfate as an end-product, whereas monosulfides can also be degraded by proton attack (H^+) in addition to an oxidant. The end-product of monosulfide oxidation is elemental sulfur (~95 %) and sulfoxyanoins such as thiosulfate and sulfate. They also indicated that ferric iron was the main oxidizing agent compared to molecular oxygen.

Schippers et al. (1999, 1996) also emphasized the different oxidation pathways for mono and disulfide minerals. The formation of sulfur compounds in the course of Fe(III) mediated chemical oxidation was analyzed. The product of pyrite oxidation was mainly sulfate, polythionates and elemental sulfur in decreasing proportions, respectively. However, monosulfides yielded more than 90 % elemental sulfur. These studies emphasized the effect of sulfide mineralogy on the oxidation product of sulfide minerals.

Although the importance of microbial activity in the oxidation of sulfide minerals is demonstrated, little has been known about the oxidation pathways of sulfide minerals. Many studies have examined the oxidation of dissolved inorganic sulfur compounds in the presence of bacteria (Pronk et al. 1990; Suzuki et al. 1994; 1965; Kelly, D. 1982; 1988; 2003). Others have investigated the effect of cell attachment during oxidation (Wakao, et al. 1984; Baldi et al. 1992). A complete understanding of oxidation pathways of sulfide minerals may depend on the bacterial mechanism of oxidation. Biological oxidation can be defined as enzymatic oxidation. Specific sulfur oxidizing enzymes were identified for some *Thiobacillus sp.*, (Kelly, 1982; Lu and Kelly, 1988; Arkesteyn, 1979). Enzymes can incorporate oxygen from O_2 or from H_2O into sulfate. Both types of enzymes were identified in *Thiobacillus sp.* (Lu and Kelly, 1988). In biological oxidation pathways, electrons can be carried via intermediate electron acceptors (electron carrier oxidation) or via direct incorporation of atmospheric oxygen into sulfate (Roy and Trudinger, 1970). In microorganism, transfer of electrons from sulfide to electron acceptors such as Fe (III) and O_2 provide energy by cycling electrons through the electron transport systems (ETS) (Elrich,1982, Kelly, 1982). It is believed that the final step in the ETS is the reduction of oxygen to water.

Biologically-mediated sulfide oxidation can be categorized into three suggested pathways: The first pathway depends on enzyme studies and electron transport system enters in the final step from sulfite to sulfate (Roy and Trudinger, 1970; Ehrlich, 1981). This pathway O_2 and H_2O derived oxygen is incorporated into sulfate. An oxygenase enzyme incorporates oxygen from O_2 except for the final step (reaction 2). In the final oxidation step, electrons have to go through the ETS whereby H_2O derived oxygen is incorporated into sulfate (reaction 3). Sulfate produced from this pathway contains 25 % H_2O derived oxygen and 75 % O_2 derived oxygen (*).

Pathways #1

$$MeS + 2H + 1/2O_2 \rightarrow S^o + H_2O \qquad (1)$$

$$S^o + O^*_2 + H_2O \rightarrow SOO^*2^{-2} + 2H+ \qquad (2)$$

$$SOO^*2^{-2} + H_2O + O^*_2 \rightarrow SO2O^*2^{-2} + H_2O^* \qquad (3)$$

$$\mathbf{MeS + 2O_2 \rightarrow SO_4^{2-} + 2H^+} \qquad \mathbf{(4)}$$

In the second pathway, all electrons from sulfide are shuttled through the electron transport system. The electrons generally enter the electron transport system at the cytochrome c level (Kelly, 1982). The following pathway equations summarize these redox reactions:

Pathways #2

$MeS + 2H + 1/2O_2 \rightarrow S^o + H_2O$ (5)

$S^o + O^*_2 + 2H_2O \rightarrow SO_3^{-2} + H_2O^* + 2H^+$ (6)

$SO_3^{2-} + H_2O + 1/2O^*_2 \rightarrow SO_4^{2-} + H_2O^*$ (7)

$MeS + 2O_2 \rightarrow SO_4^{2-} + 2H^+$ **(8)**

In this pathway, the electrons from SO_3^{2-} can be transferred to oxidized cytochrome c, and the oxygen in sulfate comes from water instead of molecular oxygen (reaction 7). The oxidation and reduction of cytochrome c result in the release of energy as ATP (reaction 7b). Molecular oxygen enters the reaction as the final electron acceptor for cytochrome oxidase (reaction 7c). These reactions produce the maximum energy for microorganisms and sulfate derives all oxygen atoms from water

SO_3^{2-} +2cyt c(ox) +H_2O → SO_4 +2cyt c(red) +2H+ (ATP) (7a)

2cyt c(red) +2cyt oxidase(ox) → 2cyt c(ox) + 2cyt oxidase(red) (+ATP) (7b)

2cyt oxidase(red) + O_2+$4H^+$ →2cyt oxidase(ox) +$2H_2O$ (7c)

$SO_3^{2-} + H_2O + 1/2O^*_2 \rightarrow SO_4^{2-} + H_2O^*$ (+2ATP) (7)

Bacterial oxidation of sulfide by ferric iron is the third oxidation pathway and all of the electrons from iron are cycled through the electron transport system (Sugio et al. 1985). The Fe (III) product is used to oxidize the sulfide mineral. In this oxidation pathway, acidity is required since chemical Fe (II) oxidation is more rapid at higher pH >4 and bacteria cannot compete with this fast reaction (Nordstrom and Southam, 1997). Furthermore, Fe(III) precipitates is more readily at more neutral pH and is less available as oxidant (Stumm and Morgan, 1989). Sulfate produced by this oxidation pathway derives all of its oxygen atoms from water (reaction 11).

Pathways #3

$$MeS + 8Fe^{3+} + 4H_2O \rightarrow Zn^{2+} + S^0 + 8Fe^{2+} + 8H^+ \quad (9)$$

$$S^0 + 6Fe^{3+} + 4H_2O \rightarrow SO_4^{-2} + 6Fe^{2+} + 8H^+ \quad (10)$$

$$\mathbf{MeS + 14Fe^{3+} + 8H_2O \rightarrow SO_4^{-2} + 16H^+} \quad \mathbf{(11)}$$

Fe(III) oxidation pathway can be called “semi biological” since it partly involves enzymes that catalyze Fe(III) production and subsequent abiotic oxidation of sulfide by Fe(III)).

All these studies suggest that the main oxidation product of mono-sulfide minerals is elemental sulfur at low pH unless it is catalyzed by bacteria (Schippers et al. 1996; Seuthel et al. 1987; Garcia, 1995b; Fowler, T., 1999; Wentzien, 1994; Crundwell, F.K., 1987). Therefore, the subsequent oxidation of elemental sulfur to sulfate may carry a unique biological signature. Oxygen and sulfur isotope composition of the sulfate product may provide a tool to elucidate such oxidation pathways of sulfides and the bacterial role. However, interpreting of isotopic composition of the sulfate product during sulfide oxidation may depend on the subsequent oxidation pathways of elemental sulfur.

There has been few studies about oxygen and sulfur isotope composition of sulfate produced during sulfide and elemental sulfur oxidation at pH <3. Previous oxygen isotope studies of sulfate formed from metal sulfide oxidation focused on pyrite (Taylor et al. 1984b; Vaneverdingen, et al. 1994; 1985).

Toran and Harris, (1989) investigated sphalerite, galena and pyrite oxidation with a mixture of *T. neopolitanus*, *T. intermedius,* and *T. ferrooxidans* at pH 5 to 6. They reported that the oxygen isotope ratios from both inoculated and sterile experiments indicated more than 50 % of the oxygen in sulfate came from water assuming no fractionation. In their biological experiments, they also demonstrated the sulfur isotope composition of sulfate was 0 to 5 ‰ lighter than the initial sulfide. Krouse et al. (1991) oxidized pentlandite with *Thiobacillus ferrooxidans* at pH 2.5 and indicated that more than ~55 % of the sulfate oxygen is derived from water and the remaining oxygen from O_2. Lloyd, (1968) calculated 68 % H_2O incorporation into sulfate during Na_2S oxidation under abiotic conditions at neutral pH. Schwarcz and Cortecci (1974) calculated a similar % H_2O using submerged pyrite. Mizutani and Rafter (1969), using elemental sulfur and soil bacteria as bacteria source, measured 100 % water-oxygen incorporation into sulfate. Suzuki et al. (1965) also reported 100 % water-oxygen incorporation into sulfate during bacterial oxidation of elemental sulfur.

Taylor et al. (1984b) conducted pyrite oxidation experiments under acidic under water submerged and wet/dry conditions, the latter being periodically exposed to air. In experiments inoculated with *T. ferrooxidans*, these authors measured 50 % water-oxygen incorporation into sulfate for the wet/dry conditions and 70-75 % for the submerged. For similar abiotic experiments, 70 % and 83 % water-oxygen incorporation was reported for the wet/dry and submerged conditions, respectively.

In this study, I investigated oxygen and sulfur isotope composition of sulfate produced by biological and abiotic oxidation of sphalerite under aerobic and anaerobic conditions. Because most sphalerite minerals contain significant amounts of Fe (II) in their crystal lattice, apart from the pure sphalerite experiments, additional experiments were carried out with a 12 % Fe-bearing sphalerite mineral to determine if Fe(II) has any effect on the oxidation reactions of sphalerite and the $\delta^{18}O_{SO4}$ value of the sulfate product. In addition to sphalerite samples, because S^o was suspected to be an important intermediate of sphalerite oxidation additional similar biotic and abiotic S^o oxidation experiments was performed and the $\delta^{34}S_{SO4}$ and $\delta^{18}O_{SO4}$ of the sulfate product also measured.

These detailed experimental studies may give an opportunity to better understand: *i)* if elemental sulfur forms during sphalerite oxidation and its subsequent oxidation to sulfate controls the final isotopic composition of sulfate and *ii)* to compare the $\delta^{18}O_{SO4}$ and $\delta^{34}S_{SO4}$ values produced during pyrite and sphalerite oxidation to reveal possible effects of sulfide mineralogy on the final $\delta^{18}O_{SO4}$ and $\delta^{34}S_{SO4}$ values.

3.2 Experimental Methods

3.2.1 Sphalerite and elemental sulfur preparation

ZnS (pure) and 12 % Fe-bearing sphalerite samples used in the current study were obtained from the Geology Museum of the Colorado School of Mines, Golden-Colorado and from the United States Geological Survey (USGS), in Denver, Colorado (USGS), respectively. The purity of the sphalerite samples were checked by analyzing the elemental composition by ICP analysis at the United States Geological Survey (USGS), in Denver, Colorado. Prior to use in all of the experiments, the samples were ground and sieved. A grain size of < 63 μm was used for the experiments. Because acid washing of sphalerite may cause the evolution of H_2S and the loss of sulfur may result in an unknown degree of sulfur isotope fractionation, precaution was taken when the sphalerite samples were prepared. Approximately 15 g of sphalerite sample were quickly rinsed by 1 M HCl and subsequently washed with deionized water and lastly with acetone (Moses et al. 1987). At the end of the experiment, insignificant sulfur isotope fractionation was observed between sulfate and ZnS (pure and Fe-bearing), thus proving that this method did not cause significant effects from sulfur loss. For elemental sulfur samples, only deionized and acetone rinsing methods were applied.

For sterilization, the mineral samples were first soaked with 70 % ethanol and spread in a thin even layer under UV radiation (germicidal) in a sterile hood for about 30 minutes to decontaminate the surface. These sterilization methods were effective since contamination effects were not observed in the abiotic control experiments. Following these treatments, the samples were immediately placed in sterile experimental containers.

3.2.2 Bacterial and abiotic aerobic experiments

In order to elucidate the reaction pathway(s) of sphalerite and elemental sulfur samples (ZnS, (Zn,Fe)S, S^o) and the relative contributions of molecular oxygen and H_2O to sulfate, biotic and abiotic sulfide oxidation experiments were performed in aqueous solution under O_2 saturated conditions and varying $\delta^{18}O_{H2O}$ values. For the bacterial experiments, sulfate and Fe(II)-free medium was used as the experimental solution (NH_4Cl, 0.6 g; $MgCl_2.6H_2O$, 0.2 g ; K_2HPO_4, 0.1 g ; Wolfe's mineral solution, 5 ml) and pH was adjusted to 3 with HCl at 25 °C. Wolfe's mineral solution was prepared with Cl salt instead of SO_4 salt to prevent sulfate contamination to the final experimental solution (1.5 g nitrilotriacetic acid , 3 g $MgCl_2.6H_2O$, 0.5 g $MnSO_4.7H_2O$, 1 g NaCl, 100 mg $FeSO_4.7H_2O$, 100 mg $CoCl_2.6H_2O$, 100 mg $CaCl_2$, 100 mg $ZnSO_4.7H_2O$, 100 mg $CuSO_4.7H_2O$, 10 mg $AlK(SO_4)_2$. $12H_2O$, 10mg H_3BO_3, 10mg $Na_2MoO_4.2H_2O$ per liter. An initial pH of 3 was used for all the experiments.

Biological sphalerite (pure and Fe-bearing) and elemental sulfur experiments were identical in terms of experimental methods and conditions. In order to keep the sulfur amount the same in the experiments, 830 mg (266 mg Sulfur in 830 mg ZnS) ZnS and Fe-bearing sphalerite and 266 mg elemental sulfur were used in the experiments. The 250 ml of microbiological medium, whose composition was described before, were placed into the 500 ml Erlenmeyer flasks and autoclaved at 121 °C for 20 minutes. After autoclaving, the flasks were kept in the sterile hood under the UV for 25 minutes to decontaminate the surfaces of the flasks. Sterilized and cleaned samples and five milliliters of the *A. Ferrooxidans* cell suspension which contained (~2.7 x 10^7 cells) was added to the medium. The biological aerobic experiments were designed both as short and long-term experiments to determine the integrity of the $\delta^{18}O_{SO4}$ values with extended incubation time and lower pH. Short-term biological sphalerite experiments were ended at pH ~2.7 (45 days). Although the long-term experiments were incubated longer to obtain the lower pH (2.1), there was no significant change in the pH. Therefore, the long-term experiments were ended at pH ~2.89 (~60 days)

To determine the kinetic oxygen isotopic fractionation effect (ε_o) during sphalerite and elemental sulfur oxidation and the relative contribution of water and molecular oxygen to the oxygen of the sulfate product, four different bacterial incubations were made for ZnS with waters having different $\delta^{18}O$ values of -15.3 ‰, -2.5 ‰, 1.8 ‰ and 13‰. Three bacterial incubations with waters having $\delta^{18}O$ values of -15.3 ‰, -2.5 ‰, 1.8 ‰ were made for Fe-bearing sphalerite and elemental sulfur experiments. The biological aerobic experiments were performed as duplicates for each given water. The short- and the long-term biological experiments were incubated in the environmental room at 25 °C and were continuously shaken (150 rpm) over the entire period of the incubations. The flasks were covered with rubber stoppers fitted with inflow and outflow tubes for aeration. Sterile air filters (0.2 μm-whatman) were connected to the inflow and exit ports to prevent microbial contamination and to minimize evaporation. The flasks were continuously bubbled with compressed air (General Air Company) and several tanks were used during these experiments. During each set of incubations, additional and separate biotic and abiotic experiments with normal laboratory water (-15.3 ‰) were also performed to monitor pH and the solution chemistry of the experimental solutions. Aliquots were taken periodically from these experiments to measure the concentration of sulfate, Zn and pH over the incubation period of each experiment.

At the end of the short and the long-term experiments, experimental solution was filtered (0.1 μm-Milipore). Some portion of the filtrate was reserved for oxygen isotope measurement of water and for sulfate concentration measurements by ion chromatography. The water samples were kept frozen until oxygen isotope measurements. To the remainder of the filtrate (~200 ml), a small amount of concentrated HCl and 10 ml of 10 % $BaCl_2$ solution were added to precipitate SO_4 as $BaSO_4$ and the precipitate was allowed to settle overnight. The barium sulfate was filtered and collected on a 0.2 μm Millipore filter, washed first with 100 ml of 1N HCl, then rinsed 3 times with total 500 ml of DI water and dried for 24 h at 100 °C. As a final purification step, all of the $BaSO_4$ powders were baked under an air atmosphere at 500 °C for 2 h. This treatment was previously shown to effectively remove any possible organic material and not interfere with $\delta^{18}O$ measurements (Mandernack et al. 2000a).

Air samples from both biotic and abiotic experiments were collected in an evacuated 200 ml collection vessel at the end of the experiments and isotopically analyzed for ^{18}O isotopic composition. Prior to sampling the gas headspace, the air source and exit port of the flask were closed and the air in the head space allowed to mix a few minutes before drawing the gas sample. The air sample was collected with a gas-tight syringe which was flushed twice before taking the final sample.

The abiotic sphalerite experiments for oxygen and sulfur isotope analysis , which were identical to the bacterial experiments but without the culture, were only carried out for ZnS samples since there was insufficient quantity of the Fe-bearing sphalerite samples. For the abiotic ZnS oxidation experiments, 3.2 gr sphalerite was added to 1 L medium to obtain enough SO_4 for isotope analysis. Sulfate concentration and pH were also monitored for the abiotic ZnS experiments. For monitoring solution chemistry during abiotic Fe-bearing sphalerite oxidation, only one abiotic Fe-bearing sphalerite experiments were performed as the abiotic ZnS experiments and the concentration of sulfate, Zinc and pH were monitored.

To determine the relative contribution of molecular oxygen and water to the sulfate product, two waters having different $\delta^{18}O$ values (13.2 and -15.3) were used for the abiotic ZnS experiments. Only one abiotic-control experiment was performed for elemental sulfur, which displayed non-detectable oxidation over 21 days of incubation.

3.2.3 Bacterial and abiotic anaerobic experiments

In order to determine the $\delta^{18}O_{SO4}$ values produced anaerobically by ferric iron oxidation of sphalerite, biotic and abiotic anaerobic experiments were carried out. For sphalerite (ZnS and Fe-bearing) experiments, 500 ml of the microbiological medium was placed into 1L serum bottles and the pH adjusted to ~2 with trace metal grade HCl. The serum bottles were then autoclaved for 20 minutes. Lower pH was necessary to keep aqueous Fe (III) in solution. Afterwards, serum bottles were purged with nitrogen for 30 minutes by using pre-sterilized inline gas filters (0.2 µm, whatman) at both the inlet and outlet in order to keep the medium sterile. After purging, the serum bottles were kept overnight in the anaerobic microbiological glove box to equilibrate with the anaerobic atmosphere before starting the experiments. The atmosphere in the glove box consisted of 5 % CO_2, 5 % H_2, and 90 % N_2. For the anaerobic experiments, approximately ~1.6 g of sphalerite was cleaned and sterilized according to the methods described above.

The ferric iron used in these experiments was prepared by dissolving ferric chloride ($FeCl_3$) into acidified DI water then filter sterilized (0.2 µm, whatman) and purged with nitrogen ~25 min. The stock ferric iron solution (1M) was kept inside the anaerobic chamber until used. To 500 ml of microbiological medium, 1.6 g of sphalerite, 5 ml of the cell culture (2.7 x10^7 cells/ml) and the $FeCl_3$ solution (100mM final) were added to each 1 liter vial and then sealed with a gas headspace inside the anaerobic chamber. As a final step, serum bottles were covered with aluminum foil to prevent iron photo oxidation/ reduction and were placed in the environmental room at 25 °C and shaken continuously at 150 rpm during the entire incubation period of the experiments (45 days).

Abiotic ZnS experiments were prepared under identical conditions as the biological experiments except that no bacterial culture was added. Fe (II) and sulfate concentrations were monitored during the course of the experiments.

Waters with different $\delta^{18}O$ value (-15.3 ‰, -2.5 ‰, 1.8 ‰, -16 ‰, 12.5 ‰) were used for the biological and abiotic experiments in order to determine the kinetic oxygen isotopic fractionation effect between water and sulfate during sphalerite oxidation. Apart from sphalerite experiments, one abiotic and biotic galena experiments were also performed under the identical conditions as sphalerite experiments.

For the incubation with elemental sulfur, one biotic and abiotic experiment was carried out. For these experiments, to 500 ml of microbiological medium 532 mg of elemental sulfur, the $FeCl_3$ solution (100 mM final) and 5 ml of the cell culture were added to each 1liter vial. The abiotic anaerobic elemental sulfur experiment was prepared without addition of the cell culture.

3.2.4 Analytical methods

The concentration of sulfate was analyzed by Ion Chromatography (IC- Dionex Series 500). Total dissolved sulfur and zinc concentration was measured by Inductively Coupled Plasma Mass spectrometry (ICP-MS). All chemical analysis were performed at the United States Geological Survey (USGS), in Denver, Colorado,. $Fe[II]_{aq}$ concentrations were measured colorometrically in the solutions by the ferrozine method.

3.2.5 Extraction of elemental sulfur from sphalerite surface

During oxidation of sulfide minerals such as pyrite and sphalerite, elemental sulfur has been reported to form on the surface (Turcotte, et al. 1993; Mcguire et al. 2001, 2001; Sasaki, et al. 1995; Sasaki, K. 1997; Mycroft, et al. 1990, Schippers, et al. 1999; Descostes, et al. 2001) . Schippers et al. (1999) demonstrated that elemental sulfur is the main sulfur species (95 % of the sulfur moiety) during oxidation of sphalerite at low pH (<3) without bacterial activity. If elemental sulfur is the main sulfur species during sphalerite oxidation, the $\delta^{34}S$ value of elemental sulfur should reflect the $\delta^{34}S$ value of sphalerite. In order to measure the $\delta^{34}S$ value of elemental sulfur, elemental sulfur was extracted from the mineral surface after sphalerite was oxidized under anaerobic conditions. For this purpose, 500 ml of the medium was filtered through 0.2 μm filter (whatman) at the end of the anaerobic experiments to obtain the sphalerite particles.

The filtering was carried out in the glove box to prevent contamination with molecular oxygen incorporation which may cause the oxidation of intermediate sulfur species. The sphalerite mineral particles collected on the filter were placed into a 50 ml beaker. The approximately 25 ml of perchloroethylene was added to the reaction beaker and the beaker was left over night at room temperature (Mcquire et al. 2000). After completion of the extraction, perchloroethylene was carefully drawn off into different beaker and left for evaporation at room temperature. Elemental sulfur was collected from the reaction beaker and analyzed for its sulfur isotope composition.

3.2.6 Isotope analysis of sulfate

Sulfur and oxygen isotope ratios of samples were determined by continuous flow isotope ratio mass spectrometry (CF-IRMS) using an elemental analyzer ($\delta\ ^{34}S$) or a Thermo-Finnigan TC/EA at 1450°C ($\delta^{18}O$) coupled to a gas source mass spectrometer in the Laboratory of Dr. Bernhard Mayer at University of Calgary , Canada and at the United States Geological Survey (USGS), in Denver, Colorado by using a Carlo Erba NC2500 elemental analyzer coupled to a Micromass Optima. Reproducibility of the $\delta^{34}S$ and $\delta^{18}O$ values for sulfate were generally better than ± 0.5 ‰. For $\delta^{18}O$ and $\delta^{34}S$, standard mean ocean water (SMOW) and Canyon Diablo Troilite (CDT) are the respective standards.

3.3 Results

3.3.1 Aerobic sphalerite experiments

The changes in solution chemistry from the ZnS and Fe-bearing sphalerite incubation experiments are indicated in Table 3.1 and 3.2, respectively. Sulfate concentration from the biological and abiotic ZnS oxidation experiments consistently increased during the incubations (Fig. 3.1). However, sulfate concentration from the abiotic-control experiments was significantly less than the biological experiments, having final concentrations (at 60 days) of 26.2 mg/L (Fig. 3.1). The total dissolved sulfur (TDS) concentration which was measured by ICP from the biological ZnS experiments increased over the period of the experiments similar to the trend of sulfate concentration. At first glance, TDS concentration appears to be less than the concentration of sulfate in both biological sphalerite experiments (Tables 3.1 and 3.2). TDS concentration should be equal to the concentration of sulfate under the experimental conditions which favor sulfate as the dominant sulfur specie over other sulfur species (Goldhaber, 1986; Schippers et al. 1996; Rimstidt and Vaungauh, 2003). When the concentration of sulfate is calculated based on the measured TDS concentration (TDSx3= SO_4), it can be seen that TDS concentration reflects the concentration of sulfate. This is especially true for ZnS experiments (Table 3.1). However, there are some disagreements between ICP and IC measurements for sulfate concentration, especially in the Fe-bearing ZnS oxidation experiments (Table 3.2). This may be simple increased analytical errors from sulfur measurements near the IC detection limit in a complex chemical matrix.

Insignificant sulfur isotope fractionation between sulfate and ZnS support the existence of the sulfur primarily as sulfate in the experiments since oxidation of sulfide to intermediate sulfur species can cause the significant sulfur isotopes fractionation between sulfate and ZnS.

Table 3.1. Solution chemistry during aerobic bacterial and abiotic pure sphalerite oxidation experiments.

	Biotic							Abiotic			
	Days	pH	SO_4 production Rate (mg/ZnS mg*day)	SO_4 (mmol/L)	SO_4 * (mmol/L)	Total Dissolved Sulfur (mmol/L)	Zn (mmol/L)	Days	pH	SO4 (mmol/L)	SO4 production Rate (mg/ZnS-mg*day)
	0	2.97	0.000	0. 18	0.17	0.17	0.04	0	3.0	0.01	
	5	3.05	0.015	0.65	0.74	0.74	0.68	5	4.2	n.d.	n.d.
	10	2.97	0.021	1.83	3.03	3.02	2.91	10	n.d.	n.d.	n.d.
	13	2.88	0.024	2.72	n.d	n.d	n.d	15	n.d.	n.d.	n.d.
	20	2.87	0.029	4.94	n.d	n.d	n.d	20	n.d.	n.d.	n.d.
	25	2.88	n.d	n.d.	5.88	5.88	5.36	25	4.5	0.11	1.2×10^{-4}
	30	2.89	0.020	5.17	n.d	n.d	n.d	30	n.d.	n.d.	n.d.
	35	2.80	0.022	6.52	7.03	7.03	6.45	35	n.d.	n.d.	n.d.
Short term	45	2.70	0.022	8.72	9.54	9.54	8.45	45	4.9	0.12	7.4×10^{-5}
	50	2.86	0.020	8.60	n.d	n.d	n.d	50	4.9	n.d.	n.d.
Long term	60	2.89	0.017	8.84	10.32	10.32	8.94	60	3.9	0.27	1.2×10^{-4}

*, calculated SO_4 concentration by using Total dissolved sulfur concentration (TDS mg/Lx3)= SO4 mmol/L

Table 3.2 . Solution chemistry during aerobic bacterial and abiotic Fe-bearing sphalerite oxidation experiments.

	Biotic							Abiotic				
	Days	pH	SO4 production Rate (mg/ZnS-mg*day)	SO_4 (mmol/L)	SO_4* (mmol/L)	Total dissolved Sulfur (mmol/L)	Zn (mmol/L)	Days	pH	SO4 production Rate (mg/ZnS-mg*day)	SO4 (mmol/L)	Zn (mmol/L)
	0	3.05	0.000	0.18	0.18	0.19	0.04	0	3.1	0.0000	0.008	0.04
	5	3.32	0.075	3.25	2.54	2.54	2.40	5	4.5	0.0008	0.03	0.27
	10	2.97	0.149	12.86	8.89	8.89	9.83	10	4.2	0.0014	0.125	0.70
	15	2.81	0.146	18.94	15.52	15.52	17.53	15	4.2	0.0000	n.d.	1.19
	22	2.75	0.153	20.68	18.12	18.12	21.23	22	3.6	0.0009	0.17	0.36
	28	2.76	0.088	21.21	20.41	20.41	23.69	28	3.6	0.0008	0.19	2.23
	33	2.71	0.089	25.46	23.64	23.64	27.84	33	4.1	0.0007	0.20	2.72
Short term	40	2.61	0.064	26.31	26.45	26.45	30.76	40	3.9	0.0007	0.23	3.47
	46	2.45	0.100	32.55	26.77	26.77	30.76	46	3.4	0.0009	0.36	3.27
Long term	54	2.44	0.059	27.35	4.36	4.36	4.95	54	3.7	0.0008	0.38	3.50

*, calculated SO_4 concentration by using Total dissolved sulfur concentration

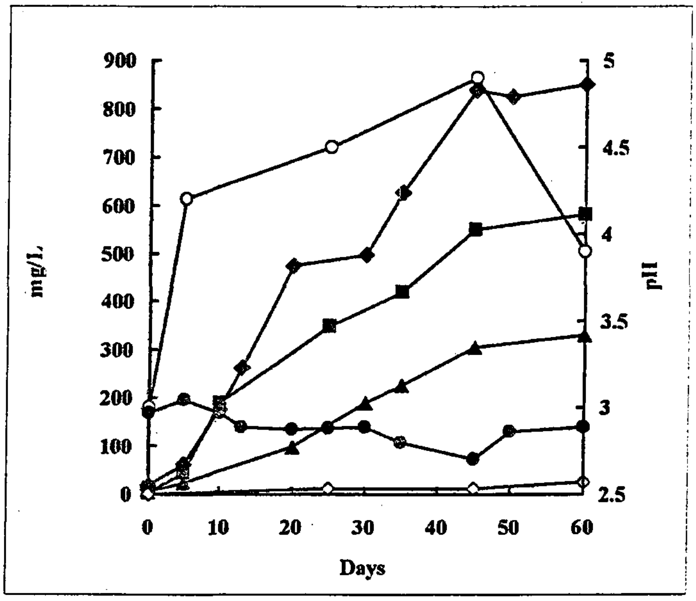

Figure 3.1. Solution chemistry during aerobic bacterial and abiotic-control Pure ZnS oxidation experiments. Sulfate concentration in the biological experiments, ◆ .Zinc concentration in the biological experiments, ■ . Total sulfur concentration in the biological experiments ,▲ pH profile of the biological experiments, ●. Sulfate concentration in the abiotic experiments, ◇ . pH profile of the abiotic experiments, ○.

The concentration of sulfate, zinc and total dissolved sulfur from the biological Fe-bearing sphalerite experiments steadily increased until 46 days and after which they plateau (Fig. 3.2). It is clear from Fig. 3.1 and 3.2 that Fe-bearing sphalerite produced higher concentrations of sulfate and zinc compared to the ZnS experiments. pH of the biological experiments is lower than that from the abiotic experiments during both types of sphalerite oxidation. pH of the biological Fe-bearing ZnS experiments even showed the lowest pH value. Figure 3.2 also shows that the amount of sulfate and Zn dissolved with bacteria are higher than those without bacteria during both types of sphalerite oxidation experiments.

The pH of the biological experiments showed interesting trend. In the biotic ZnS experiments, pH was almost stable (±0.1) over the period of the experiments (Fig. 3.1). In contrast, pH dropped from 3 to 2.4 at 54 days in the biological Fe-bearing sphalerite experiments (Fig. 3.2). In contrast to the biotic experiments, slight increases in pH were observed during the abiotic ZnS and Fe-bearing ZnS oxidation experiments.

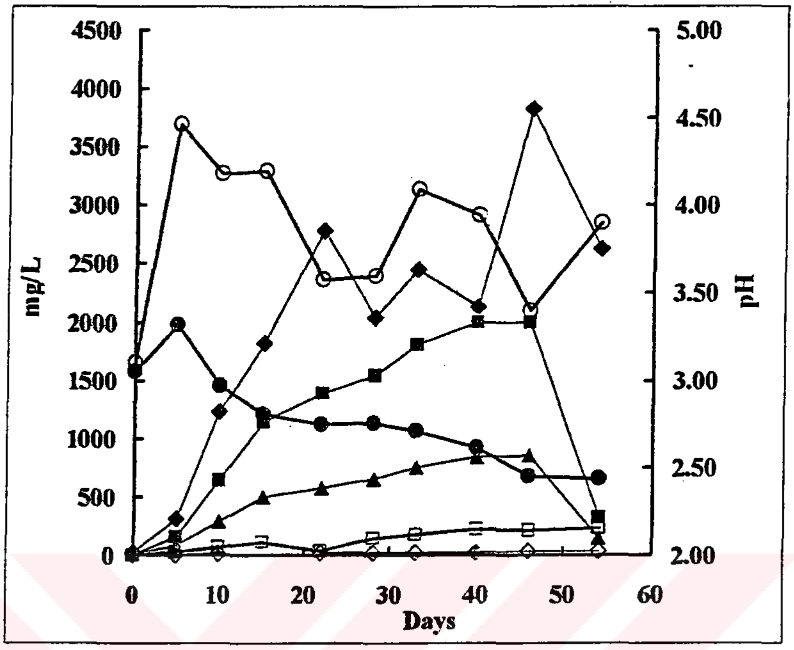

Figure 3.2 Solution chemistry during aerobic bacterial and abiotic control Fe-bearing sphalerite oxidation experiments. Sulfate concentration in the biological experiments, ◆. . Zinc concentration in the biological experiments, ■ . Total sulfur concentration in the biological experiments , ▲. pH profile of the biological experiments,●. Sulfate concentration in the abiotic experiments,◇ Total sulfur concentration in the abiotic experiments,△. Zinc concentration in the biological experiments,□ pH profile of the abiotic experiments, ○ .

3.3.2 Anaerobic sphalerite experiments

The changes in solution chemistry from the anaerobic ZnS and Fe-bearing sphalerite oxidation experiments are given in Table 3.3. The concentration of sulfate increased with time and was very similar in both the biotic and the abiotic experiments during both types of sphalerite oxidation experiments (Figs. 3.3a,3.3b). Fe-bearing sphalerite experiments produced slightly higher sulfate than the ZnS experiments. Sulfate production rate decreased with time, particularly in the ZnS experiments. This decreasing trend could be indicative of the formation of different sulfur species such as elemental sulfur. Formation of elemental sulfur was reported by previous studies under the same conditions as the current study (Schippers, et al. 1999; Sand et al. 2001). It is also possible that formation of Fe(III)-sulfate bearing minerals can contribute to this decreasing trend. An increase in the Fe (II) aq concentration throughout the course of the experiments indicates continues sphalerite oxidation by ferric iron without producing sulfate.

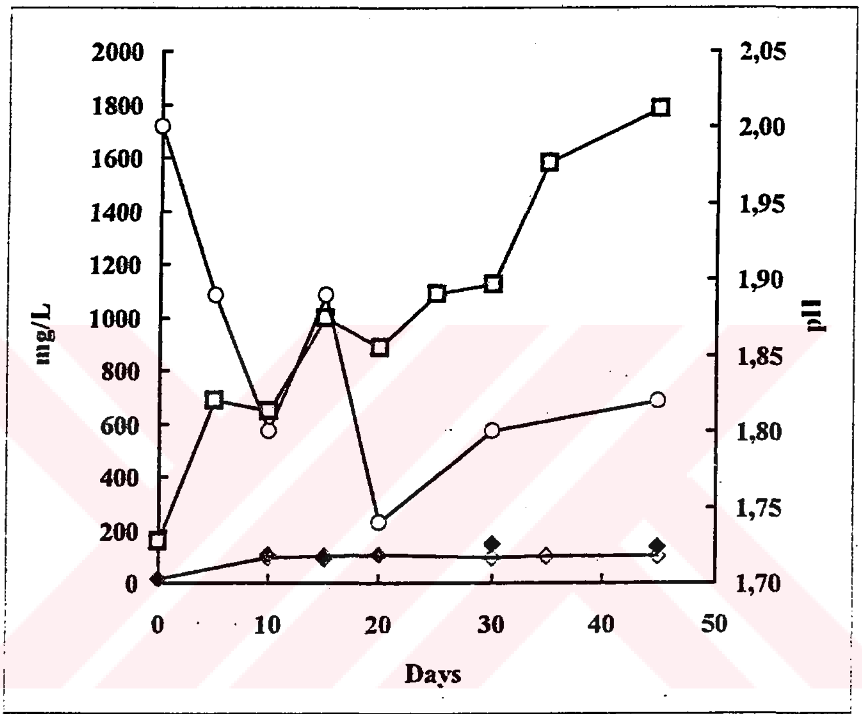

Figure 3.3a Solution chemistry during anaerobic bacterial and abiotic ZnS sphalerite oxidation experiments. Sulfate concentration in the biological experiments,◆. Fe(II) concentration in the biological experiments,■. pH of the biological experiments, ●. Sulfate concentration in the abiotic experiments,◇ . Fe(II) concentration in the biological experiments,□ . pH of the abiotic experiments, ○ .

3.3.3 Bacterial and abiotic aerobic and anaerobic elemental sulfur experiments

Biological aerobic elemental sulfur oxidation experiments were ended after 20 days since when the pH of the solution had dropped to 2.1 (Fig. 3.4). The 20 day time point corresponds to the long-term experiments whereas the short-term experiments were ended when the pH dropped to 2.7 after 10 days (Table 3.4).

Table 3.3 Solution chemistry during sphalerite oxidation under anaerobic conditions.

	Biotic					Abiotic			
	Days	pH	Fe(II) mg/L	SO_4 (mg/L)	SO_4 production Rate (mg/ZnSmg*day)	pH	Fe(II) mg/L	SO_4 (mg/L)	SO_4 production Rate (mg/ZnSmg*day)
(Zn,Fe)S	0	2.00	324	11.2	0.0000	2.00	319	10	0.0000
	10	1.74	435	124.5	0.0078	1.74	335	69	0.0043
	30	1.72	3280	157.0	0.0033	1.72	3160	48	0.0010
	45	1.75	4080	150.2	0.0021	1.75	4100	147	0.0020
ZnS	0	2.00	158	13	0.0000	2.00	158	13	0.0000
	5	1.89	688	n.d	n.d	1.89	688	n.d	n.d
	10	1.80	646	106	0.0066	1.80	646	96	0.0060
	15	1.89	1000	91	0.0038	1.89	1000	100.9	0.0042
	20	1.74	885	108	0.0034	1.74	885	108	0.0034
	25	n.d	1090	n.d	n.d	n.d	1090	n.d	n.d
	30	1.80	1125	145	0.0030	1.80	1125	94	0.0020
	35	n.d	1580	n.d	n.d	n.d	1580	101	0.0018
	45	1.82	1780	137	0.0019	1.82	1780	100	0.0014

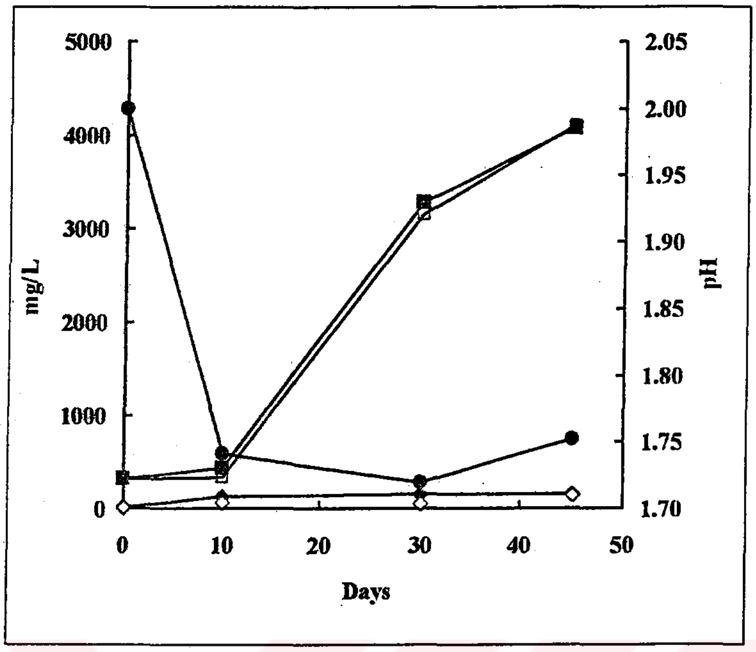

Figure 3.3b Solution chemistry during anaerobic biotic and abiotic Fe-bearing ZnS oxidation experiments. Sulfate concentration in the biological experiments,◆ Fe(II)concentration in the biological experiments,■ . pH profile of the biological experiments, ●. Sulfate concentration in the abiotic experiments,◇ Fe(II)concentration in the biological experiments, □. pH profile of the abiotic experiments, ○

In contrast to the sphalerite experiments, the pH displayed a gradual and consistent drop throughout the bacterial incubation. The concentration of sulfate increased linearly over the period of the experiments and was very similar to the sulfate production rate during the ZnS oxidation experiments at respective days (10 and 20 days), but significantly less than the rate observed for the Fe-bearing sphalerite experiments.

In the Fe-bearing sphalerite experiments, it is most likely that Fe(III) produced by bacterial reaction may have acted as oxidizing agent in addition to molecular oxygen and produced more elemental sulfur which was subsequently oxidized to sulfate by bacteria (reaction 11). The abiotic elemental sulfur oxidation experiments produced insignificant sulfate during the 20 days incubation period and pH was stable (Table 3.4). Although biotic and abiotic anaerobic elemental sulfur oxidation experiments were carried out, no oxidation was observed as evidenced by a complete lack of sulfate production (data not shown).

Table 3.4 Solution chemistry during elemental sulfur oxidation by *A. ferrooxidans* and abiotically

Biotic					Abiotic		
Days	pH	SO_4 (mg/L)	SO_4* production Rate (mg/ ZnS mg*day)	SO_4 production Rate (mg/ S° mg*day)	pH	SO_4 (mg/L)	SO_4 production Rate (mg/S° mg*day)
0	3.0	28	0.000	0.000	3.0	0.3	0.00000
5	2.9	58	0.045	0.044	3.2	0.3	0.00022
10	2.7	126	0.064	0.050	2.9	1.2	0.00045
15	2.4	365	0.074	0.092	3.0	1.3	0.00033
20	2.1	450	0.086	0.085	3.0	2.5	0.00047

*, SPR calculated from aerobic biological pure ZnS oxidation experiments based on only the sulfur weight of the ZnS sample used in the experiments (~274 mg S in 830 mg ZnS)

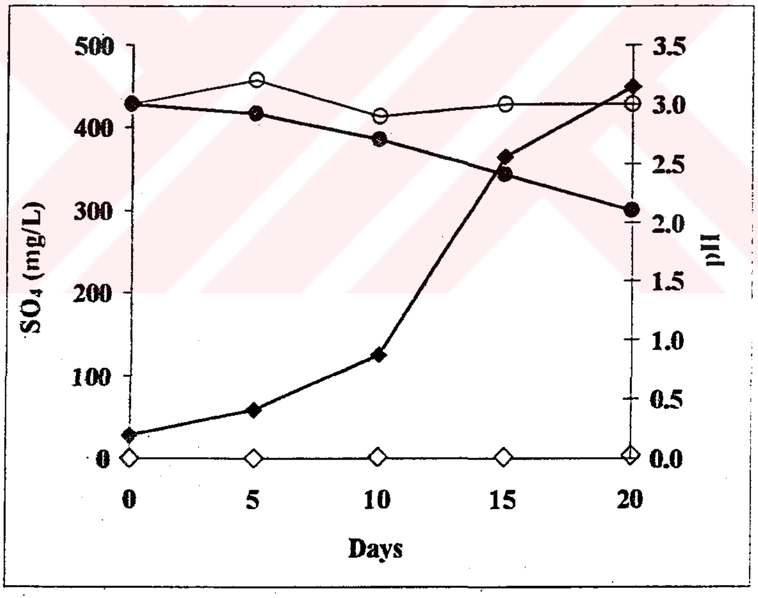

Figure.3.4 Solution chemistry during aerobic elemental sulfur oxidation experiments. Sulfate concentration in the biological experiments, ◆ . Sulfate concentration in the abiotic experiments, ◇. pH profile of the biological experiments, ● . pH profile of the abiotic experiments, ○.

3.3.4 Oxygen and sulfur isotopic composition of sulfate produced under aerobic conditions

Table 3.5 shows the $\delta^{18}O_{SO4}$ and the $\delta^{34}S_{SO4}$ values of sulfate produced during the aerobic biological and abiotic ZnS and biological Fe-bearing sphalerite oxidation experiments. The $\delta^{18}O_{SO4}$ values from the biological ZnS and Fe-bearing sphalerite experiments showed strong linear dependence on the $\delta^{18}O_{H2O}$ values (Table 3.5, Fig. 3.5 and Fig. 3.6). During the short and long-term biological ZnS experiments, the linear regression between the $\delta^{18}O_{SO4}$ and the $\delta^{18}O_{H2O}$ values has a slope of m= ~0.96, indicating that ~100 % of the sulfate-oxygen is derived from water-oxygen. The standard deviation for the slope and the intercept were estimated as m= ± 0.1, ± 0.7 and m=± 0.1, ±0.8 for the short and long-term biological experiments, respectively.

The values for standard deviation are tested according to t-test. Oxygen isotope fractionation effect ($\Delta^{18}O_{SO4-H2O}$) between water and sulfate were estimated from the linear regression between the $\delta^{18}O_{SO4}$ and the $\delta^{18}O_{H2O}$ values as 9.1± 0.7‰, 8.9± 0.8 ‰ for the short and the long-term biological ZnS experiments, respectively (Fig. 3.5). The amount of O_2 incorporated into sulfate was insignificant and therefore ($\Delta^{18}O_{SO4-O2}$) values were not necessary to calculate.

The linear regression between the $\delta^{18}O_{SO4}$ and $\delta^{18}O_{H2O}$ values obtained from the biological Fe-bearing sphalerite experiments provided slopes of m= 1.00±0.1 and m= 0.94±0.1 for the short-term and the long-term experiments, respectively. These results also indicate ~ 100 % water-oxygen incorporation into sulfate in both experiments.

The fractionation of oxygen isotopes between sulfate and water was estimated to be +8.2±0.8 ‰ for the short-term and +7.2±1.1 ‰ for the long-term experiments (Fig. 3.6). Although the oxidation rate of the Fe-bearing sphalerite is significantly faster than the ZnS experiments, the $\delta^{18}O_{SO4}$ values and oxygen isotope fractionation effect ($\Delta^{18}O_{SO4-H2O}$) between both experiments is similar (Table 3.5) The $\delta^{34}S_{SO4}$ values from the biological ZnS oxidation experiments were not significantly different from the $\delta^{34}S_{ZnS}$ value. The kinetic sulfur isotope fractionation effect ($\Delta^{34}S_{SO4-ZnS}$) was estimated to be ±0.1 ‰ (Table 3.8).

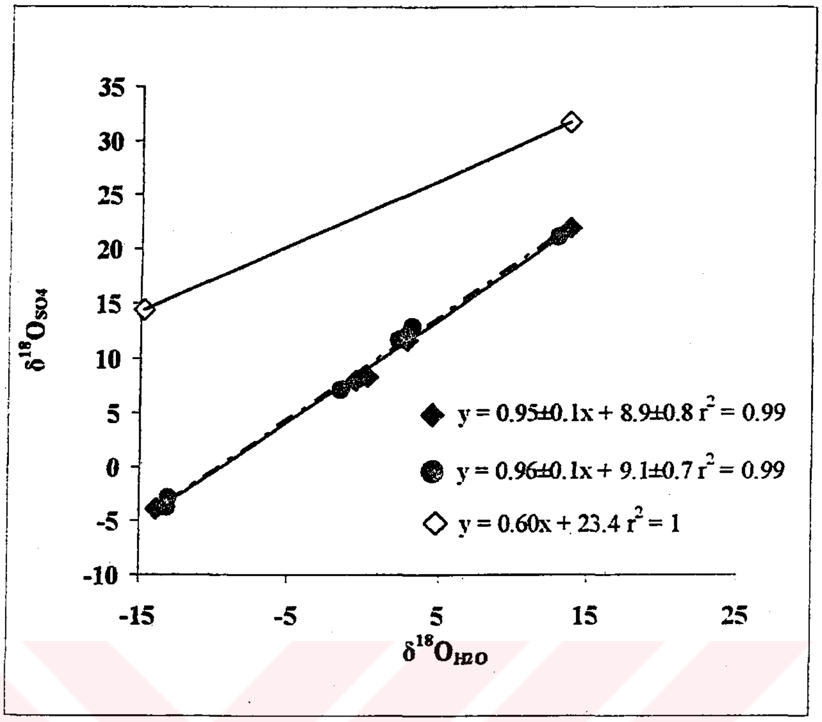

Figure 3.5. Relationship of the $\delta^{18}O$ of the SO_4 relative to the $\delta^{18}O$ of the experimental H_2O during aerobic oxidation of ZnS by *A.ferrooxidans* and abiotically. Short-term bacterial (pH: 2.7 , 45 days),●. Long-term bacterial (pH: 2.9 , 60 days),◆. Abiotic (pH ~3),◇.

Similar to the ZnS experiments, the $\delta^{34}S_{SO4}$ and $\delta^{34}S_{(Zn,Fe)S}$ values were also closely matched and indicated no significant sulfur isotope fractionation (Table 3.8). The abiotic control ZnS experiments produced sulfate that had 60 % incorporation of oxygen from H_2O and 40 % from molecular O_2 (Fig. 3.5). Only two abiotic ZnS oxidation were performed due to insufficient amount of ZnS sample. Although the oxygen isotope fractionation effect between sulfate and water, and between sulfate and molecular oxygen was not able to be determined for the abiotic experiments due to insufficient data points (n=2), based on the higher O_2 incorporation into sulfate, it is reasonable to predict that the $\Delta^{18}O_{SO4-H2O}$ values will be different than those for biotic experiments.

Table 3.5. Oxygen and sulfur isotope composition of sulfate from aerobic bacterial and abiotic pure ZnS and Fe-bearing ZnS oxidation experiments

Biological		$\delta^{18}O_{H2Oinitial}$ (‰)	$\delta^{18}O_{H2Ofinal}$ (‰)	Avg.$\delta^{18}O_{SO4}$ (‰)	Avg.$\delta^{34}S_{SO4}$ (‰)
ZnS	**Short-term**	-15.3	-12.9	-2.9	-7.9
		-15.3	-13.0	-3.8	-7.8
		-2.5	-1.5	7.0	-7.9
		-2.5	n.d	n.d	n.d
		1.8	2.3	11.6	-8.0
		1.8	3.2	12.9	-8.0
		13.2	13.0	21.1	-7.2
	Long term	-15.3	-13.8	-3.9	-7.9
		-2.5	-0.6	7.9	-7.6
		-2.5	0.2	8.3	-7.8
		1.8	2.7	12.1	-7.4
		1.8	2.8	11.7	-7.7
		13.2	13.8	22.0	-7.4
Abiotic	**Long term**	-15.3	-14.7	14.5	**-10.3**
		13.2	13.7	31.7	-7.9
Biological		-15.3	-14.1	-5.5	0.2
(Zn,Fe)S	**Short-term**	-15.3	-14.1	-6.1	0.2
		-2.5	n.d	n.d	0.3
		-2.5	-1.9	5.8	0.5
		1.8	2.1	10.7	0.4
		1.8	2.2	10.5	0.2
	Long-term	-15.3	-14.3	-6.2	0.2
		-15.3	-14	-5.9	0.2
		-15.3	-14.3	-6.2	0.3
		-2.5	-1.6	5.4	0.4
		-2.5	-1.4	6.9	0.3
		1.8	n.d	n.d	n.d
		1.8	2.9	9.6	0.3

$\delta^{34}S$ value of pure sphalerite was -7.7 ‰ and $\delta^{34}S$ value of Fe-bearing sphalerite was 0.0 ‰ .

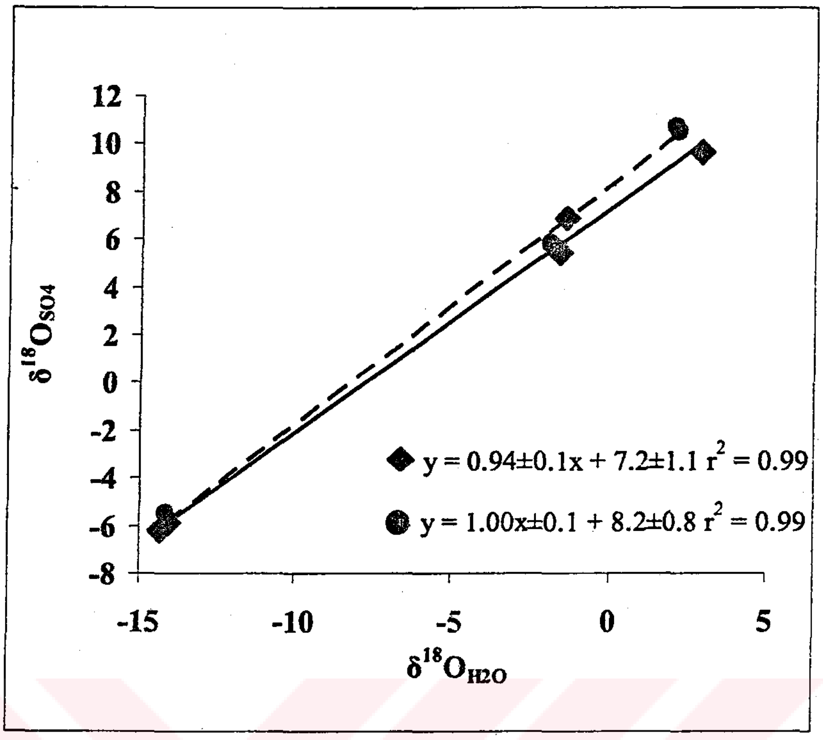

Figure 3.6 Relationship of the $\delta^{18}O$ of the SO_4 relative to the $\delta^{18}O$ of the experimental H_2O during aerobic oxidation of Fe-bearing ZnS by *A.ferrooxidans.* Short-term bacterial (pH: 2.6 , 40 days), ●. Long-term bacterial (pH: 2.44, 54 days),◆ .

A sulfur isotope fractionation ($\Delta^{34}S_{SO4-ZnS}$) of ~ -2.6 ‰ was measured from one of the abiotic experiments (Table 3.5). However, since the other abiotic experiment did not show the same fractionation effect, the observed -2.6 ‰ fractionation may have been an artifact of the experimental conditions or due to analysis error.

3.3.5 Oxygen and sulfur isotopic composition of sulfate under anaerobic conditions

The linear regressions generated for $\delta^{18}O_{SO4}$ versus $\delta^{18}O_{H2O}$ from the anaerobic experiments yielded slopes of m=1.0±0.4 and m= 0.98±0.0 for the biotic and abiotic ZnS experiments, respectively and the corresponding values for the Fe-bearing sphalerite experiments are m=0.96±0.1 and m=0.99±0.0. These results suggest that all oxygen atoms of sulfate are derived from water-oxygen during anaerobic sphalerite oxidation irrespective of mineralogical difference and experimental conditions (biotic vs. abiotic) (Table 3.6 and Fig. 3.7).

The oxygen isotope fractionation effect ($\Delta^{18}O_{SO4-H2O}$) was estimated to be 7.02±0.9 ‰ and 7.0±0.7 ‰ for the biotic and abiotic Fe-bearing ZnS oxidation experiments, respectively and 9.6±4.7‰ and 7.6 ±1.1 ‰ for the biotic and abiotic ZnS oxidation experiments, respectively. Note that the value for $\Delta^{18}O_{SO4-H2O}$ of 9.6 ‰ has a relatively large error and is therefore not significantly different than the 3 other reported values. It is clear from these results that the oxygen isotope fractionation effect between sulfate and water is similar for both types of sphalerite during biotic and abiotic anaerobic oxidation (Table 3.6).

It is interesting to note that both the biological aerobic and anaerobic sphalerite experiments produced sulfate derived of 100 % water-oxygen and with similar $\Delta^{18}O_{SO4-H2O}$ values (Table 3.8).

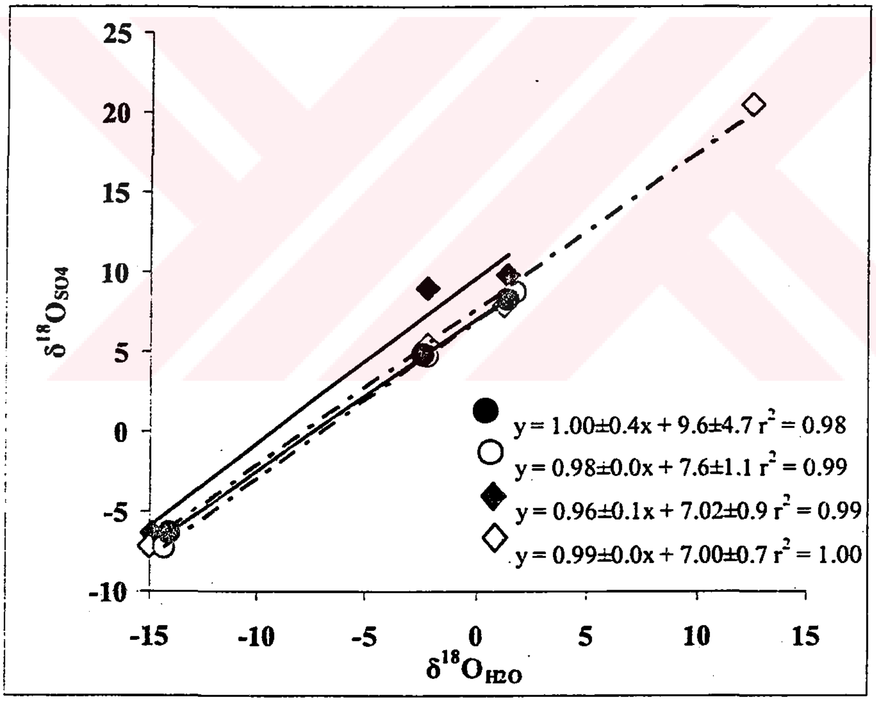

Figure 3.7 Relationship of the $\delta^{18}O$ of the SO_4 relative to the $\delta^{18}O$ of the experimental H_2O during anaerobic oxidation of ZnS and Fe-bearing sphalerite by A.ferrooxidans and abiotically. Bacterial ZnS, ●. Abiotic ZnS, ○. Bacterial Fe-bearing sphalerite, ◆. Abiotic Fe-bearing sphalerite, ◇ .

The $\delta^{34}S_{SO4}$ values from the anaerobic sphalerite experiments are depleted by ~2.6 ‰ relative to the $\delta^{34}S$ values of the ZnS and Fe-bearing sphalerite, indicating a sulfur isotope fractionation effect of ~ - 2.6 ‰ for both types of sphalerite (Table 3.8). The $\delta^{34}S$ value of elemental sulfur which was extracted from the ZnS and Fe-bearing sphalerite surface closely reflects the $\delta^{34}S$ value of the sphalerite source (Table 3.8).

Biotic and abiotic anaerobic galena experiments did not produce sulfate (data not shown). The XRD patterns taken from the filtered particulates at the end of the galena experiments showed that the solids were elemental sulfur, supporting that elemental sulfur was the only oxidation product. Furthermore, the sulfur isotope composition of these S^o particles were identical to that of galena, (Table 3.8). All these results from the galena experiments are consistent with the results of the study performed by Schippers et al. (1999).

3.3.6 Oxygen and sulfur Isotopic composition of sulfate from aerobic and anaerobic elemental sulfur experiments

The $\delta^{18}O_{SO4}$ values from the biotic S^o oxidation experiments, when plotted relative to $\delta^{18}O_{H2O}$ for the waters of preparation yielded slopes of 1.04 during both the short and the long-term experiments (Table 3.7) (see Fig. 3.8). The slopes obtained from both experiments indicate 100 % water-oxygen incorporation into sulfate. The oxygen isotope fractionation effect ($\Delta^{18}O_{SO4\text{-}H2O}$) is estimated to be 8.02 ± 0.92 ‰ and 8.9±1.15 ‰ for the short and long-term experiments, respectively (Fig. 3.8, Table 3.7).

The $\delta^{18}O_{SO4}$ values and oxygen isotope fractionation ($\Delta^{18}O_{SO4\text{-}H2O}$) effect from elemental sulfur experiments are almost identical to those obtained from both types of aerobic sphalerite oxidation experiments.

The $\delta^{34}S_{SO4}$ values are depleted by 1.2 – 2.0 ‰ during the short-term experiments, this depletion diminished with the extent of the reaction as inferred from the long-term experiments (Table 3.7). The sulfur isotope fractionation effect ($\Delta^{34}S_{SO4\text{-}S^0}$) was estimated as -2 ‰ and -1.2 ‰ for the short-term and long-term experiments, respectively.

Table 3.6 Oxygen and sulfur isotope composition of sulfate from short-term anaerobic bacterial and abiotic ZnS (pure ZnS and Fe-bearing ZnS) oxidation experiments.

	$\delta^{18}O_{H2Oinitial}$ (‰)	$\delta^{18}O_{H2Ofinal}$ (‰)	Avg.$\delta^{18}O_{SO4}$ (‰)	Avg.$\delta^{34}S_{SO4}$ (‰)	Avg.$\delta^{34}S_{S^0}$ (‰)
ZnS	-16.0	-15.1	-6.0	-9.4	n.d
Biological	-15.3	-14.9	-6.4	-10.4	-7.1
	-2.5	-2.2	9.0	-10.5	-8.0
	1.8	1.4	9.8	-10.2	-6.9
Abiotic	-16.3	-16.0	-7.4	-9.9	n.d
	-15.3	-15.0	-7.2	-10.2	-7.7
	-2.5	-2.2	5.5	-10.4	-7.4
	1.8	1.2	7.9	-10.8	-7.9
	12.5	12.5	20.5	n.d	n.d
(Zn,Fe)S	-15.3	-14.0	-6.4	-2.4	0.8
Biological	-15.3	-14.0	-6.4	-2.4	n.d
	-2.5	-2.4	4.8	-2.6	n.d
	1.8	1.4	8.3	-2.2	n.d
	-15.3	-14.3	-7.3	-2.1	0.4
Abiotic	-2.5	-2.2	4.7	-2.4	-0.1
	1.8	1.7	8.7	-2.4	n.d
Galena					
Biological					2.1
Abiotic					2.1

$\delta^{34}S$ value of galena was 2.1 ‰
$\delta^{34}S$ value of pure sphalerite was -7.7 ‰ and
$\delta^{34}S$ value of Fe-bearing sphalerite was 0.0 ‰ .

Sulfate also could not be obtained from the biotic and abiotic anaerobic elemental sulfur experiments (data not shown). Although replicate abiotic control experiments were performed with elemental sulfur as with the biological experiments, the concentration of sulfate produced was negligible and insufficient for isotopic analysis. These results are consistent with previous studies (Kortia, 1998) and indicate that abiotic reactions were insignificant for producing sulfate based on my experimental conditions.

Table 3.7. Oxygen and sulfur isotope composition of sulfate from aerobic bacterial elemental sulfur oxidation experiments.

Biological	$\delta^{18}O_{H2Oinitial}$ (‰)	$\delta^{18}O_{H2Ofinal}$ (‰)	Avg.$\delta^{18}O_{SO4}$ (‰)	Avg.$\delta^{34}S_{SO4}$ (‰)
	-15.3	-15.2	-7.6	2.5
	-15.3	-15.3	-8.5	2.3
	-2.5	-2.4	6.2	2.9
Short-term	-2.5	-2.4	6.3	n.d
	-2.5	-2.4	6.0	2.2
	1.8	1.8	9.3	2.6
	1.8	1.8	9.2	2.9
Long term	-15.3	-14.5	-5.1	3.4
	-15.3	-15.2	-7.1	3.2
	-2.5	-2.6	6.0	3.3
	-2.5	-2.7	6.4	3.5
	1.8	1.3	10.2	3.3

The $\delta^{34}S_S{}^o$ value used in the experiments was 4.4 ±0.1‰

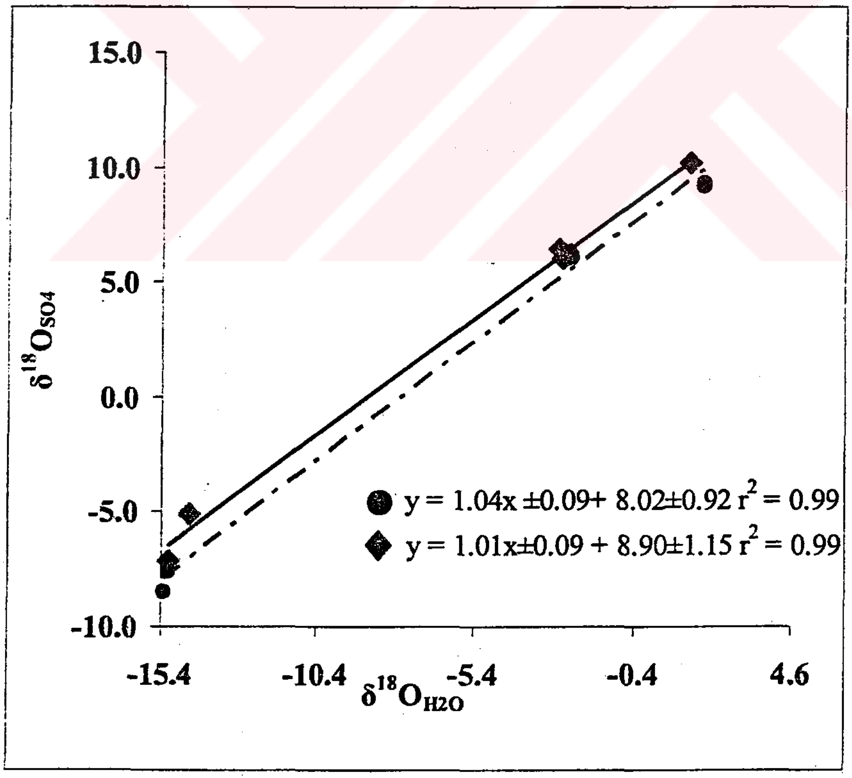

Figure 3.8 Relationship of the $\delta^{18}O$ of the SO_4 produced by *A.ferrooxidans* during aerobic elemental sulfur oxidation relative to the $\delta^{18}O$ of the experimental H_2O. Short-term (pH: 2.7 , 10 days), ●. Long-term(pH: 2.1, 20 days), ◆.

Table 3.8. Summary of oxygen and sulfur isotope fractionation during ZnS and S^o experiments.

Sample		% oxygen H_2O[a]	$\Delta_{SO4-H2O}$[b]	$\Delta_{SO4-ZnS}$	Δ_{SO4-S^o}	Δ_{S^o-ZnS}[c]
			Isotopic Fractionation			
ZnS	**Aerobic Exps.**					
	Short-term Biotic	96	9.0	-0.2	n.d	n.a
	Abiotic	60		-2.6	n.d	n.a
	Long-term Biotic	95	8.9	0.0	n.d	n.a
	Anaerobic Exps.					
	Biotic	104	9.6	-2.6	-3.0	0.4
	Abiotic	98	7.7	-2.6	-2.7	0.1
(Zn,Fe) S	**Aerobic Exps.**					
	Short-term Biotic	100	8.2	-0.3		
	Abiotic	n.d.	n.d	n.d	n.d	n.d
	Long-term Biotic	94	7.2	-0.3	n.d	n.d
	Anaerobic Exps.					
	Biotic	96	7.0	-2.4	-3.2	0.8
	Abiotic	100	6.9	-2.3	-2.6	0.3
S^o	**Aerobic Exps.**					
	Short-term Biotic	104	8.0		-2.0	
	Abiotic	n.d.	n.d	n.d	n.d	n.d
	Long-term Biotic	101	8.9		-1.2	
	Anaerobic Exps.					
	Biotic	n.d	n.d	n.d	n.d	n.d
	Abiotic	n.d	n.d	n.d	n.d	n.d

[a] % estimated from linear regressions between SO_4 and H_2O

[b] $\Delta_{SO4-H2O}$ = obtained from the intercept calculated from linear regressions.

[c] $\Delta_{S^o-ZnS} = (\delta^{34}S_{SO4}) - (\delta^{34}S_{S^0})$

3.4 Discussion

3.4.1 Rates of sphalerite and elemental sulfur oxidation

My experimental results illustrate that sphalerite is oxidized faster by bacterial reactions compared to abiotic reactions irrespective of the mineralogical composition (Fig. 3.1 and Fig. 3.2). According to sulfate production rates (SPR), Fe-bearing sphalerite is oxidized even faster compared to pure ZnS experiments. SPR is 0.022 (mg/ZnS-mg-day) for ZnS after 45 days whereas it is 0.100 (mg/ZnS-mg-day) for Fe-bearing sphalerite after 46 days. This result seems to be consistent with previous studies which indicated that the presence of iron within the gap bands make electron transfer more favorable and thus accelerates the oxidation rate (Crundwell, 1988). Furthermore, it is possible that the number of bacteria became higher in the Fe-bearing sphalerite experiments than in the ZnS experiments because *A. ferrooxidans* can obtain energy from Fe (II) oxidation in addition to sulfur, which result in a higher oxidation rate in the Fe-bearing sphalerite experiments. It should be note that the decrease in sulfate concentration at 54 days in the Fe-bearing sphalerite experiments may have resulted for the formation of Ferric iron-sulfate minerals. The drop in zinc concentration at this time suggests that zinc may have co-precipitated with the iron oxides (Fig. 3.2).

The SPR from the biotic and the abiotic anaerobic experiments is very similar for both types of sphalerite samples and significantly less than the aerobic experiments (Tables 3.1, 3.2 and 3.4). The SPR shows a decreasing trend with the extent of the reaction irrespective of mineralogical composition of sphalerite. This may be explained by the formation of non-sulfate sulfur species, such as elemental sulfur as suggested by previous studies (Turcotte, et al. 1993; Mcguire et al. 2001,; Sasaki, et al. 1995; Sasaki, 1997; Mycroft, et al. 1990, Schippers, et al. 1999; Descostes, et al. 2001). An increase in the Fe(II) concentration which was produced during oxidation of sphalerite by ferric iron is in agreement with this and suggests that the oxidation of sphalerite continues without sulfate production.

The SPR from the biological aerobic elemental sulfur experiments is similar to the SPR measured in the biological ZnS experiments at respective days (Table 3.4). For this comparison, the SPR from aerobic biological pure ZnS experiments is calculated by using only sulfur weight of the ZnS sample without the weight of Zn to make the starting weight of ZnS sample same with the elemental sulfur (266 mg) (Table 3.1 and Table 3.4). Similar SPR rate may be due to the formation and oxidation of elemental sulfur during ZnS oxidation experiments. The insignificant change in the pH profile during the ZnS experiments further suggests the formation of elemental sulfur as an intermediate, whose subsequent oxidation to sulfate equally produces an H^+ (reactions 2) after an H^+ is consumed via reaction 1.

The current experimental study shows that the oxidation of sphalerite and elemental sulfur at pH <3 under aerobic condition is largely controlled by biological reactions. Moreover, it is also showed that chemical oxidation of sphalerite by Fe(III) produce elemental sulfur as the main oxidation product.

3.4.2 Reaction mechanisms of elemental sulfur oxidation under aerobic conditions

The $\delta^{18}O_{SO4}$ values from the short and long-term biological aerobic elemental sulfur oxidation experiments showed that sulfate derived all of its oxygen atoms from water (Fig. 3.8) even though O_2 was the electron acceptor during oxidation. Bacterial oxidation of solid elemental sulfur proceeds via stepwise reactions in which SO_3^{2-} is an intermediate and other compounds such as thiosulfate and polythionates may form (Suzuki, et al. 1994; 1966; Pronk et al. 1990; Kelly, 1982). When *A. ferrooxidans* cells were incubated with elemental sulfur at pH 5, significant amounts of sulfite accumulated, indicating that sulfite can be an intermediate of elemental sulfur oxidation (Pronk et al. 1990). Oxidation of elemental sulfur at lower pH values does not result in the accumulation of sulfite, demonstrating that sulfite oxidation to sulfate by *A. ferrooxidans* is favored at low pH conditions (Pronk, J.T. et al. 1990). Similarly, oxidation of elemental sulfur to sulfate by *Thiobacillus thiooxidans*, all of the sulfate derived its oxygen atoms from water and did not include any oxygen from ^{18}O-labeled O_2 (Suzuki, et al. 1966, 1965). Mizutani and Rafter (1969) used soil as a source of bacteria to oxidize elemental sulfur with two waters having distinctly different oxygen isotopic composition. They found that water contributed all of the sulfate oxygen with an insignificant kinetic oxygen isotope fractionation effect ($\Delta_{SO4-H2O}$ = ~0). My experimental results are consistent with the results of the previous studies.

The complete incorporation of water-oxygen into sulfate may occur due to 1-) oxygen isotope exchange between a sulfite intermediate and water, 2-) an enzymatic electron transport system where O_2 does not make directly contact with the sulfur atoms (as pathway 2). As previous studies suggested, sulfite is more likely an intermediate during elemental sulfur oxidation. It is been demonstrated that oxygen isotope exchange between water and sulfite is on the order of nanoseconds at low pH (<3) (Holt et al. 1981). Therefore, one can safely assume that this process may be partly responsible for the water-oxygen incorporation into sulfate. The electron transport system (ETS) for S^o oxidation may also explain the complete incorporation of water oxygen into sulfate. *Thiobacillus spp*., derive energy from sulfur oxidation, but the electrons from S^o pass through several steps of the ETS before they reduce O_2 to water in the final step. Consequently, the reduction of O_2 to water can be physically separated from the final oxidation of SO_3^{2-} to SO_4^{2-} and the oxygen in sulfate likely was derived from water (Kelly, 1982). The transfer of electrons from sulfur to the electron acceptor (O_2) provides energy by cycling electrons through the electron transport system (Ehrlich, 1981). The final step in the electron transport system is reduction of oxygen to form water, not incorporate into sulfate.

Based on my own work here and previous studies, the following pathway is proposed for bacterial oxidation of elemental sulfur (Kelly, 1982). According to the pathway, elementa sulfur is first oxidized to sulfite.

$$S^o + O^*_2 + 2\cancel{H_2}O \rightarrow \cancel{SO}_3^{-2} + \cancel{H_2}O^* + 2H^+ \qquad (15)$$

$$S\cancel{O}_3^{2-} + \cancel{H_2}O + 1/2O^*_2 \rightarrow SO_4^{2-} + H_2\cancel{O}^* \qquad (16)$$

$$S^o + H_2O + 3/2\,O_2 \rightarrow SO_4^{2-} + 2H^+ \qquad (17)$$

Sulfite may be enzymatically oxidized directly to sulfate by a cytochrome c-linked oxidoreductase (reactions 16a-c), incorporating water-oxygen into sulfate (16a). The oxygen isotope exchange between sulfite and water could also occur at step 16a.

$$SO_3^{2-} + 2cyt\ c(ox) + H_2O \rightarrow SO_4 + 2cyt\ c(red) + 2H+ \ (ATP) \quad (16a)$$

$$2cyt\ c(red) + 2cyt\ oxidase(ox) \rightarrow 2cyt\ c(ox) + 2cyt\ oxidase(red) \ (+ATP) \quad (16b)$$

$$2cyt\ oxidase(red) + O_2 + 4H^+ \rightarrow 2cyt\ oxidase(ox) + 2H_2O \quad (16c)$$

$$SO_3^{2-} + H_2O + 1/2O^*{}_2 \rightarrow SO_4^{2-} + H_2O^* \quad (16)$$

This mechanistic pathway suggests the complete incorporation of H_2O derived oxygen, consistent with my experimental results, even though the net stoichiometry (17) does not suggest this.

The kinetic oxygen isotope fractionation effect between sulfate and water was estimated to be 8 ‰ for the short-term and 8.9 ‰ for the long-term lower pH experiments (Fig. 3.8, Table 3.8). These results appear to contradict the results of Mizutani and Rafter (1965) who reported no oxygen isotope fractionation between sulfate and water during oxidation of elemental sulfur by soil bacteria. Mizutani and Rafter attributed this fractionation to insignificant oxygen isotope exchange between sulfite and water However, these authors do not report if the bacteria were in fact sulfur–oxidizers. Therefore, it is not clear that the 0 ‰ fractionation effect was due to sulfur oxidizing bacteria. The kinetic oxygen isotope fractionation measured in this study could be due to oxygen isotope exchange between sulfite and water, which increases with decreasing pH and thus might occur rapidly at the pH of our experiments (Pearson and Rightmire, 1980; Holt et al. 1981; Chiba and Sakai, 1985).

The abiotic elemental sulfur experiments did not produce significant amounts of sulfate, indicating that elemental sulfur oxidation is largely controlled by biological reactions which consistent with previous studies (Curutchet, et al. 1996; Garcia et al. 1995a, 1995b)

3.4.3 Reaction mechanisms of sphalerite oxidation under aerobic conditions

In good agreement with the $\delta^{18}O_{SO4}$ values from the bacterial aerobic S^o oxidation experiments, the $\delta^{18}O_{SO4}$ values from both the ZnS and Fe-bearing sphalerite experiments also indicate complete incorporation of water-oxygen into sulfate during the biotic short and long-term experiments (Fig. 3.5 and Fig. 3.6). Although the

$\delta^{18}O_{SO4}$ values were similar between the biological aerobic Fe-bearing sphalerite and pure ZnS oxidation experiments, suggesting similar reactions for each, there was no mass balance for the sulfate and zinc products for the Fe-bearing sphalerite. This is likely due to precipitation of ferric iron-sulfate minerals (e.g., jarosite, schwertmannite) as evidenced by decreasing sulfate concentrations (Fig. 3.2). It is also expected that the solution chemistry during the Fe-bearing sphalerite oxidation would be more heterogeneous since Fe (II) oxidation and precipitation of Fe-oxides can also occur. Therefore, it would be difficult to obtain mass balance as for the pure ZnS experiments. These results are surprising since previous studies indicate direct oxidation of pyrite which involves enzymatic reactions incorporated O_2 into the sulfate product (Taylor et., al; 1984a; 1984b). Given the similar $\delta^{18}O_{SO4}$ values from the aerobic sphalerite and S^o oxidation experiments, oxidation of sphalerite also likely utilizes the same cyt-pathway (15, 16a-c) as for S^o oxidation. Therefore, as previously discussed for S^o oxidation, all the electrons from the sulfur-side of sphalerite are shuttled through the electron transport system (ETS) where aerobic respiration takes place, resulting in the formation of water from O_2 reduction (Elrich, 1981, Kelly, 1982). The energy obtained from the ETS goes into high-energy adenosine triphosphate (ATP) bonds which are needed by bacteria for energy consuming reactions (Kuenen, et al. 1975; Kelly, 1982). The only major difference between oxidation of sphalerite and S^o is the initial oxidation of ZnS to an S^o intermediate as shown below in reaction 18. Elemental sulfur formation during bacterial and abiotic sphalerite oxidation was previously reported elsewhere (Garcia, 1995b; Fowler, and Crundwell, 1999)

$$ZnS + 1/2O_2 + \cancel{2H^+} \rightarrow \cancel{S^o} + \cancel{H_2O} + Zn^{+2} \qquad (18)$$

$$\cancel{S^o} + 2\cancel{H_2O} + O^*_2 \rightarrow \cancel{SO_3^{2-}} + \cancel{H_2O}^* + \cancel{2H^+} \qquad (19)$$

$$\cancel{SO_3^{2-}} + \cancel{H_2O} + 1/2O^*_2 \rightarrow SO_4^{2-} + \cancel{H_2O}^* \qquad (20)$$

$$\mathbf{ZnS + 2O_2 \rightarrow SO_4^{2-} + Zn^{+2}} \qquad \mathbf{(21)}$$

In this oxidation pathway, the dissolution of sphalerite is initiated by proton attack (H^+) followed by a series of reactions giving rise to elemental sulfur (reaction 18) (Schippers et al. 1999; Sand et al. 2001; Mcguire, et al. 2001;Mycroft, et al. 1990;

Sasaki et al. 1995; Turcotte, et al. 1993; Hazeu et al. 1988). Because the solubility of elemental sulfur in the water is very low (Steudel, et al. 1987; Roy et al. 1970), only in the presence of sulfur oxidizing bacteria does continued oxidation of elemental sulfur to sulfate occur. This likely explains why the abiotic sphalerite oxidation experiments produced very little amount of sulfate compared to the biological reactions (Fig. 3.1 and Fig. 3.2). The subsequent oxidation of elemental sulfur causes the formation of sulfite and yields protons needed for further dissolution of ZnS (reactions 18, 19). According to this proposed pathway, pH should be stable during sphalerite oxidation since production and consumption of protons are in equilibrium (reactions 18 and 19). The constant pH profile observed during the biological ZnS oxidation experiments is consistent with this ides (Fig. 3.1, Table 3.1).

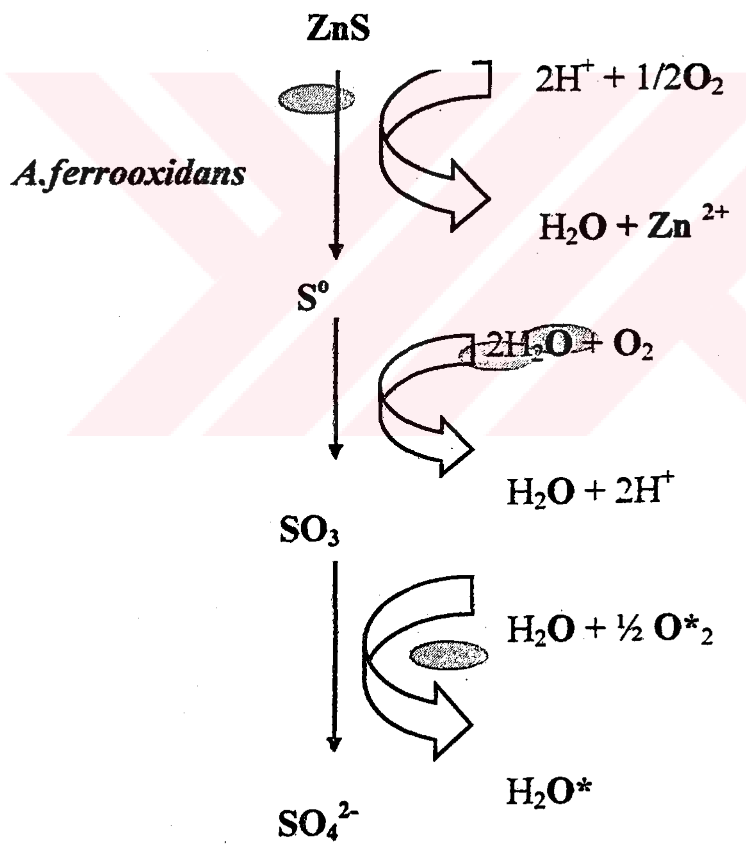

$$ZnS + 2O_2 \longrightarrow SO_4^{2-} + Zn^{2+}$$

Figure 3.9 Proposed sphalerite and elemental sulfur oxidation pathways for biological experiments under aerated conditions, as originally presented for sulfide oxidation by Kelly et al. (1982).

If reaction 21 represents the net stoichiometry of the proposed sphalerite oxidation pathways, then accordingly, if no sulfate is lost from the system by precipitation reactions, then the molar sulfate concentration should equal the molar concentration of dissolved zinc (reaction 21). In fact the sulfate and zinc concentrations are similar at 60 days from the biological ZnS oxidation experiments in agreement with the net stoichiometry of reaction 21 (Table 3.1). Nonetheless, as illustrated for the S^o oxidation experiments, the net stoichiometry does not represent the actual oxygen sources to sulfate.

Abiotic control ZnS experiments produced sulfate that has 60 % oxygen atoms from H_2O and 40 % from molecular O_2. Larger molecular O_2 incorporation into sulfate suggests that sulfide oxidation may occur via a metal centered oxidation in which sulfur side of sphalerite is directly attacked by molecular O_2 (or an intermediate derived from O_2) and electron transfer proceeds via an inner-sphere mechanism as proposed theoretical studies by Luther III, (1990); Wehrli, (1990). The difference in the oxygen source of sulfate between the abiotic and biological experiments may stem from different oxidation mechanisms. It is most likely that elemental sulfur also formed during abiotic sphalerite oxidation since the pH of the solution was acidic (pH 3) at the beginning of the experiments. The increase in pH during aerobic abiotic oxidation may be explained by the formation of elemental sulfur which consumes protons (Fig. 3.1, reaction 18). It is well known that the formation of a porous layer of elemental sulfur product on the surfaces of sphalerite may limit the rate of reaction by preventing the diffusion of soluble reactants through this layer, as previously reported for the chemical leaching of sphalerite (Fowler and Crundwell, 1999). The relatively low rates of sulfate production in the abiotic experiments are consistent with this.

Sulfate formed in the abiotic reactions was likely due to proton attack on the sphalerite. During the attack, hydrogen sulfide (H_2S) first forms prior to its oxidation to S^o (Schippers et al. 1999). Since the experimental flask was continuously purged with air, H_2S should be quickly oxidized to sulfate by O_2. Although hydrogen sulfide could not be measured during the experiments, hydrogen sulfide odor was noted and was likely the source of sulfate during the abiotic sphalerite oxidation.

3.4.4 Reaction mechanisms of sphalerite oxidation under anaerobic conditions

Sphalerite can be oxidized by ferric iron in addition to O_2 molecules (Fowler and Crundwell, 1999; Crundwell, 1987). Because Fe (III) is a strong oxidant and its concentration is generally high under acidic conditions, oxidation of sphalerite by ferric iron may significantly contribute to the formation of AMD sites. Therefore, it is important to reveal oxidation pathway of sphalerite by ferric iron and to observe whether the sulfate product has a unique $\delta^{18}O$ value compared to sulfate produced during aerobic ZnS oxidation.

The $\delta^{18}O_{SO4}$ values from the anaerobic sphalerite experiments (ZnS and Fe-bearing) showed 100 % water-oxygen incorporation into sulfate and a very similar oxygen isotope fractionation effect as for the aerobic sphalerite and elemental sulfur oxidation experiments (Table 3.6,Fig. 3.7).

The following reaction steps, explain the oxidation of sphalerite by Fe (III) ions at pH 2 (Sand et al. (2001)). According to this pathway, the first product of sphalerite oxidation is the formation of hydrogen sulfide followed by additional oxidation to elemental sulfur (reactions 22-23) (Sand et al. 2001; Schippers et al. 1999; Tributsch, et al. 1981). Furthermore, H_2S can be oxidized to H_2S^{*+} radical which oxidized to elemental sulfur by Fe (III) through chain elongation of the polysulfides (Steudel, R., 1996).

$$ZnS + Fe^{3+} + H \longrightarrow Zn^{2+} + 0.5\ H_2S_n + Fe^{2+} \qquad (22)$$

Thiosulfate may arise by a side reaction 23 or 24 through oxidation of bisulfite formed during oxidation of hydrogen sulfide (Sand et al. 2001).

$$H_2S_n + 6Fe^{3+} + 3H_2O \longrightarrow H_2S_2O_3^- + [(n-2)/8]\ S_8 + 6Fe^{2+} + 6H^+ \qquad (23)$$

$$\text{Or } 1/8\ S_8 + \underset{\substack{\uparrow\downarrow\ H_2O \\ SO_4}}{HSO_3^-} \longrightarrow HS_2O_3^- \qquad (24)$$

A minor amount of sulfate forms as product of thiosulfate reaction 25

$$HS_2O_3^- + 8Fe^{3+} + 5H_2O \longrightarrow 2SO_4^{2-} + 8Fe^{2+} + 10H^+ \quad (25)$$

Elemental sulfur forms as a major species during anaerobic (reaction 23) and aerobic sphalerite oxidation. The sulfate concentrations from the anaerobic experiments are significantly less than those produced from the aerobic experiments (Table 3.3). This is likely due to elemental sulfur not being further oxidized to sulfate in the anaerobic experiments. Although it is demonstrated that *A. ferrooxidans* has the ability to oxidize elemental sulfur under anaerobic conditions by using Fe(III) as electron acceptor (Sugio, et al. 1985), similar sulfate concentrations were measured in the biotic and abiotic anaerobic sphalerite experiments. This suggests that chemical oxidation of sphalerite by $Fe(III)_{aq}$ was dominant in both types of experiments. Biological and abiotic anaerobic elemental sulfur oxidation experiments showed no significant sulfate production by Fe^{3+} oxidation (data not shown). These results suggest that elemental sulfur oxidation (biological and abiotic) could not have occurred under anaerobic conditions. Therefore, it is reasonable to speculate that sulfate production during the anaerobic experiments was likely due to decomposition of the hydrogen sulfide radicals (reactions 23-25) as suggested by Sand et al, (2001).

3.4.5 Oxygen isotope fractionation

The oxygen isotope fractionation effect ($\Delta^{18}O_{SO4-H2O}$) was estimated as 9.6 ‰ and 7.7 ‰ for the biotic and abiotic anaerobic ZnS experiments, respectively. The respective values were 7 ‰ and 6.9 ‰ for the Fe-bearing ZnS experiments. These results are similar to those obtained from the biological aerobic sphalerite and elemental sulfur experiments, and suggests that oxygen isotope exchange between water and sulfite may be responsible for the similar oxygen isotope fractionation effect between all of these experiments (reaction 24).

The similar oxygen isotope fractionation effect between sulfate and water ($\Delta^{18}O_{SO4-H2O}$) for all of the sphalerite and S^o oxidation experiments may be due to a common and rate-controlling oxidation step that primarily controls this fractionation. Sulfite is a common intermediate during both sphalerite and elemental sulfur oxidation.

Oxygen isotope exchange between sulfite and water is likely to occur under the low pH of our experimental conditions and may be responsible for the similar oxygen isotope fractionation effect. It is reported that oxygen isotope exchange between sulfite and water is on the order of nanoseconds under acidic conditions in contrast to sulfate-oxygen and water-oxygen exchange reactions (Lloyd, 1968; Pearson et al. 1980; Holt et al. 1981). The time required for oxygen isotope exchange between sulfate and water was estimated to be on the order of 250.000 yr, at pH 7 and 25 °C (Llyod, 1968). Zak et al. (1980) reported no evidence of oxygen isotope exchange between sulfate and water for pore waters taken from deep marine sediments. Further, Chiba and Sakai (1985)'results from laboratory experiments indicate a water-sulfate oxygen exchange rate in the oceans of ~10^9 year ($t^{1/2}$) at 100 to 300 °C and pH 2 to 7. Extrapolating the experimental data of Hoering and Kennedy (1957) and Chiba and Sakai (1985), at pH 0, 1 and 2, the respective half times required for SO_4 –H_2O oxygen isotopic exchange is ~1 to 30 year , 25 to 100 years, and ~10^3 to 10^5 years. Based on these results, it can be assumed that sulfate–water oxygen isotopic exchange is unlikely under our experimental conditions.

Sulfite-water oxygen isotope exchange reactions seem more likely under my experimental conditions. Holt et al., (1981) investigated the oxygen isotope fractionation effect during sulfite oxidation to sulfate under different experimental conditions, some of which are similar to acid mine drainage. For SO_3^{2-} in isotopic equilibrium with water, data from their experiments indicate $\Delta^{18}O_{SO4\text{-}H2O}$ + 10 ‰ when sulfite reacts with O_2 stoichiometrically at 24°C and $\Delta^{18}O_{SO4\text{-}H2O}$ +8 ‰ during sulfite oxidation by bromine.

The results of my experiments seems to be consistent with the range reported by these studies. Although the oxidation rate is significantly different for both types of sphalerite and elemental sulfur experiments, the similar $\Delta^{18}O_{SO4\text{-}H2O}$ values suggest that isotopic fractionation may be controlled largely by isotopic equilibrium between water and sulfite. Fractionation was not a function of oxidation rate under the experimental conditions, which is consistent with SO_3^{2-} - H_2O oxygen isotope exchange rates of a few nanoseconds at pH ~2 (Holt et al. 1983, 1981)

Alternatively, Mizutani et al. (1969, 1973) and Fritz, et al. (1973) indicated oxygen isotope exchange between sulfate and water proceeds through enzyme-bound intermediates during the bacterial reduction of sulfate. Similar enzyme mediated oxygen isotope exchange processes may also have occurred during sulfide oxidation to sulfate in my experiments. However, because the biotic and abiotic anaerobic sphalerite oxidation experiments showed similar oxygen isotope fractionation as the aerobic biological experiments, enzyme mediated processes are not as likely as oxygen isotope exchange between H_2O and sulfite.

These results from all of the sphalerite oxidation experiments contrast significantly from the anaerobic pyrite oxidation experiments where $\Delta^{18}O_{SO4-H2O}$ was ~3.6 ‰ This fractionation is significantly different than those obtained from anaerobic pyrite oxidation (3.6 ‰). In contrast to sphalerite experiments, higher sulfate concentrations also resulted from the anaerobic pyrite oxidation, possibly a result of different oxidation mechanisms. Furthermore, anaerobic galena oxidation experiments only produced elemental sulfur, further suggesting a different oxidation mechanism. Differences in oxygen isotope fractionation between sulfate and water may suggest different oxidation mechanism for particular metal sulfide minerals as suggested by previous studies (Schippers et al,. 1996, 1999; Sand et al. 2001).

3.4.6 Sulfur isotope fractionation associated with aerobic and anaerobic sphalerite oxidation and aerobic elemental sulfur oxidation

The $\delta^{34}S_{SO4}$ values from both aerobic sphalerite (ZnS & Fe-bearing) oxidation experiments were very similar to the $\delta^{34}S$ of the parent minerals and thus showed insignificant sulfur isotope fractionation (Table 3.8). These results may indicate that most of sulfur moiety of sphalerite is oxidized to sulfate under acidic conditions. These results are consistent with the fact that sulfur isotope fractionation associated with oxidation of solid phase metal sulfides is insignificant compared to oxidation of aqueous HS^- (Nakai and Jensen, 1964; Taylor et al. 1984; Fry et al. 1986, McCready and Krouse, 1982; Mandernack et al. 2003). Sulfur isotope fractionation during sulfide oxidation under different experimental conditions was reported in previous studies (Kaplan and Rafter, 1958; Kaplan and Rittenberg, 1964; Fry et al. 1988; Sakai, 1957; Fry et al. 1986, 1988 ; Taylor, et al. 1984b; Seal and Wandless, 1997). The largest sulfur isotope fractionation of ~-15 ‰ was reported by Kaplan and Rittenberg (1964) during oxidation of dissolved Na_2S in experiments inoculated with *T. thiooxidans*. They attributed the fractionation to isotopic exchange between the intermediate sulfur species and sulfate. Toran and Harris (1989) measured a sulfur isotope fractionation of -2 to -5.5‰ for FeS_2 and ZnS oxidation experiments inoculated with a mixture of *T. neopolitanus*, *T. intermedius*, and *T. ferrooxidans* and run at a pH of 5 to 6. A major difference between our experiments and Toran and Harris's study is pH, which may control the formation and oxidation of intermediate sulfur species to sulfate and thus influence the net fractionation. A fractionation of -4.7 ‰ was reported by Chamber and Trudinger (1978) during oxidation of thiosulfate by *T. intermedius* at neutral pH. Fry et al., (1988) reported fractionation of 5.2 ‰ during abiotic oxidation of Na_2S in aqueous solution at pH 11. These results indicate that fractionation is possibly caused by the formation of intermediate sulfur species as a function of pH (Kaplan and Rittenberg, 1964; Goldhaber, 1983).

In contrast to pH conditions ≥ 7, and consistent with my experimental results Taylor and Wheeler (1994) did not observe significant sulfur isotope fractionation between sulfide mineral and sulfate at low pH (<3). Fry et al. (1986) reported no fractionation during oxidation of thiosulfate by *T. versutus* at pH 8.5.

Aerobic biological oxidation of elemental sulfur produced sulfate enriched in ^{32}S by 2 ‰ during the short-term experiments (Table 3.8). This enrichment decreased with the extent of the reaction and was estimated as 1.2 ‰ during the long-term biological experiments. These results are consistent with those of McCready and Krouse (1982) who reported ~-1 ‰ sulfur isotope fractionation between sulfate and the elemental sulfur substrate in experiments inoculated with *Thiobacillus*. Sulfur isotope fractionation observed in our experiments may be due to sulfur isotope exchange between intermediate sulfur species as a function of pH. Decreasing fractionation with decreasing pH, as inferred from the long-term lower pH experiments, seems to be consistent with this possibility.

In contrast to the aerobic biological sphalerite experiments, one of the aerobic abiotic ZnS oxidation experiments produced sulfate enriched in ^{32}S~ 2.6 ‰. This result is consistent with the $\delta^{34}S_{SO4}$ values from the biotic and abiotic anaerobic ZnS and Fe-bearing sphalerite experiments, where Fe^{3+} was the oxidant and bacterial influence probably non-existing. The similar sulfur isotope fractionation between these experiments may have occurred due to same oxidation pathway and incomplete oxidation of intermediate sulfur species (e.g. elemental sulfur) to sulfate. Because pH of the both experimental solutions was acidic, sphalerite may have been first oxidized to hydrogen sulfide which undergoes additional oxidation to S^o under both experimental conditions (Sand, et al. 2001; Schippers et al. 1999). Because bacterial activity non-exist in the both systems, subsequent quantitative oxidation of S^o to sulfate may have not occurred, causing sulfur isotope fractionation between sulfate and the source sphalerite. The insignificant sulfur isotope fractionation between the sphalerite and the elemental sulfur which was extracted from the surface of sphalerite in the anaerobic experiments indicates that hydrogen sulfide formed during oxidation of sphalerite was largely oxidized to elemental sulfur and thus provide further support for incomplete oxidation to sulfate (Table 3.8). Furthermore, significant sulfur isotope fractionation between sulfate and the source sphalerite during anaerobic oxidation further support that sulfate was the minor oxidation product. Therefore, it is reasonable to conclude that the similar sulfur isotope fractionation between the aerobic abiotic and anaerobic experiments is likely due to incomplete oxidation of sulfur moiety of sphalerite to sulfate. This result is also consistent with chemical sphalerite oxidation pathway proposed by Sand et al. (2001) and Schippers et al. (1999) under aerobic and anaerobic conditions.

The results from the anaerobic (biotic and abiotic) and aerobic abiotic sphalerite oxidation experiments showed that the $\delta^{34}S_{SO4}$ values produced by chemical oxidation of sphalerite at low pH (<3) enriched in ^{32}S ~-3 ‰ relative to the aerobic biological experiments. Therefore, -3 ‰ sulfur isotope fractionation effect ($\Delta^{34}S_{SO4-ZnS}$) can be used to elucidate chemical oxidation of sphalerite whereas insignificant sulfur isotope fractionation effect (~±0.3 ‰) could be good indicative of sphalerite oxidation by bacteria under O_2 saturated conditions.

In contrast to sphalerite experiments, the $\delta^{34}S_{SO4}$ values from biological and abiotic pyrite oxidation experiments under both anaerobic and aerobic conditions closely reflect the $\delta^{34}S$ of the source pyrite. These results indicate that sulfur mineralogy may have a control on oxidation pathways of sulfide minerals and fractionation of sulfur isotopes.

4 IRON ISOTOPE FRACTIONATION DURING MICROBIALLY-STIMULATED FE[II] OXIDATION AND FE[III] PRECIPITATION

4.1 Introduction

Iron is common in freshwater, marine, and soil environments and is often coupled to the cycling of C, N, S, and O (Ehrlich, 1990; Ferris et al., 1989; Nealson et al., 1988; Jones, 1986; Ghiorse, 1984). Ferric oxyhydroxides serve as important electron acceptors for the anaerobic decomposition of organic carbon in many aquatic and terrestrial environments (Kappler, et al., 2004; Glasauer, et al., 2003; Lovely, et al., 1987; 1986a and b). Ferric oxyhydroxides formed during Fe[II] oxidation also scavenge many trace metals in aquatic environments such as acid mine drainage (AMD) and thus strongly influence the fate and transport of heavy metals (Blowes et al., 2003; Jambor et al., 2003). In oxygenated, low pH (<3) environments, Fe[II] oxidation is largely driven by bacteria due to slower kinetics associated with chemical reactions (Savic et al., 1998; Singer and Stumm, 1970; Nordstrom et al.,1997; Lizama et al., 1989). Iron oxidation at low pH is often mediated by *Acidothiobacillus* and *Leptosprillum* species that are commonly found in AMD (Brett, 2003; Schrenk et al., 1998; Nordstrom et al., 1997). Conversely, Fe[II] oxidation often proceeds abiotically in oxygenated environments at higher pH.

Biological and chemical oxidation of ferrous iron aqueous species ($Fe[II]_{aq}$) to ferric iron precipitate ($Fe[III]_{ppt}$) occurs through a variety of $Fe[II]_{aq}$ and ferric iron aqueous species ($Fe[III]_{aq}$) depending on the particular geochemistry of a given system. Following oxidation of $Fe[II]_{aq}$, various $Fe[III]_{aq}$ anion complexes may form [e.g. $Fe(OH)_3$, $Fe_2(CO_3)_3$, $Fe_2(SO_4)_3$] depending on pH and anion concentrations in the water (Jambor et al., 2003). Subsequent precipitation of different $Fe[III]_{ppt}$ minerals occurs, and the crystal form may be influenced by the $Fe[III]_{aq}$ species. Biological and/or chemical oxidation pathways may leave a unique Fe isotope "fingerprint" on the resulting ferric iron precipitates. Therefore, Fe isotope signatures of these solids may be a useful tool for tracing the geochemical conditions and/or biological influences controlling Fe[II] oxidation (Anbar, 2004; Croal et al., 2004; Beard et al., 2003).

Recent studies have revealed that metabolic processes, which include multiple enzymatic oxidation steps, can apparently produce significant isotopic fractionation of Fe. Beard et al. (1999) observed a ~ -1.3 ‰ fractionation between $Fe[II]_{aq}$ and a ferrihydrite substrate during microbial Fe[III] reduction by *Shewanella algae*. Croal et al. (2004) reported a similar fractionation (-1.5 ‰) between $Fe[II]_{aq}$ and $Fe[III]_{ppt}$ during Fe[II] oxidation by an anaerobic and photoautotrophic bacteria. It is further hypothesized that Fe isotope variations that have been seen in sedimentary rocks, ferromanganese nodules, and Precambrian banded iron formation [ranging from -1.6‰ to 0.9 ‰ when compared to terrestrial igneous rocks (0‰, ±0.1‰)], could be indicative of biological origins (Beard et al., 1999; 2003). However, Mandernack et al. (1999) observed no significant Fe isotope fractionation between aqueous Fe[II] and magnetite produced intra-cellularly by two different strains of magnetotactic bacteria, one of which was grown in replicate under micro-aerophilic and anaerobic conditions with different iron salts. They suggested that iron isotopes on their own might not always be useful for tracing biological origins in geological and extraterrestrial materials.

In addition to the demonstration of microbial Fe isotope fractionation, several recent studies have shown that abiotic chemical reactions can produce significant fractionation of Fe isotopes (e.g., Roe et al., 2003; Johnson et al., 2002; Skulan et al., 2002; Matthews et al., 2001; Anbar et al., 2000). For example, Bullen et al. (2001) conducted field and laboratory studies of abiotic Fe[II] oxidation and subsequent precipitation of ferrihydrite under oxygenated conditions at circum-neutral pH. $Fe[III]_{ppt}$ produced experimentally was observed to have $\delta^{56}Fe$ as much as 2‰ greater than that of co-existing aqueous Fe. They proposed that the extent of this fractionation could depend on the complexation of Fe[II] with various anionic ligands. For example, they suggested that readily oxidized $Fe[II](OH)_x$ aqueous species may have greater $\delta^{56}Fe$ than bulk $Fe[II]_{aq}$. Thus, the resulting mineral product of oxidation could carry the isotopic signature of this reactive Fe[II] aqueous species or some reaction intermediate. On the other hand, Schauble et al. (2001) provided theoretical estimates of equilibrium Fe isotope fractionation of ~3 to 6‰ among different Fe[II] and Fe[III] aqueous species bonded to different anionic ligands at 25°C . In response to these earlier studies, Johnson et al. (2002) and Welch et al. (2003) carried out isotope exchange experiments using isotopically-enriched Fe tracers, and observed a ~2.9 ‰ fractionation between $Fe[III]_{aq}$ and $Fe[II]_{aq}$ at 22 ±2°C, which they attributed to the equilibrium isotope effects.

Based on these previous studies, it is clear that the extent and direction of Fe isotope fractionation accompanying biologic and non-biologic processes are similar. Thus, our ability to determine whether biological and/or chemical reactions have contributed to Fe isotopic fractionation observed in the rock record remains unclear. If we hope to be able to assess potential biological origins of natural ferric iron precipitates from their measured $\delta^{56}Fe$ values, it is valuable to simulate and attempt to distinguish biological and non-biological Fe isotope fractionation processes in controlled laboratory experiments. The low pH environment (i.e., pH < 3) provides an ideal experimental condition to test the ability of various processes to fractionate Fe isotopes. However, no data currently exists related to biological Fe isotope fractionation at low pH. Experiments at low pH are particularly attractive due to general sluggishness of many (but not all) non-biological reactions, broad co-stability of Fe[II] and Fe[III] aqueous species, and availability of numerous acidophilic bacteria that stimulate Fe redox processes. For example, study of the reaction intermediates leading to Fe[III] precipitates at low pH as a result of biological and non-biological Fe[II] oxidation may help to determine: 1) if bacteria that stimulate the oxidation step are capable of imparting a unique iron isotope "biosignature" to the products, and 2) if the Fe isotope contrast between $Fe[II]_{aq}$ and $Fe[III]_{ppt}$ is determined by fractionation accompanying the oxidation step, by equilibrium exchange between Fe[II] and Fe[III] aqueous species, by speciation of $Fe[II]_{aq}$ and $Fe[III]_{aq}$ with various anionic ligands, by kinetic effects related to Fe[III] precipitation, or by some combination of these factors.

In this study I investigated the biological and non-biological influences on the $\delta^{56}Fe$ values of coexisting $Fe[II]_{aq}$, $Fe[III]_{aq}$, and $Fe[III]_{ppt}$ formed as a result of Fe[II] oxidation during controlled laboratory experiments with *Acidothiobacillus ferrooxidans* at pH <3. This experimental work is a critical part of a larger study of Fe redox and cycling processes in a natural acid mine drainage setting. Rather than just focusing on the Fe isotope contrast between $Fe[II]_{aq}$ and $Fe[III]_{ppt}$ as in previous studies of biological Fe isotope fractionation (e.g., Beard et al., 1999; Croal et al., 2004), I also measured the Fe isotope fractionation between coexisting $Fe[II]_{aq}$ and $Fe[III]_{aq}$, and conducted experiments to determine the controls on Fe isotope fractionation during subsequent precipitation of $Fe[III]_{ppt}$. Consequently, from this experimental approach, it is possible to more accurately asses the possible biological influence of Fe isotope fractionation during Fe[II] oxidation.

4.2 Experimental Design

4.2.1 Bacterial cultures

The acidophilic Fe[II] oxidizing bacterium, *Acidithiobacillus ferrooxidans* (23270) (*A.ferroxidans* formerly, *Thiobacillus ferrooxidans*) was obtained from the American Type Culture Collection (ATCC) and used in all biological experiments. Bacteria were maintained in a modified 2039-ATCC medium that contains the following per liter: 0.8 g $NH_4(SO_4)$, 2 g $MgSO_4 \cdot 7H_2O$, 0.1 g K_2HPO_4; 22 g $FeSO_4.7H_20$ and 5 ml Wolfe's mineral solution (1.5 g nitrilotriacetic acid , 3 g $MgSO_4.7H_2O$, 0.5 g $MnSO_4.7H_2O$, 1 g NaCl, 100 mg $FeSO_4.7H_20$, 100 mg $CoCl_2.6H_2O$, 100 mg $CaCl_2$, 100 mg $ZnSO_4.7H_2O$, 100 mg $CuSO_4.7H_2O$, 10 mg $AlK(SO_4)_2.\ .12H_2O$, 10mg H_3BO_3, 10mg $Na_2MoO_4.2H_2O$ per liter). The medium was prepared by adding the above and 5 ml Wolfe's mineral solution to 795 ml de-ionized (DI) water. This salt solution was then filter-sterilized using pre-sterilized 0.2μm cellulose acetate filters (Gelman sciences) and the salt solution was adjusted to 2.3 with trace-metal grade H_2SO_4 acid. $FeSO_4.7H_20$ (22 gr) salt was then added to 200 ml acidified-DI water and immediately filter-sterilized. The salt medium and the Fe[II] solution were aseptically combined. *A. ferrooxidans* was subcultured three times before being grown for the iron isotope experiments.

4.2.2 $FeSO_4$ oxidation at 25 °C

The first set of biological experiments was carried out at 25°C. For these experiments, 100 ml of filter-sterilized ferrous sulfate medium was added to 200 ml sterile-serum bottles inoculated with 2 ml of the *A.ferrooxidans* culture. The culture had been incubating for 10 days inside the closed serum bottles. To reduce inevitable carry over of iron oxides from the inoculating culture to the experimental solution, the bacterial inoculum was centrifuged at 1500 rpm (Sampson et al., 2000; Donati et al., 1997) to remove Fe-oxides and the supernatant containing the bacteria was used to inoculate the serum bottles. Replicate abiotic control experiments were set up using the same medium but were not inoculated with *A. ferrooxidans*. For each set of biological experiments, four serum bottles were incubated at 25°C for up to 6 weeks (Table 4.1). Due to the slower rates of chemical Fe[II] oxidation, only two serum bottles were prepared for each set of abiotic experiments. The pH of the medium was monitored throughout the experiments. At each sampling point (7, 14, 28, and 42 days) during the incubation period, one serum bottle was filtered using 0.1µm-cellulose acetate Millipore filters under aseptic conditions. The filtered precipitate and an aliquot of the filtrate were frozen and later analyzed for Fe isotopic compositions. Total iron and $Fe[II]_{aq}$ concentrations in the culture medium were measured using a DR/700 Hach colorimeter at each sampling point (Table 4.1). $Fe[III]_{aq}$ concentrations were calculated as the difference between total iron and $Fe[II]_{aq}$. In order to separately measure the $\delta^{56}Fe$ values of both the $Fe[II]_{aq}$ and $Fe[III]_{aq}$ pools, a separate portion of the filtrate was reserved for the chemical separation of $Fe[III]_{aq}$ from each product solution, the method for which is discussed in detail below.

4.2.3 $FeSO_4$ oxidation at 4°C

In addition, biological experiments with $FeSO_4$ medium were carried out at 4°C (environmental room) in order to determine possible temperature effects on bacterial Fe[II] oxidation rates and resulting Fe isotope compositions. The composition of the medium used in these experiments was identical to that in the $FeSO_4$ experiments conducted at 25°C with the exception that DI water used for medium preparation was first cooled to 4°C; the medium was prepared by using this DI water as described before. One hundred milliliters of filter sterilized ferrous sulfate medium, which had previously been refrigerated at 4°C, was added to 200 ml sterile-serum bottles inoculated with 2 ml of the *A. ferrooxidans* culture, which was also kept at 4°C in the environmental room overnight. Abiotic control experiments were set up using the same medium but were not inoculated. For each set of biological experiments, four serum bottles were incubated at 4 °C for up to 10 weeks. Because chemical Fe[II] oxidation is slower, only two serum bottles were prepared for each set of abiotic experiments. The pH of the medium was monitored over the period of the experiments. At each sampling point (28, 42, 56, and 70 days) during the incubation period, one serum bottle was filtered using 0.1µm-cellulose acetate (Milipore) filters and the filtered precipitate and an aliquot of the filtrate were frozen. The measurements of total iron and Fe (II) concentrations in the culture medium, as well as the Fe(II)/Fe (III) separation experiments, were carried out at 4°C in the environmental room. All experimental solutions used for the measurements and separation experiments (e.g. NaOH and DI water) were equilibrated at 4°C before use in the experiments.

4.2.4 $FeCl_2$ oxidation at 25°C

To observe possible speciation effects on biological Fe isotope fractionation resulting from possible anionic ligand interactions with $Fe[II]_{aq}$ and/or $Fe[III]_{aq}$, a second set of experiments were carried out using a $FeCl_2$ medium at 25°C. For these experiments, 6g of $FeCl_2$ replaced the ferrous sulfate in the 2039 medium and the Wolfe's mineral solution was made using ferrous chloride instead of ferrous sulfate. According to this modification, 1L of modified medium contains: 0.6 gr $NH_4(Cl)$; 0.1 gr K_2HPO_4; 1.59 gr $MgCl_2.6H_2O$, ~ 6 gr of $FeCl_2$ and 5 ml modified Wolfe's mineral solution (with Cl^- salt). The pH of the medium was adjusted to 2.3 using trace metal grade HCl. The amount of Fe[II] added was adjusted in order that chloride concentrations were kept to a minimum, as high concentrations (> 5 g/L) have an inhibitory effect on *A. ferrooxidans* (Harahuc, 2000; Suzuki, 1999). In addition, these experiments were inoculated with bacteria that were grown in a starter medium that had been modified to minimize carry over of sulfate. Because the bacteria grow more slowly in the chloride medium (Fry et al., 1986), this experiment ran for 77 days (Table 4.2). As before, abiotic control experiments were set up under the same experimental conditions.

4.2.5 Fe[II]/Fe[III] separation experiments

In order to measure the $\delta^{56}Fe$ values of $Fe[II]_{aq}$ and $Fe[III]_{aq}$ that co-exist in solution at pH <3.0, chemical methods were developed to quantitatively separate $Fe[II]_{aq}$ and $Fe[III]_{aq}$. 50 ml aliquots of medium were taken at each sampling point and ~0.1 ml of 10 M NaOH was added to adjust the sample to a final pH of ~5. This method forces rapid precipitation of any $Fe[III]_{aq}$ and generally results in >90% separation of $Fe[II]_{aq}$ from $Fe[III]_{aq}$. Because Fe[II] in aqueous solutions is unstable in the presence of oxygen at pH>3 and could spontaneously oxidize, the separations were carried out in an anaerobic chamber. Prior to separation, both the sample medium and NaOH were purged with pure nitrogen gas for 30 minutes. The sample medium was purged directly inside the serum bottles using a pre-sterilized inline gas filter (0.2 μm, Whatman) and an outlet port. After purging but before NaOH addition, solutions were kept overnight in the anaerobic chamber to equilibrate with the anaerobic atmosphere. After the addition of NaOH, the sample was filtered using 0.1 μm cellulose acetate filters to obtain the precipitated $Fe[III]_{aq}$ and the filtrate was retained for determining the $Fe[II]_{aq}$ concentrations. Following separation procedures, the filtrate was acidified with trace metal grade HCl to prevent possible $Fe[II]_{aq}$ oxidation. Both the precipitate and filtrate were kept frozen for subsequent Fe isotope analysis. Total iron and $Fe[II]_{aq}$ concentrations were measured colorometrically in the solutions by the ferrozine method before and after separation with NaOH to determine the amount of $Fe[III]_{aq}$ and $Fe[II]_{aq}$ recovered (Table 4.1 and 4.2). Recovery was usually between 90-98 %. In general, better recovery for both $Fe[II]_{aq}$ and $Fe[III]_{aq}$ was obtained from the chloride solution.

4.2.6 Abiotic ferric iron precipitation experiments

In order to assess whether isotopic fractionation of $Fe[III]_{aq}$ occurs during Fe-oxyhydroxide precipitation and to assess possible ionic speciation effects on Fe isotopic fractionation, precipitation experiments were conducted using ferric chloride and ferric sulfate solutions over a narrow pH range (2.2-3.5). This pH range covers that used in the biological experiments and mimics the range associated with many AMD sites. For these experiments, ferric chloride and ferric sulfate were dissolved in DI water. The ferric chloride solution had an initial Fe[III] concentration of ~1300 mg/L and the ferric sulfate solution had an initial Fe[III] concentration of ~1400 mg/L. 100 ml aliquots of DI water with varying amounts of concentrated NaOH were mixed with 100 ml aliquots of the ferric solutions to achieve the appropriate pH. After mixing, solutions were allowed to stand for 5 minutes and then were sequentially filtered through 0.8 and 0.1 μm cellulose acetate filters (Table. 4.5). Aliquots of the filtrates were collected along with the two precipitate fractions for analysis of Fe isotopic composition. For the ferric sulfate precipitation experiments, the following final pH's were used: 2.54, 2.67, 2.85, 3.22, and 3.35. An anaerobic duplicate of the pH= 2.85 experiment was also completed in order to determine whether the presence of dissolved oxygen might also influence Fe isotope fractionation associated with Fe[III] precipitation. For the ferric chloride experiments, the following pH's were used: 2.38, 2.55, 2.89, and 3.22.

In order to assess whether Fe[III] concentration has an effect on iron isotope fractionation during precipitation, a second set of the above experiments was conducted using a ferric chloride solution with 60 mg/L Fe[III] and a ferric sulfate solution with 100 mg/L Fe[III]. For the ferric sulfate solution, the following pH's were used: 2.51, 2.72, 3.24, and 3.54. For the ferric chloride solution, the following pH's were used: 2.22, 2.51, 2.76, 3.27, and 3.54. These samples were filtered using only the 0.1 μm cellulose acetate filters, as the precipitates were not coarse enough to be trapped by the 0.8 μm filter.

In addition to these short-term precipitation experiments, longer-term precipitation experiments were conducted at a single pH of 2.7 and 2.5, respectively, for ferric sulfate and ferric chloride solutions (Table 4.6). For this experiment separate solutions containing 600 mg/L Fe[III] from ferric chloride and 450 mg/L Fe[III] from ferric sulfate were brought to their respective pH's and allowed to stand, in the dark (to prevent photo oxidation/reduction) at room temperature for 7 to 14 days. Samples were taken and filtered through 0.1 μm cellulose acetate filters at 30 min, 24 hours, 1 week, and 2 weeks (ferric chloride solution only). Both precipitates and filtrates were retained for isotopic analysis. At the two-week time point, there was no precipitate in the ferric sulfate solution and thus no data is available. The pH of the solutions was taken at the time of sampling to monitor possible temporal changes.

4.2.7 Determination of Fe isotope composition

For this study, the isotopic composition of Fe was determined using "double spike" measurement techniques on two different mass spectrometric analytical platforms. Thermal ionization mass spectrometry (TIMS) was used early in the study, while multi-collector inductively coupled plasma mass spectrometry (MC-ICPMS) was used later in the study. The TIMS analysis was accomplished on a Finnigan MAT 261 adjustable collector instrument in Menlo Park, CA. The MC-ICPMS analysis was accomplished on two different Thermo-Electron "Neptune" instruments, one at

BRGM in Orleans, France and the other at the University of California at Santa Cruz. In both cases, the Neptune instruments were operated in "high-resolution" mode, allowing effective resolution of the Fe ion beams from Ar-N,O,H ion beams (Arnold et al., 2004). The Fe isotope data obtained for this study are presented in Tables 4.1, 4.2, 4.4 and 4.5 in which each isotopic determination is keyed to its appropriate analysis platform.Sample preparation differed for the different analytical approaches. For the TIMS analysis, an aliquot of each experimental product (i.e., reactant solution or acid digest of filter) sufficient to provide ~1.25 μg of Fe was mixed with a set amount of ^{57}Fe-^{58}Fe mixed "double spike" enriched tracer, and the mixture was allowed to homogenize overnight on a warm plate (~50°C). The solution was then taken to dryness and re-dissolved in 1 mL of 6*N* HCl. The acid solution was loaded onto a small Teflon column containing 2 mL of AG-1-X8 anion resin and then washed with 10 mL of 6*N* HCl to strip other ions from the solution. Fe was then eluted from the column using 7 mL of 0.1*N* HCl, and the resulting solution was taken to dryness. An amendment solution consisting of 10 μg of colloidal silica, 1 μg of alumina and 40 μL of 0.15*M* H_3PO_4 was added to the Fe, and the solution was again taken to dryness. The product solid was taken up in 5 μL of Teflon-distilled H_2O and loaded onto a single Re filament ribbon for mass spectrometry.

For the MC-ICPMS analysis, an aliquot of each experimental product sufficient to provide ~7 μg of Fe was taken to dryness and re-dissolved in 1 mL of 7*N* HNO_3. The acid solution was loaded onto a small Teflon column containing 1 mL of REE-Spec resin (Eichrom Industries) and then washed with 10 mL of 7*N* HNO_3 to strip other major ions from the solution. By using strong nitric acid, ferric iron and the rare earth elements are quantitatively retained on this resin, while other cations and anions are effectively separated in the wash. Fe and the rare earths were then eluted from the column using 7 mL of 0.35*N* HNO_3 (i.e., 2% HNO_3, the acid strength used for the MC-ICPMS method). A 1 mL aliquot was collected from each resulting solution and measured for Fe concentration on a Perkin-Elmer Elan 6000 quadropole icpms in order to demonstrate quantitative recovery of Fe from the column. Prior to isotopic measurement on the Neptune instruments, 1 mL of each purified solution was mixed with a set amount of the same ^{57}Fe-^{58}Fe "double spike" enriched tracer used for the TIMS analysis. Isotopic measurements resulted in determination of the $^{56}Fe/^{54}Fe$ ratio of the sample, and used the $^{57}Fe/^{58}Fe$ ratio of the sample-double spike mixture as a measure of isotopic fractionation due to mass spectrometry procedures. For the TIMS approach, individual isotopic determinations given in the data tables comprised at least 60 scans, each consisting of four 4-second measurements: a simultaneous measurement of ^{54}Fe and ^{56}Fe, a simultaneous measurement of ^{56}Fe, ^{57}Fe and ^{58}Fe, and measurements of ^{52}Cr and ^{60}Ni in order to correct for isobaric interferences of Cr and Ni (although these corrections were generally negligible). For the MC-ICPMS approach, individual isotopic determinations given in the data tables comprised 60 scans, during which ^{54}Fe, ^{56}Fe, ^{57}Fe and ^{58}Fe as well as ^{52}Cr and ^{60}Ni were measured simultaneously for 8 seconds. In both cases, the $^{56}Fe/^{54}Fe$ ratio of the sample was mathematically extracted from the measured composition of the sample-double spike mixture using an algorithm similar to that originally proposed by Russell et al. (1978) and employed for all isotope ratio determinations based on the double spike method at Menlo Park (e.g., Johnson et al., 2000; Bullen et al., 2001).

The isotopic data are reported here in terms of $\delta^{56}Fe$, the per mil difference of the $^{56}Fe/^{54}Fe$ ratio of a sample from that of BIR-1, and a U.S.G.S. basalt standard. The internal precision of an isotope composition determination is 0.15‰ or better for the TIMS method and 0.10‰ or better for the MC-ICPMS method (2σ, minimum 60 component ratio determinations). BIR-1 is used as the reference standard because: 1) as an igneous rock it should have $\delta^{56}Fe \sim 0.0$‰ (cf., Johnson and Beard, 2000); and 2) it has a complex chemical matrix that must be processed through the entire analytical procedure in order to obtain purified Fe for analysis. Thus, reproducibility of its Fe isotope composition provides a measure of external precision of the analytical methods. External precision on the determination of the Fe isotope composition of BIR-1 was 0.11‰ for the TIMS method (2σ, n=20), 0.07‰ for the MC-ICPMS method on the Neptune instrument at Orleans (2σ, n=9), and 0.07‰ from the MC-ICPMS method on the Neptune instrument at Santa Cruz (2σ, n=25). In addition, the Fe isotope composition of the IRMM-014 Fe standard was determined on the Neptune instrument at Orleans, with external precision of 0.10‰ (2σ, n=15). Relative to BIR-1, IRMM-014 gave $\delta^{56}Fe$ of -0.02‰, identical within analytical uncertainty to the composition of this standard relative to igneous rocks reported by Beard et al. (2003).

4.3 Results

Data for the biological and abiotic oxidation experiments are presented in Table 4.1 (ferrous sulfate medium) and Table 4.2 (ferrous chloride medium). In these tables, it is included both the raw data for $Fe[II]_{aq}$, $Fe[III]_{aq}$ and $Fe[III]_{ppt}$ (concentration and isotopic composition) and corrected data for $Fe[II]_{aq}$ and $Fe[III]_{aq}$, adjusted to account for small amounts of $Fe[III]_{aq}$ and $Fe[II]_{aq}$, respectively, carried over into the precipitate formed during the separation of $Fe[III]_{aq}$ with NaOH from the experimental solutions. Data for the ferric iron precipitation experiments are presented in Table 4.4 (short term experiments) and Table 4.5 (long term experiments). In Table 4.4, both the raw data for $Fe[III]_{aq}$ and $Fe[III]_{ppt}$, as well as a calculated composition for $Fe[III]_{ppt}$ based on mass balance determined as the difference between the starting composition and the $Fe[II]_{aq}$ fraction are included.

4.3.1 Efficiency of separation method

The efficiency of the separation method was tested by performing the following mass balance calculation:

$$\delta^{56}Fe_{mix} = \delta^{56}Fe[II]_{aq}.X_{Fe[II]aq} + \delta^{56}Fe[III]_{aq}.X_{Fe[III]aq} \qquad (1)$$

where $X_{Fe[II]aq}$ and $X_{Fe[III]aq}$ are the concentrations of $Fe[II]_{aq}$ and $Fe[III]_{aq}$, respectively. Fe_{mix} is the solution containing both $Fe[II]_{aq}$ and $Fe[III]_{aq}$ used in the separation experiments. $\delta^{56}Fe_{mix}$ was measured directly; as noted above, $\delta^{56}Fe[II]_{aq}$ and $\delta^{56}Fe[III]_{aq}$ values required a correction. Using the concentration and isotopic values of the Fe phases obtained for each sampling point, $\delta^{56}Fe_{mix}$ values were calculated using equation (1) and compared to the measured $\delta^{56}Fe_{mix}$ values (Table 4.1 and 4.2). If there had been significant isotopic exchange or fractionation during the separation of $Fe[II]_{aq}$ from $Fe[III]_{aq}$, then the calculated and the measured $\delta^{56}Fe[II]_{aq}$ values would have revealed significant differences.

The similarity between the measured and the calculated values for $\delta^{56}Fe_{mix}$ indicates that the separation experiments were quantitative within the uncertainty limits of the isotopic analysis ($2\sigma < \pm0.15‰$).

4.3.2 Rates of Fe[II] oxidation

A.ferrooxidans oxidized Fe[II] in both the ferrous sulfate and ferrous chloride media under all experimental conditions, this oxidation resulted primarily in the accumulation of aqueous Fe[III] and a small amount of ferric oxyhydroxides. However, the oxidation rates differed between the experiments (Fig. 4.1). Because sulfate stimulates bacterial Fe[II] oxidation, the oxidation rate was significantly greater in the sulfate medium compared to that in the chloride medium. The maximum Fe[II] oxidation rate was 1.4 mM/day for the $FeSO_4$ medium and ~0.25 mM/day for the $FeCl_2$ medium.

The maximum fractions of total Fe[II] oxidized were 81% (ferrous sulfate medium, 42 days) and 40% (ferrous chloride medium 77 days) (Tables 4.1 and 4.2). The amount of precipitation of ferric oxyhydroxides increased with the extent of reaction. While abiotic Fe[II] oxidation occurred in the non-biological experiments, rates were much lower when compared to the biological experiments and in all cases less than 10 % of the Fe[II] was oxidized (Tables 4.1 and 4.2).

Abiotic precipitation of ferric oxyhydroxides occurred only in the $FeSO_4$ medium. The oxidation process can be effectively modeled as a second-order reaction, where f (the proportion of reactant remaining after time t; f = 1 at t = 0) is described by the equation:

$$f = (1 + kt)^{-1} \tag{4.1}$$

where k is the reaction rate constant. This relationship solves the general rate equation:

$$(1-f)/f = kt \tag{4.2}$$

Table 4.1 Chemical and Fe isotope compositions of biological and abiotic oxidation experiments using ferrous sulfate medium

Day	Pre-separation:				Post-separation:					δ^{56}Fe:						
	pH	Fe[II] (mg)	Fe[III] (mg)	[a]f	[b]pH	[c]Fe[II] (mg)	[d]Fe[III] (mg)	[e]Fe[II] (%)	[f]Fe[III] (%)	[g]Fe_{mix} (‰)	[h]$Fe[II]_{aq}$ (‰)	[h]$Fe[III]_{aq}$ (‰)	[h]$Fe[III]_{ppt}$ (‰)	[i]$Fe[II]_{aq}$ (‰)	[i]$Fe[III]_{aq}$ (‰)	[i]Fe_{mix} (‰)
25°C-A																
0	2.31	4670	10	1.00	-	-	-	-	-	-0.22	-	-	-		-	-
7	2.31	3490	930	0.75	6.10	3130	130	90	86	-0.35 [o]	-1.40 [o]	2.05 [o]	2.82 [o]	-1.58	3.68	-0.47
14	2.16	3200	1180	0.68	6.10	2910	180	91	85	-0.38 [o]	-1.10 [o]	1.49 [o]	1.55 [o]	-1.29	2.30	-0.32
28	2.21	2660	1370	0.57	6.10	2640	250	99	82	-0.60 [o]	-1.40 [o]	1.80 [o]	1.70 [o]	-1.71	1.86	-0.49
42	2.11	2390	2090	0.51	5.60	2350	20	98	99	-0.30 [o]	-1.39 [o]	1.03 [o]	0.68 [o]	-1.41	1.08	-0.25
25°C-B																
0	2.30	4300	100	0.98	-	-	-	-	-	-0.20 [o]	-	-	-		-	-
7	2.41	3580	820	0.81	5.60	3260	85	92	90	-0.20 [o]	-0.60 [o]	1.14 [o]	0.25 [o]	-0.66	1.92	-0.18
14	2.35	2960	1390	0.67	5.10	2740	30	93	98	-0.25 [o]	-1.10 [o]	1.27 [o]	0.44 [o]	-1.13	1.66	-0.24
28	2.31	2540	1690	0.58	5.00	2200	50	90	97	-0.26 [o]	-1.20 [o]	0.91 [o]	0.88 [o]	-1.25	1.36	-0.21
42	2.29	820	2520	0.19	4.90	720	60	88	98	-0.36 [o]	-3.70 [o]	0.58 [o]	0.36 [o]	-4.06	.77	-0.42
4°C																
0	2.40	4435	85	0.98	-	-	-	-	-	-0.20 [o]	-	-	-		-	-
28	2.81	3650	1100	0.81	5.60	3140	80	86	93	-0.20 [o]	-1.05 [o]	1.59 [o]	2.90 [o]	-1.14	2.95	-0.19
42	2.92	3180	1540	0.70	5.55	2990	190	94	94	-0.20 [o]	-0.88 [o]	1.21 [o]	0.78 [o]	-1.02	1.52	-0.19
56	3.32	2950	2110	0.65	5.20	2800	130	95	94	-0.24 [o]	-1.35 [o]	1.33 [o]	0.43 [o]	-1.48	1.54	-0.22
70	3.03	2430	1750	0.54	5.40	2190	10	90	99	-0.20 [o]	-1.58 [o]	0.79 [o]	1.65 [o]	-1.59	1.12	-0.46
25°C-Abiotic																
0	2.30	4250	15	0.99	-	-	-	-	-	-0.18 [s]	-	-	-		-	-
14	2.35	4051	200	0.95	4.20	4054	6	100	97	-0.34 [s]	-0.38 [s]	1.75 [s]	1.85 [s]	-0.38	1.75	-0.28
42	2.29	3800	360	0.89	4.20	3795	5	100	99	-0.31 [s]	-0.55 [s]	1.13 [s]	1.29 [s]	-0.55	1.13	-0.40

[a] proportion Fe[II] remaining; [b] pH used in the separation experiments; [c,d] concentration after separation; [e,f] percent recovery during separation; [g] measured value of mixture used for separation; [h] measured values; [i] calculated values based on mass balance (calculated $Fe[III]_{aq}$ = measured $Fe[III]_{aq}$ less $Fe[II]_{aq}$ carryover fraction); dash indicates values not determined. Superscripts on measured Fe isotope values indicate technique: o, Orleans Neptune multi-collector ICPMS; s, UC Santa Cruz Neptune multi-collector ICPMS.

Table 4.2 Chemical and Fe isotope compositions of biological and abiotic oxidation experiments using ferrous chloride medium

	Pre-separation:				Post-separation:					δ^{56}Fe:						
Day	pH	Fe[II] (mg)	Fe[III] (mg)	[a]f	[b]pH	[c]Fe[II] (mg)	[d]Fe[III] (mg)	[e]Fe[II] (%)	[f]Fe[III] (%)	[g]Fe_{mix} (‰)	[h]$Fe[II]_{aq}$ (‰)	[h]$Fe[III]_{aq}$ (‰)	[h]$Fe[III]_{ppt}$ (‰)	[i]$Fe[II]_{aq}$ (‰)	[i]$Fe[III]_{aq}$ (‰)	[i]Fe_{mix} (‰)
25°C																
0	2.30	2840	50	0.98	-	-	-	-	-	-0.15^{s}	-	-	-		-	-
35	2.16	2120	590	0.73	4.44	2010	40	95	93	-0.27^{o}	-0.51^{o}	1.20^{o}	0.85^{o}	-0.55	1.55	-0.09
56	2.07	1890	940	0.65	5.00	1850	30	98	97	-0.27^{o}	-1.15^{o}	1.72^{o}	1.04^{o}	-1.20	1.85	-0.19
70	2.07	1715	760	0.59	4.80	1620	20	94	97	-0.45^{o}	-1.25^{o}	1.32^{o}	1.75^{o}	-1.28	1.65	-0.38
77	2.05	1830	720	0.63	4.60	1860	0	102	100	-0.40^{o}	-1.10^{o}	1.49^{o}	1.64^{o}	-1.10	1.49	-0.37
25°C-Abiotic																
0	2.00	2740	0	1.00	-	-	-	-	-	-0.13^{s}	-	-	-		-	-
56	2.00	2700	40	0.99	4.20	2630	0	97	100	-0.18^{s}	-0.18^{s}	1.06^{s}	-	-0.18	3.23	-0.13

[a] proportion Fe[II] remaining; [b] pH used in the separation experiments; [c,d] concentration after separation; [e,f] percent recovery during separation; [g] measured value of mixture used for separation; [h] measured values; [i] calculated values based on mass balance (calculated $Fe[III]_{aq}$ = measured $Fe[III]_{aq}$ less $Fe[II]_{aq}$ carryover fraction); dash indicates value not determined. Superscripts on measured Fe isotope values indicate technique: o, Orleans Neptune multi-collector ICPMS; s, UC Santa Cruz Neptune multi-collector ICPMS.

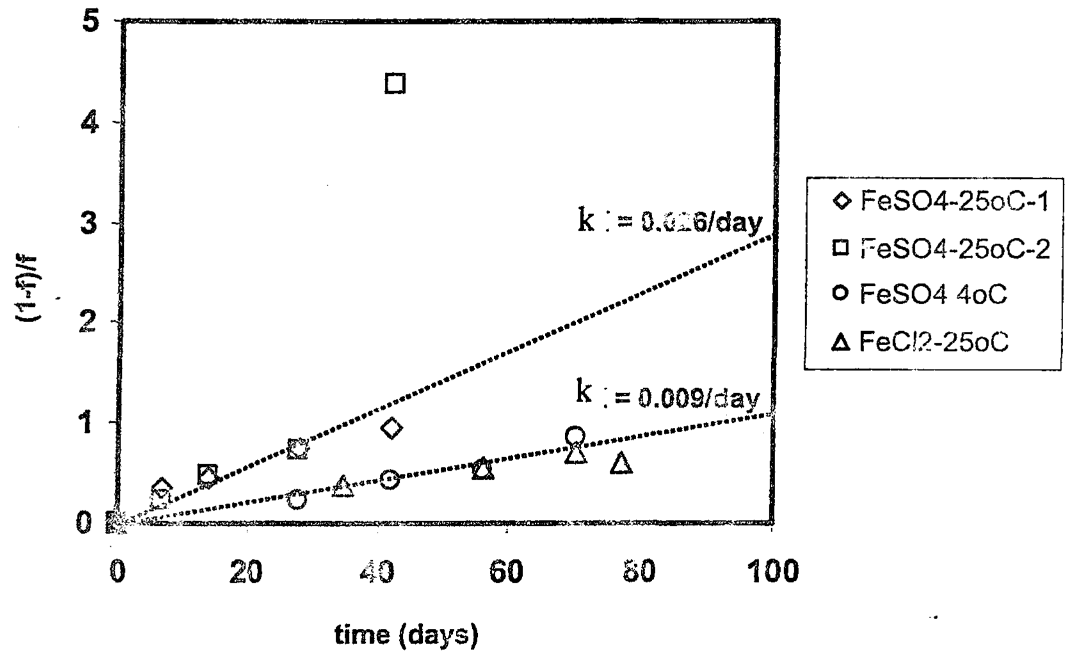

Figure 4.1. Regression of data for all biological oxidation experiments, using second-order rate law (Eq. 3) forced through a zero intercept. f is the proportion of $Fe[II]_{aq}$ remaining; the slope of the line through any given data array is equivalent to k, the reaction rate constant.

The data for the biological experiments are plotted in Figure 4.1, where the y-axis is (1-f)/f and the x-axis is time. Thus the slope of the straight line fitted through the data is equivalent to k, the reaction rate constant. Straight lines can be fitted through all data for the first 25°C ferrous sulfate experiment, the 4°C ferrous sulfate experiment and the 25°C ferrous chloride experiment. However, the data for the second 25°C ferrous sulfate experiment are non-linear, with the 42-day time point being clearly at odds with the other data. Noting that the earlier time points for this second experiment are consistent with those of the first 25°C ferrous sulfate experiment, it is suggested that the errant 42-day time point sample was affected by enhanced oxidation due to an additional, unknown process. Disregarding that one point, the rate constant determined for both 25°C ferrous sulfate experiments is ~0.026/day, while that for the 4°C ferrous sulfate and 25°C ferrous chloride experiments is ~0.009/day. The data thus demonstrate clear compositional and temperature effects on oxidation rate. It is noted that treating the oxidation process as either a zeroeth-order (i.e., f vs. t) or first-order (i.e., ln f vs. t) reaction results in less linearity of the data, providing support for the second-order reaction model.

$$df/dt = -k_n f^n \qquad (4.3)$$

where n=2 (cf., Johnson et al., 2002). Equation 1 can be recast as a simple function of time. Regardless, rate constants determined for zeroeth, first and second order reaction models using best linear fits through the data do not differ significantly.

4.3.3 Isotopic fractionation in the biological experiments

Tables 4.1 and 4.2 give the Fe isotope compositions of $Fe[II]_{aq}$, $Fe[III]_{aq}$ and $Fe[III]_{ppt}$ for the biological and abiotic oxidation experiments. Throughout the experiments, the $\delta^{56}Fe[II]_{aq}$ values are consistently lower than those of coexisting $Fe[III]_{aq}$ and $Fe[III]_{ppt}$. As shown in Figure 4.2a, the data for $Fe[II]_{aq}$ in the biological experiments considered together exhibit apparent Rayleigh type behavior, which can be described by the following natural log function: isotopic composition of each data point and the small extent of reaction in this experiment.

However, simple Rayleigh behavior during biological oxidation is less tenable when corresponding $\delta^{56}Fe[III]_{aq}$ values are likewise considered. As shown in Figure 4.2b,

$$\delta^{56}Fe[II]_{aq} = \varepsilon \ln(f) \qquad (4.4)$$

where $\delta^{56}Fe[II]_{aq}$ is the isotopic composition of the remaining $Fe[II]_{aq}$ at a given time during the reaction; epsilon (ε) is the isotopic enrichment factor that is described by $\varepsilon = 1000(\alpha - 1)$, where $\alpha = (^{56}Fe/^{54}Fe_{Fe[III]})/(^{56}Fe/^{54}Fe_{Fe[II]})$; and f is the proportion of $Fe[II]_{aq}$ remaining after time t as defined above. If the oxidation reaction follows Rayleigh behavior, a plot of $\delta^{56}Fe[II]_{aq}$ versus ln(f) will yield a straight line, the slope of which is equal to ε (Mariotti et al.,1983). The data for all the biological experiments plotted in Figure 4.2a describe a strong linear relationship ($r^2 = 0.93$) and define a value for ε of 2.2‰, which can be interpreted to reflect an apparent Rayleigh fractionation associated with the oxidation of $Fe[II]_{aq}$ to $Fe[III]_{aq}$. A statistical analysis of this regression reveals that the slope of this line, which equals ε, falls between 1.7 and 2.5 ‰ at the 99% confidence interval, which is significantly less than the ~2.9‰ reported for equilibrium isotopic exchange between Fe[II]- and Fe[III]-hexaquo species at low pH (Johnson et al., 2002; Welch et al., 2003), and might provide evidence of a "biological effect". In fact, simple linear regression through the three data points obtained in my abiotic ferrous sulfate oxidation experiment (Table 4.1) provide a value for ε of 3.4‰.

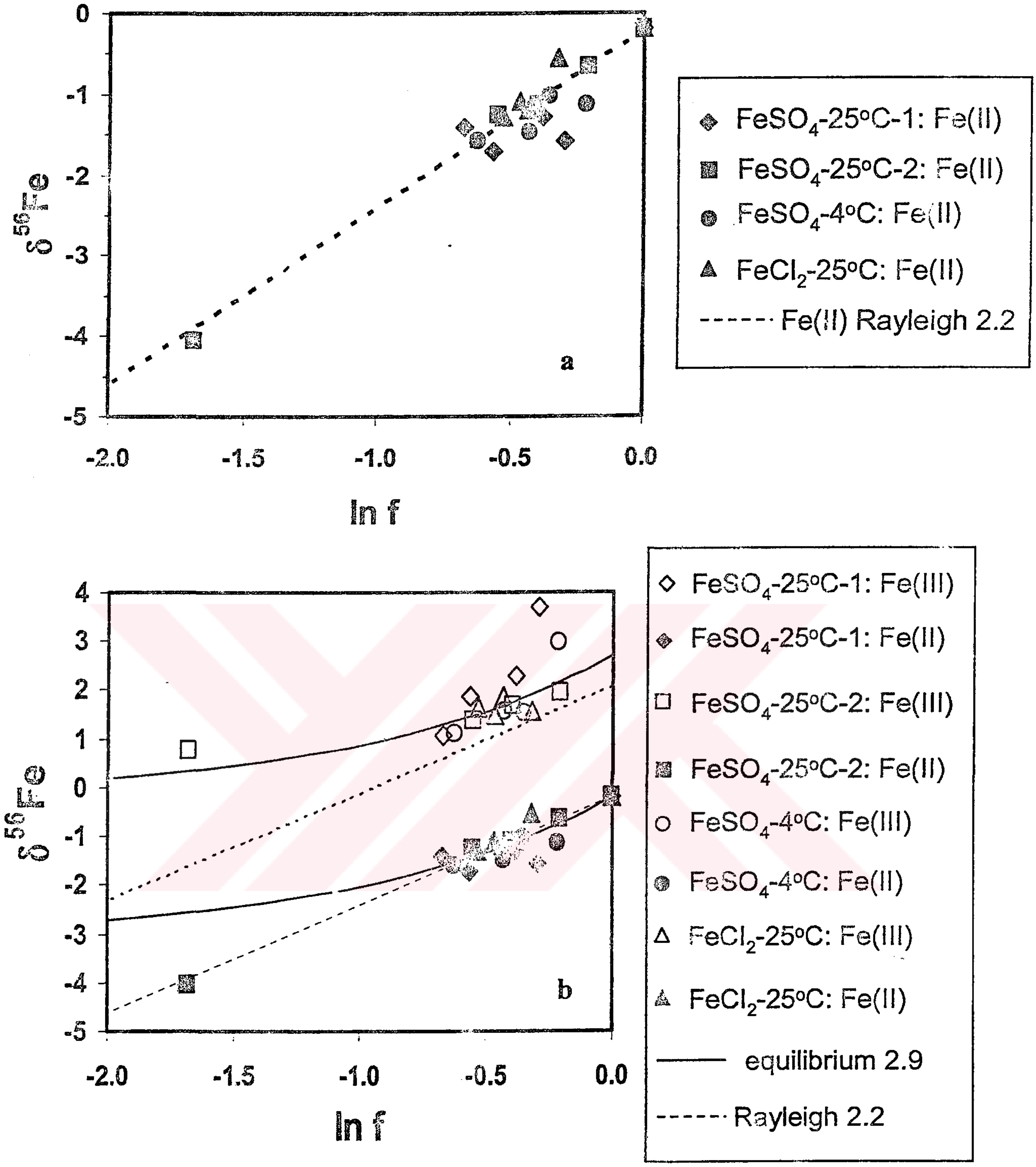

Figure 4.2. $\delta^{56}Fe$ of corrected aqueous components for all biological oxidation experiments, plotted against ln(f), where f is the proportion of $Fe[II]_{aq}$ remaining. a) Corrected $Fe[II]_{aq}$ components only, fitted with least-squares regression line having slope of 2.2 (r^2=0.91). On this log-linear plot, the slope of the regression line gives the apparent Rayleigh isotopic enrichment factor ε, which for the overall data array is 2.2‰. b) Corrected $Fe[II]_{aq}$ and $Fe[III]_{aq}$ components, plotted in comparison to both Rayleigh fractionation trends (ε=2.2‰) and equilibrium fractionation trends (ε=2.9‰).

This value is consistent with equilibrium isotopic exchange between $Fe[II]_{aq}$ and $Fe[III]_{aq}$ given the uncertainty on the $Fe[III]_{aq}$ data for all the biological experiments as a group have consistently greater $\delta^{56}Fe$ than the Rayleigh model (ε = 2.2‰) would predict. On the other hand, the bulk of the $Fe[II]_{aq}$ and $Fe[III]_{aq}$ data are well described by equilibrium fractionation curves based on ε = 2.9‰. Some of the data are clearly at odds with a simple equilibrium model, particularly the 42-day time point for the second 25°C ferrous sulfate experiment, which was noted above to be errant with respect to a simple second-order rate mechanism. I note that in general, when data deviate from the simple equilibrium model lines, they do so in a complementary fashion: for a given time point, when $\delta^{56}Fe[III]_{aq}$ lies above the $Fe[III]_{aq}$ model line in Figure 4.2b, the corresponding $\delta^{56}Fe[II]_{aq}$ lies below the $Fe[II]_{aq}$ model line, and vice versa. In addition, there is an apparent isotope mass balance in the offset: when the concentration of $Fe[II]_{aq}$ is greater than $Fe[III]_{aq}$ (i.e., early in each experiment), $\delta^{56}Fe[III]_{aq}$ is further displaced from the equilibrium curve than $\delta^{56}Fe[II]_{aq}$, and vice versa. These relationships apparently point to an additional process that may overprint the isotopic fractionation resulting from oxidation.

A wide range of isotopic fractionation between $Fe[III]_{aq}$ and $Fe[III]_{ppt}$ was observed in all the biological experiments. In general, the fractionation was greater in the earlier part of each experiment than in the later part, although the decrease was clearly not monotonic as each experiment progressed (Table 4.3). Interestingly, no obvious fractionation between $Fe[III]_{aq}$ and $Fe[III]_{ppt}$ was observed in the abiotic ferrous sulfate oxidation experiment.

These results suggest that there is significant and complex isotopic fractionation that occurs during precipitation of the ferric oxyhydroxide solids that may be related to biological processes, and that $\delta^{56}Fe_{ppt}$ does not provide a useful surrogate of $\delta^{56}Fe[III]_{aq}$.

4.3.4 Abiotic Fe[III] precipitation experiments

Short- and long-term abiotic precipitation experiments using ferric chloride and ferric sulfate starting solutions were performed at high and low Fe concentrations to help determine possible isotopic fractionation effects associated with differing rates of Fe[III]-oxyhydroxide precipitation.

Table 4.3 Summary of Fe isotope fractionation among different Fe pools

Experiment	Day	f	$\Delta_{Fe[III]ppt-Fe[II]aq}$ (‰)	$\Delta_{Fe[III]aq-Fe[III]ppt}$ (‰)	$\Delta_{Fe[III]aq-Fe[II]aq}$ (‰)
$Fe[II]SO_4$ 25°C-A	7	0.75	4.40	0.86	5.26
	14	0.68	2.84	0.75	3.59
	28	0.57	3.41	0.16	3.57
	42	0.51	2.09	0.40	2.49
$Fe[II]SO_4$ 25°C-B	7	0.81	0.91	1.67	2.58
	14	0.67	1.57	1.22	2.79
	28	0.58	2.13	0.48	2.61
	42	0.19	4.42	0.41	4.83
$Fe[II]SO_4$ 4°C	28	0.81	4.04	0.05	4.09
	42	0.70	1.80	0.74	2.54
	56	0.65	1.81	1.11	3.02
	70	0.54	3.24	-0.53	2.71
$Fe[II]Cl_2$ 25°C	35	0.73	1.40	0.70	2.10
	56	0.65	2.24	0.81	3.05
	70	0.59	3.03	-0.10	2.93
	77	0.63	2.74	-0.15	2.59
$Fe[II]SO_4$ 25°C-abiotic	14	0.95	2.23	-0.10	2.13
	42	0.91	1.84	-0.16	1.68
$Fe[II]Cl_2$ 25°C-abiotic	56	0.99	-	-	3.41

In these experiments, pH was used as a proxy for precipitation rate (i.e., lower pH resulted in slower precipitation rate). In the high concentration experiments, various size fractions were collected (>0.8 μm and 0.1–0.8 μm) to determine whether precipitate size affected $\delta^{56}Fe$ values, which might reflect different fractionation effects during different stages of precipitation. Precipitate size also varied with the rate of precipitation, in that the larger size fraction required a greater amount of time to form.

In all cases, precipitation resulted in solids having lesser $\delta^{56}Fe$ than that of co-existing $Fe[III]_{aq}$ and for the high Fe concentration experiments, slower rates of precipitation resulted in greater Fe isotopic contrast between $Fe[III]_{aq}$ and $Fe[III]_{ppt}$. In the high Fe concentration experiments, the >0.8 μm precipitate fraction displayed a greater difference in Fe isotopic composition between $Fe[III]_{aq}$ and $Fe[III]_{ppt}$ (i.e., $\Delta^{56}Fe_{aq-ppt}$) for each pH than did the 0.1-0.8 μm precipitate fraction (Table 4.4). In these experiments, the isotopic contrast decreased with increasing pH and rate, particularly in the case of the 0.1-0.8 μm fraction (Table 4.4). Using $\delta^{56}Fe$ values of the bulk precipitate calculated by mass balance, a pH/rate effect was evident in the $Fe_2(SO_4)_3$ experiment that was more similar to that observed in the 0.1-0.8 μm fraction, although with different values of $\Delta^{56}Fe_{aq\text{-}ppt}$ observed for each. For the chloride system, in the pH/rate effect observed in the bulk precipitate more closely approximated the >0.8 μm fraction. These results suggest that the Fe isotope fractionation associated with solid precipitation can be expressed in both size fractions, and the pH/rate effect is consistently expressed during the formation of smaller, colloidal Fe-oxyhydroxides, but may also be expressed during re-crystallization and precipitation of larger-sized Fe[III]-oxyhydroxides in some systems (e.g., $FeCl_3$).

Isotopic fractionation between ferric aqueous and precipitate pools tended to be much greater in the experiments using ferric sulfate solution than in those using ferric chloride solution (Table 4.4), suggesting differing importance of factors such as anion ligand effects preceding precipitation, solid-liquid boundary layer dynamics or within-solid diffusional gradients leading to kinetic isotope effects. Similar patterns emerged in the precipitation experiments carried out at lower concentrations. Specifically, $\Delta^{56}Fe_{aq\text{-}ppt}$ was greater in the ferric sulfate experiment than in the ferric chloride experiment at given pH/rate, and there was a significant pH/rate effect in the ferric sulfate experiment but essentially there is no effect in the ferric chloride experiment (Table 4.4).

Therefore, the kinetic fractionation effects associated with precipitation are apparently not influenced by $Fe[III]_{aq}$ concentration to any measurable extent. Mineralogy of the precipitates may also play a role in the observed differences between the chloride and sulfate systems, as X-ray diffraction of the precipitates revealed that the sulfate solutions precipitated schwertmannite while the chloride solutions precipitated akaganeite.

In order to determine if the precipitation effects discussed above were largely due to kinetic or equilibrium effects, long-term (2-3 weeks) precipitation experiments were conducted. For the ferric sulfate system at pH=2.66, the data can be interpreted to indicate that isotopic equilibrium between ferric aqueous and precipitate pools was approached within 24 hours, with an isotopic contrast of ~0.7‰ (Table 4.5). This is ~0.6‰ less than the 1.29‰ difference obtained using the calculated isotopic

Table 4.4 Ferric chloride and ferric sulfate precipitation experiments (short-term)

	Fe_{aq} (mg/L)	% $Fe[III]_{aq}$ remaining	[a] $\delta^{56}Fe_{aq}$	[a] $\delta^{56}Fe_{ppt}$ (0.1-0.8 μm)	$\Delta^{56}Fe_{aq\text{-}ppt}$ (0.1-0.8 μm)	[a] $\delta^{56}Fe_{ppt}$ (>0.8 μm)	$\Delta^{56}Fe_{aq\text{-}ppt}$ (>0.8 μm)	[b] $\delta^{56}Fe_{ppt}$ (calculated)	[c] $\Delta^{56}Fe_{aq\text{-}ppt}$
$Fe[III]Cl_3$:									
pH = 1.90	653	100	-0.22^{m}	-	-	-	-	-	-
2.38	614	94	-0.19^{m}	-0.45^{s}	0.26	-0.80^{m}	0.61	-0.69	0.50
2.55	444	68	-0.09^{m}	-0.20^{s}	0.11	-0.50^{m}	0.41	-0.50	0.41
2.89	78	12	-0.02^{m}	-0.05^{s}	0.03	-0.28^{m}	0.26	-0.25	0.23
3.22	7	1	0.00^{m}	-0.06^{s}	0.06	-0.24^{m}	0.24	-0.22	0.22
1.90	75	100	-0.18^{s}	-	-	-	-	-	-
2.22	39	51	0.03^{s}	-0.22^{s}	0.25	-	-	-0.49	0.52
2.51	29	39	0.12^{s}	-0.18^{s}	0.30	-	-	-0.44	0.56
2.76	20	27	-0.02^{s}	-0.22^{s}	0.20	-	-	-0.29	0.27
3.27	16	21	0.10^{s}	-0.13^{s}	0.23	-	-	-0.31	0.41
3.53	13.5	18	0.35^{s}	-0.12^{s}	0.47	-	-	-0.34	0.69
$Fe[III]_2(SO_4)_3$:									
pH = 1.90	715	100	-0.20^{o}	-	-	-	-	-	-
2.54	640	89	-0.03^{m}	-0.51^{m}	0.48	-1.13^{m}	1.10	-1.65	1.62
2.54	634	89	-0.02^{o}	-0.49^{o}	0.47	-	-	-1.61	1.59
2.67	493	69	0.20^{o}	0.08^{s}	0.12	-0.91^{o}	1.11	-1.09	1.29
2.85	91	13	0.82^{o}	0.45^{s}	0.37	-0.15^{o}	0.97	-0.34	1.16
2.86	95	13	0.90^{m}	0.60^{m}	0.30	-0.20^{m}	1.10	-0.37	1.27
3.22	5.7	1	0.64^{o}	0.60^{s}	0.04	-0.14^{o}	0.78	-0.21	0.85
3.35	7	1	0.77^{m}	0.65^{m}	0.12	-0.19^{m}	0.96	-0.21	0.98
1.90	60	100	-0.23^{s}	-	-	-	-	-	-
2.51	47	78	0.26^{s}	-0.03^{s}	0.29	-	-	-1.86	2.12
2.72	33	55	0.66^{s}	-0.07^{s}	0.73	-	-	-1.24	1.90
3.24	7	12	0.89^{s}	-0.39^{s}	1.28	-	-	-0.34	1.23
3.54	2.7	4.5	1.00^{s}	-0.46^{s}	1.46	-	-	-0.26	1.26

[a] measured values; [b] total precipitate calculated by mass balance assuming concentration and Fe isotope composition of $Fe[III]_{aq}$ is correct; [c] fractionation factor based on calculated total precipitate; dash indicates value not determined. Superscripts on measured Fe isotope values indicate technique: m, Menlo Park TIMS; o, Orleans Neptune multi-collector ICPMS; s, UC Santa Cruz Neptune multi-collector ICPMS.

composition of the bulk precipitate in the short-term experiment conducted at a similar pH of 2.67 (Table 4.4; Fig. 4.3). For the ferric chloride system at pH = 2.50, the long-term precipitation experiment revealed that isotopic equilibrium between ferric aqueous and precipitate pools was probably attained after 1 week, with an isotopic contrast of ~0.9‰ (Table 4.5). This is (~0.5‰) greater than the 0.41‰ difference obtained using the calculated bulk precipitate in the short-term precipitation experiments conducted at similar pH (Tables 4.4; Fig. 4.3).

Thus, short-term precipitation in both the sulfate and chloride systems apparently produces ferric oxyhydroxides that are not in isotopic equilibrium with their host solutions, but with increased contact and/or aging of solid, equilibrium may be approached in each system although from opposite directions.

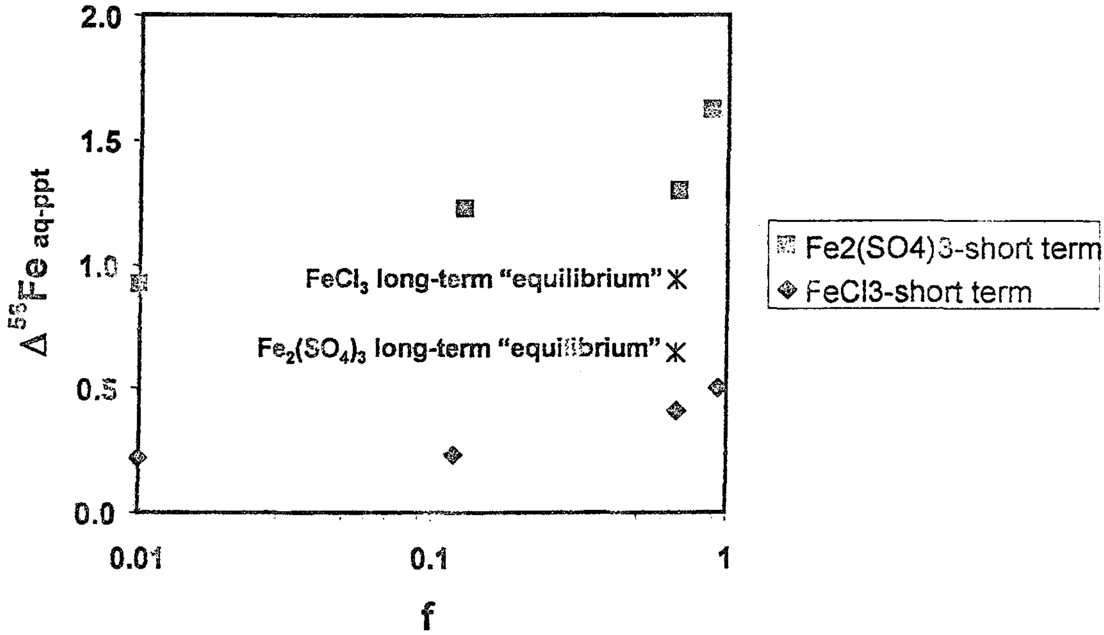

Figure 4.3. Isotopic contrast ($\Delta^{56}Fe_{aq\text{-}ppt}$) between $Fe[III]_{aq}$ and $Fe[III]_{ppt}$ in ferric iron precipitation experiments, plotted against f, the proportion of $Fe[III]_{aq}$ remaining (note logarithmic scale). "Equilibrium" values obtained from the long-term precipitation experiments represent average of the 1- and 2-week samples for the chloride system, and the 24 hour and 1 week samples for the sulfate system.

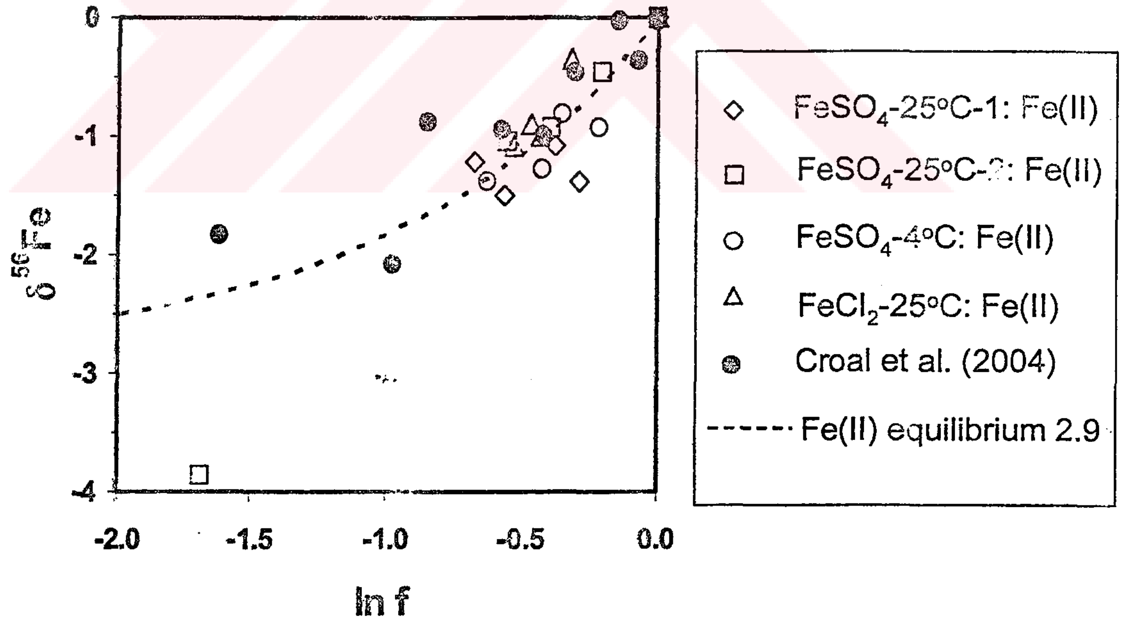

Figure 4.4. $\delta^{56}Fe$ of corrected $Fe[II]_{aq}$ components for all biological oxidation experiments, plotted against ln(f), where f is the proportion of $Fe[II]_{aq}$ remaining. Data from experiments of Croal et al. (2004) are included for comparison. Data are plotted relative to starting material for each experiment, where the initial value is taken to be 0‰. Dashed line represents the equilibrium fractionation trend having an isotopic enrichment factor of ε=2.9‰.

Table 4.5 Ferric chloride and ferric sulfate precipitation experiments (long-term)

Sample Time	pH	Fe_{aq} (ppm)	$\delta^{56}Fe_{aq}$ [a]	$\delta^{56}Fe_{ppt}$ [a]	$\Delta^{56}Fe_{aq-ppt}$
$Fe[III]Cl_3$:					
Time = 0 min	2.50	600.00	-0.22 [o]	-	-
30 min	2.50	420.00	-0.05 [o]	-0.65 [o]	0.60
24 hours	2.45	430.00	0.00 [o]	-0.60 [o]	0.60
1 week	2.46	410.00	0.20 [o]	-0.66 [o]	0.89
2 weeks	2.43	400.00	0.18 [o]	-0.80 [o]	0.98
$Fe[III]_2(SO_4)_3$:					
Time = 0 min	2.66	465.00	-0.19 [o]	-	-
30 min	2.66	320.00	0.06 [o]	-0.52 [o]	0.58
24 hours	2.60	300.00	-0.01 [o]	-0.67 [o]	0.66
1 week	2.46	320.00	0.09 [o]	-0.60 [o]	0.69

[a] measured values; dash indicates value not determined. Superscripts on measured Fe isotope values indicate technique: o, Orleans Neptune multi-collector ICPMS.

4.4 Discussion

4.4.1 Isotopic fractionation between $Fe[II]_{aq}$ and $Fe[III]_{aq}$ pools

In my experiments, net Fe isotope fractionations between the $Fe[II]_{aq}$, $Fe[III]_{aq}$ and $Fe[III]_{ppt}$ pools were determined by three competing processes: 1) an oxidation of $Fe[II]_{aq}$, 2) an equilibration via electron exchange between $Fe[II]_{aq}$ and 3) $Fe[III]_{aq}$, and precipitation of $Fe[III]_{aq}$ as either schwertmannite or akaganeite. The fundamental basis of the study design was to set up experiments in which oxidation of ferrous iron was driven by microbial activity. If a biological effect was able to be expressed in the ferric iron products, then either the oxidation or precipitation effect would have had to overprint the equilibration effect. Johnson et al. (2002) and Welch et al. (2003) conducted abiotic exchange experiments at pH ~2.5 to determine the time required to reach isotopic equilibrium between $Fe[III]_{aq}$ and $Fe[II]_{aq}$. For these experiments, $FeCl_2$ and $FeCl_3$ solutions that differed substantially in Fe isotope composition were mixed and allowed to stand for a period of time at 22 ± 2°C. In this experimental system, the principal aqueous species were $[Fe[II](H_2O)_6]^{2+}$ (>97% of $Fe[II]_{aq}$ species) and $[Fe[III](H_2O)_6]^{3+}$ (>82% of $Fe[III]_{aq}$ species). For this system, the time required to reach isotopic equilibrium was relatively quick (< 1 minute), and the process was modeled as a second-order reaction with rate constant ~ $0.2 sec^{-1}$ (~ $17{,}000 day^{-1}$). Thus, one might have initially predicted that given the anticipated slow rates of bacterial Fe[II] oxidation (rate constant ~$0.01\text{-}0.03 day^{-1}$ for my experiments; Fig. 4.1), equilibrium between $Fe[II]_{aq}$ and $Fe[III]_{aq}$ should have been the dominant control on isotopic distribution among aqueous species. However, it was not possible to *a priori* rule out a biological control on $Fe[III]_{aq}$ chemistry (e.g., strong Fe[III]-ligand formation) that might have hindered or even prevented back reaction of the Fe[III] aqueous pool with the remaining Fe[II] aqueous pool. In fact, if only the $Fe[II]_{aq}$ data for the biological experiments are considered, then a reasonable interpretation of my data would be that isotopic distribution during the microbial oxidation process was governed by a Rayleigh mechanism having ε ~2.2‰ (Fig. 4.2a). This value is substantially less than the 2.9‰ value determined by Johnson et al. (2002) and Welch et al. (2003) for $Fe[II]_{aq}$-$Fe[III]_{aq}$ equilibrium exchange, and could be interpreted as reflecting a biological control on the isotopic distribution. Croal et al. (2004), in a study of Fe isotope fractionation by Fe[II] oxidizing photoautotrophic bacteria, obtained broadly similar results to mine in that the isotopic contrast between their hydrous ferric iron precipitates and aqueous ferrous iron was ~1.5‰ (compare with Table 4.3) and the isotopic compositions of the Fe[II] aqueous reactants in their two experiments using different enrichment cultures were consistent with control by a Rayleigh mechanism having ε ~1.1‰ and 1.8‰, respectively. They concluded that the observed fractionation between $Fe[III]_{ppt}$ and $Fe[II]_{aq}$ was due either to an equilibrium effect produced by biological ligands or to a kinetic effect produced by precipitation of hydrous ferric oxides overlaid upon equilibrium exchange between Fe[II] and Fe[III] aqueous species. However, in the absence of measurements of the isotopic composition of the $Fe[III]_{aq}$ fraction that would be difficult to isolate given the circum-neutral pH conditions of their experiments, it was not possible to decide between these contrasting mechanisms. By determining the Fe isotope composition of the $Fe[III]_{aq}$ products of my biological experiments, it is possible to better constrain the actual fractionation between the Fe[II] and Fe[III] aqueous pools. As shown in Figure 4.2b, the data for aqueous Fe are generally well described by an equilibrium mechanism between $Fe[II]_{aq}$ and $Fe[III]_{aq}$ having ε ~2.9‰, consistent with the experimental work of Johnson et al. (2002) and Welch et al. (2003). This result suggests that isotopic equilibration between Fe[II] and Fe[III] due to electron transfer dominates any isotopic effects associated with microbial Fe[II] oxidation or Fe[III] precipitation. As shown in Figure 4.4, the $Fe[II]_{aq}$ data of Croal et al. (2004) cluster with the data from my biological experiments, suggesting a similar interpretation of their experimental results. However, in order to confirm this interpretation, it will be necessary to develop novel and clever techniques with which to actually determine the Fe isotope composition of the minor $Fe[III]_{aq}$ pool formed at the circum-neutral pH conditions used in the experiments of Croal et al. (2004).

4.4.2 Isotopic fractionation associated with $Fe[III]_{aq}$ precipitation

In order to interpret isotopic fractionation between $Fe[II]_{aq}$ and Fe[III]-oxyhydroxides properly, an important goal of my study was to assess causes of isotopic fractionation between $Fe[III]_{aq}$ and Fe[III]-oxyhydroxide pools during Fe[III] precipitation. In the short-term Fe[III] precipitation experiments (Table 4.4; Fig. 4.3), a range of pH's were used in order to investigate the possible effects of precipitation rate on fractionation. In these experiments, pH was used as a proxy for precipitation rate. Recent work on carbonates by Adkins et al. (2003) contested the use of pH as a proxy for precipitation rate and maintained that isotope effects associated with changes in pH are a function of changes in speciation among ionic components containing the isotopes in question. However, it is unlikely that changes of Fe aqueous speciation with changing pH controlled the fractionation observed in my experiments. For example, over the pH range used in the precipitation experiments with ferric sulfate, concentrations of Fe aqueous species (calculated using the WATEQ4f speciation code; Ball and Nordstrom, 1991) changed little (i.e., at pH=1.9 vs. 3.5: $Fe(SO_4)_x$ = 92.8% vs. 91.5%, $Fe(OH)_x$ = 0.2% vs. 4%, $Fe(H_2O)_6$ = 7% vs. 4.5%), yet $\Delta^{56}Fe_{aq-ppt}$ decreased by ~0.8‰. Over the same pH range used in the experiments with ferric chloride, concentrations of Fe aqueous species changed considerably (i.e., at pH=1.9 vs. 3.5: $FeCl_x$ = 39% vs. 19.7%, $Fe(OH)_x$ = 1.5% vs. 34.8%, $Fe(H_2O)_6$ = 39.5% vs. 45.5%), yet $\Delta^{56}Fe_{aq-ppt}$ barely decreased. It is contend that the isotopic changes seen during these experiments are more likely related to the rate at which the precipitates formed.

Skulan et al. (2002) experimentally precipitated hematite (Fe_2O_3) from hot nitric acid solutions over varying reaction times. During "rapid" precipitation of hematite (~12 hours), $\Delta^{56}Fe_{aq-ppt}$ ~1.3‰ was observed. However, when protracted precipitation/dissolution was allowed to occur over a longer time (~200 days), $\Delta^{56}Fe_{aq-ppt}$ approached 0‰. My long-term precipitation experiments were run for a much shorter time than the long-term equilibration experiments of Skulan et al.

(2002). Regardless, $\Delta^{56}Fe_{aq\text{-}ppt}$ using the ferric sulfate medium was significantly less in the long-term experiment than in the short-term experiment (i.e., ~0.7‰ vs. 1.29‰), consistent with the trend observed by Skulan et al. (2002) of decreasing fractionation with increasing reaction time. However, $\Delta^{56}Fe_{aq\text{-}ppt}$ using the ferric chloride medium was significantly greater in the long-term experiment than in the short-term experiment (i.e., ~0.9‰ vs. 0.44‰), opposite to the trend observed by Skulan et al. (2002).

Although it is clear from my experiments that different reaction times at a given pH result in different $\Delta^{56}Fe_{aq\text{-}ppt}$, it remains unclear whether equilibrium values of $\Delta^{56}Fe_{aq\text{-}ppt}$ are in the 0.7-0.9‰ range for the ferric sulfate and chloride systems as measured in my long-term experiments or are closer to 0‰ as observed by Skulan et al. (2002) for the ferric oxide system. Regardless, in order for equilibrium effects to be expressed, slow rates of precipitation apparently are required. This is supported by the theoretical work of Watson (2004) who looked at near-surface kinetic controls on the isotopic composition of carbonates. Watson's (2004) model predicts that during rapid precipitation of carbonate, the surface of the precipitating crystal represents a reaction front that can have an isotopic composition that is not at equilibrium with that of the surrounding water, depending primarily on the isotopic equilibration rate that is largely diffusion limited. If the precipitation rate exceeds the isotopic equilibration rate, this non-equilibrium isotopic signature will be incorporated into the mineral.

The differences in $\Delta^{56}Fe_{aq\text{-}ppt}$ of the different size fractions in my precipitation experiments apparently support such a model. In those experiments, the smaller size fraction (0.1–0.8 μm) is intermediate in isotopic composition between that of the >0.8 μm and $Fe[III]_{aq}$ fractions, and tends to be significantly heavier (by as much as ~1.0‰) than the >0.8 μm fraction. The 0.1-0.8 μm fraction may be associated with earlier and/or faster rates of precipitation and might reflect the isotopic composition of a colloidal intermediate, while the >0.8μm fraction may be associated with later and/or slower rates of precipitation. With time, amalgamation and dissolution/re-crystallization occurs and larger Fe[III]-oxyhydroxide precipitates form. At the slowest rates of precipitation, the net isotopic fractionation observed may be the additive fractionation effects associated with the formation of each size fraction, depending primarily on the ability of early-formed solids to re-equilibrate with the evolving $Fe[III]_{aq}$ pool. If true, this suggests that multiple rate-controlling steps occur during slower Fe[III] precipitation at lower pH and the fractionation effects of each step may be expressed in the final product.

Decreasing $\Delta^{56}Fe_{aq-ppt}$ with increasing Fe[III]-oxyhydroxide precipitation rate observed in my experiments is consistent with the observations of Johnson et al. (2002), who developed a rapid precipitation technique to physically separate isotopically-enriched $Fe[III]_{aq}$ from a $Fe[II]_{aq}$-$Fe[III]_{aq}$ mixture with little to no effect on isotopic composition. However, as noted above, Skulan et al. (2002) observed the opposite trend, increasing $\Delta^{56}Fe_{aq-ppt}$ with increasing precipitation rate, during experimental precipitation of hematite. This apparent contradiction is likely related to the time scale and kinetics of the various experiments. My slowest experiments (i.e., at lowest pH) may be most analogous to the "rapid" hematite precipitation experiments of Skulan et al. (2002) that occurred over a 12-hour timeframe. At the precipitation rate corresponding to this time scale, kinetic isotope effects perhaps related to diffusion gradients in the growing solid (cf., Gussone et al., 2003) and resulting in positive $\Delta^{56}Fe_{aq-ppt}$ are best expressed. At more rapid precipitation rates, diffusion gradients in the liquid immediately adjacent to the growing solid may limit the ability of residual, isotopically heavy $Fe[III]_{aq}$ in this liquid boundary layer to equilibrate isotopically with the remaining $Fe[III]_{aq}$ pool. Progressive precipitation under this condition would result in $\Delta^{56}Fe_{aq-ppt}$ approaching 0‰. At slower precipitation rates (e.g., the 200-day "equilibrium" experiment of Skulan et al., 2002), there would be the greatest potential for true isotopic equilibrium between solid and liquid.

Dependence of $\Delta^{56}Fe_{aq-ppt}$ on precipitation rate may help to explain the variability of $\Delta^{56}Fe_{aq-ppt}$ observed in my biological experiments. In all biological experiments conducted at 25°C. $\Delta^{56}Fe_{aq-ppt}$ is greatest in the earlier stages and least in the later stages of Fe[II] oxidation (Table 4.3). Precipitation of Fe[III]-oxyhydroxide is presumably a first-order reaction (Beard and Johnson, 2004), and thus precipitation rate should correlate with ln ($Fe[III]_{aq}$). Thus, in the earlier stages of Fe[II] oxidation when $Fe[III]_{aq}$ concentrations are low, the precipitation rate should be correspondingly slow and $\Delta^{56}Fe_{aq-ppt}$ also should be greatest. As $Fe[III]_{aq}$

concentrations increase with protracted Fe[II] oxidation, the precipitation rate should increase and $\Delta^{56}Fe_{aq\text{-}ppt}$ should decrease toward 0‰. However, although simple precipitation rate considerations can account for the results of the experiments conducted at 25°C, the results of the experiment using ferrous sulfate at 4°C argue for additional controls. In that experiment, $\Delta^{56}Fe_{aq\text{-}ppt}$ actually increased through the 56-day time point, then decreased to a negative value by the 70-day time point (Table 4.3). Although one can speculate about unique kinetics associated with precipitation of Fe[III]-oxyhydroxides in this low-temperature condition, there is little hard evidence that can be used to account for this different behavior. Furthermore, abiotic controls prepared at 4°C resulted in no measurable oxidation and thus offer no additional interpretive insight.

5 CONCLUSIONS and SUGGESTIONS FOR FUTURE STUDIES

The aim of this study was to examine bacterial influence on sulfide minerals and Fe(II) oxidation as inferred from oxygen, sulfur isotopes of sulfate and Fe isotopes of Fe-oxides at pH <3.

The $\delta^{18}O_{SO4}$ and $\delta^{34}S_{SO4}$ values from bacterial and abiotic pyrite oxidation

Pyrite oxidation occurred by both biological and abiotic pathways under aerobic conditions at pH <3. However, it was observed that the oxidation rate of pyrite was higher when bacteria present, indicating that the oxidation of pyrite was largely controlled by bacterial activity at pH < 3 and under O_2 saturation conditions. Sulfate production rate from anaerobic experiments confirmed that the chemical oxidation of pyrite by Fe (III) was dominant in both biotic and abiotic experiments.

Water was the most important source of oxygen in sulfate for both biotic and abiotic oxidation mechanisms under aerobic and anaerobic conditions. The percentage of water-oxygen incorporation into sulfate ranged from 87 to 95 % during aerobic biotic and abiotic experiments. Water-oxygen incorporation into sulfate increased with decreasing pH. ~100 % water-oxygen incorporation into sulfate was determined for both biotic and abiotic experiments under anaerobic conditions. The similar oxygen isotope fractionation effect between sulfate and water from both biotic and abiotic experiments under anaerobic conditions indicate that the chemical oxidation of pyrite by Fe(III)aq was dominant over biological experiments. Because the solubility of Fe (III)-oxides is very low and the concentration of soluble Fe (III) could be too low for FeS_2 oxidation at pH <4, the $\delta^{18}O_{SO4}$ values produced by oxidation of pyrite by Fe(III) can be a good indicative of terrestrial environments when compared to higher pH environments, such as marine environments.
Experimental results from aerobic long-term biological pyrite oxidation showed that water–oxygen incorporation into sulfate may not always be indication of oxidation

of pyrite by Fe(III) ions as suggested by previous studies. The long term experimental results indicated the increasing water-oxygen incorporation into sulfate with decreasing pH, suggesting that the $\delta^{18}O_{SO4}$ values may be largely controlled by the other processes such as oxygen isotope exchange between water and intermediate sulfur species which increase water-oxygen incorporation into sulfate. These exchange reactions appears to be a function of pH and may overprint the biological signature.

Although it is clear that pyrite oxidation is largely controlled by biological reactions as inferred from the high sulfate concentration, the $\delta^{18}O_{SO4}$ values can not be used to distinguish biotic vs. abiotic oxidation of pyrite because of the similar oxygen isotope signatures. For example, ~90 % incorporation of oxygen from water was obtained for both biotic and abiotic experiments.

The $\delta^{34}S_{SO4}$ values closely reflect the $\delta^{34}S$ value of pyrite under aerobic conditions, indicating the quantitative oxidation of pyritic sulfur to sulfate. Therefore, the $\delta^{34}S_{SO4}$ values can be a useful tool to determine the source of sulfate.

Consequently, elucidation of pyrite oxidation mechanism in any natural environments requires a combination of geochemical, isotopic and microbiological data.

The $\delta^{18}O_{SO4}$ and $\delta^{34}S_{SO4}$ values from bacterial and abiotic sphalerite and elemental sulfur oxidation

ZnS and Fe-bearing sphalerite oxidation occurred by both biological and abiotic experiments and the oxidation rate was higher in the biological experiments than abiotic experiments. Fe-bearing sphalerite experiments even produced higher sulfate concentration during both biotic and abiotic experiments relative to pure sphalerite experiments, indicating that Fe (II) in the crystal lattice of sphalerite has effect on oxidation rate.

The $\delta^{18}O_{SO4}$ values from aerobic biological ZnS and Fe-bearing sphalerite experiments showed 100 % water–oxygen was incorporated into sulfate during the short- and long-term experiments. 100 % water–oxygen incorporation into sulfate suggests that *A. ferrooxidans* catalyze sphalerite oxidation via ETS (electron transport system) as a source of energy and they incorporate H_2O–derived oxygen rather than oxygen from molecular oxygen into the oxidized sulfate. The $\delta^{18}O_{SO4}$ values from aerobic experiments proved that the net stoichiometry of oxidation reactions (reaction 21) not always represent the actual oxygen source of sulfate, although it explains overall mass transformation phenomenon.

In contrast to biological ZnS experiments, the $\delta^{18}O_{SO4}$ values from aerobic abiotic ZnS experiments point out 40 % water and 60 % molecular oxygen incorporation into sulfate. The difference between biotic and abiotic experiments may indicate different oxidation mechanisms for each experiments (biotic vs. abiotic).

The $\delta^{18}O_{SO4}$ values from anaerobic pure and Fe-bearing sphalerite experiments are very similar for both biotic and abiotic experiments, suggesting that the chemical oxidation of sphalerite by Fe (III) ions was the dominant in both experiments and the $\delta^{18}O_{SO4}$ values can not reflect bacterial influence.

This study also showed that elemental sulfur is the main sulfur intermediate and the actual sulfur moiety which was oxidized to sulfate during sphalerite oxidation may have been elemental sulfur. The identical $\delta^{18}O_{SO4}$ values between biological elemental sulfur and sphalerite experiments under O_2 saturated conditions further support this idea. Experimental results from anaerobic sphalerite oxidation showed that elemental sulfur forms on the surface of sphalerite as major oxidation product during chemical oxidation of sphalerite by $Fe(III)_{aq}$. The formation of elemental sulfur on the surface of sphalerite has implications for understanding the role and distribution of various microorganism involved in the oxidation of sulfides. Additionally, elemental sulfur at the mineral surface may be a determining factor in the type of microorganism which involve in the oxidation. Although the $\delta^{18}O_{SO4}$ values from ZnS and Fe-bearing sphalerite experiments are very similar, these values are different than the $\delta^{18}O_{SO4}$ values from pyrite experiments. The $\delta^{18}O_{SO4}$ values from sphalerite experiments tend to be more enriched in O^{18} (~9 ‰) relative to water compared to the $\delta^{18}O_{SO4}$ values from pyrite experiments (~4 ‰). These results may imply that sulfide mineralogy, especially oxidation state of sulfur of each mineral, have effect on the $\delta^{18}O_{SO4}$ values. Therefore, the $\delta^{18}O_{SO4}$ values can be used to determine the source of sulfide mineral (pyrite vs. sphalerite).

The conclusions drawn from these studies revealed that bacteria can influence the rates of sulfide minerals oxidation. The Oxygen isotope studies of the sulfate product can serve as useful tools for understanding processes involved in their formation. The $\delta^{18}O_{SO4}$ values measured in the laboratory and field clearly indicate that water-oxygen is incorporated into sulfate during oxidation. Because oxygen isotope exchange between sulfate and water is very slow at pH <3 the $\delta^{18}O_{SO4}$ values can preserve the $\delta^{18}O_{H2O}$ values. It can be hypothesized that the $\delta^{18}O_{SO4}$ values measured for sulfate in acidic environments (pH<3) may be useful for determining the paleo-temperature at the time of their formation when the proper oxygen isotope fractionation effect ($\Delta^{18}O_{SO4\text{-}H2O}$) is applied.

Fe isotopes of Fe-oxides

This is the first study to measure the Fe isotope distribution between $Fe[II]_{aq}$, $Fe[III]_{aq}$ and $Fe[III]_{ppt}$ during bacterial and abiotic Fe[II] oxidation in ferrous sulfate and ferrous chloride solutions at low pH conditions that might be typically reflect acid mine drainage environments. Although the original purpose of this study was to determine the impact of biological processes on the Fe isotope composition of the ferric iron products of oxidation, my main conclusion is that the isotopic distribution between the various Fe pools was controlled by abiotic processes. Using a novel method to separate the product $Fe[III]_{aq}$ from residual $Fe[II]_{aq}$, which follows oxidation over varying reaction times, I found that both $\delta^{56}Fe[III]_{aq}$ and $\delta^{56}Fe[III]_{ppt}$ were consistently greater than $\delta^{56}Fe[II]_{aq}$, and that overall the aqueous data are well explained by an equilibrium model having ε = 2.9‰. This fractionation factor is identical to that of previously established for equilibrium between Fe[II]- and Fe[III]-hexaquo species due to electron transfer. My results argue against a role for biologically-induced ligand formation that could hinder or prevent back reaction of $Fe[III]_{aq}$ with $Fe[II]_{aq}$, and thus impart a biological signature on the ferric iron products of oxidation. In a series of abiotic experiments in which schwertmannite or akaganeite were precipitated from ferric sulfate and ferric chloride solutions, respectively it was found that $\delta^{56}Fe[III]_{aq}$ was consistently greater than $\delta^{56}Fe[III]_{ppt}$, and that $\Delta^{56}Fe_{aq-ppt}$ depends largely on rate of precipitation. Fractionation between ferric aqueous and precipitate pools was substantially greater in the sulfate system when compared to that in the chloride system, perhaps due to differences in ligand formation prior to precipitation, or to greater diffusion limitation either at the solid-liquid interface or within precipitates in the sulfate system in comparison to chloride system. Overall, the results of this study suggest that, at least under low pH conditions, unique Fe isotope "biosignatures" related to microbial oxidation of ferrous iron that similar to those used in the current study, may not be expressed in the ferric iron products of the oxidation process, and thus will be absent in the geologic record.

5.1 Future Studies

The current study showed that the oxidation state of sulfur of sulfide minerals have effect on the $\delta^{18}O_{SO4}$ values. Therefore, more sulfide minerals which have different sulfur oxidation state should be used for future studies.

Biological pyrite oxidation experiments indicated larger water-oxygen incorporation into sulfate with decreasing pH. New experiments should be carried out under different pH values in order to investigate if $\delta^{18}O_{SO4}$ values change systematically with changing pH. This study may give an opportunity to use the oxygen isotope fractionation effect between sulfate and water ($\Delta^{18}O_{SO4-H2O}$) to predict pH values which sulfate formed and eventually geochemical conditions. More metal sulfide oxidation experiments should be performed by using different experimental conditions to investigate the possible effect of environmental conditions on the $\delta^{18}O_{SO4}$ and $\delta^{34}S_{SO4}$ values.

REFERENCES

Adkins, J. F., Boyle, E. A., Curry, W. B., and Lutringer, A., 2003. Stable isotopes in deep-sea corals and a new mechanism for "vital effects". *Geochmica et Cosmochimica Acta.* **67**, 1129-1143.

Anbar, A.D, Roe, J. E., Barling, J. and Nealson, K. H., 2000. Nonbiological fractionation of iron isotopes. *Science* **288**, 126-128.

Anbar, A.D., 2004. Iron stable isotopes: beyond biosignatures, *ESPL Frontiers*, **217**, 223-236.

Arkesteyn, G.J M.W., 1979. Pyrite oxidation by T. ferrooxidans with special reference to the sulfur moiety of the mineral. *Antonie van Leeuwenhoek.* 45, 423-435.

Baldi,F., Clark, T., Pollack, S. S., and Olson, G.J., 1992. Leaching of pyrites of various reactivities by T.ferroxidans. *Appl.Environ. Microbiol.* **58**, 1853-1856.

Ball, J.W. and Nordstrom, D.K., 1991. WATEQ4f—User's manual with revised thermodynamic data base and test cases for calculating speciation of major, trace and redox elements in natural waters. U.S. *Geological Survey Open-File Report*, 91-183, 185.

Beard, B. L. and Johnson, C. M., 1999. High precision iron isotope measurements of terrestrial and lunar materials. *Geochimica et Cosmochimica Acta.* **63**, 1653-1660.

Beard, B. L., Johnson, C. M., Cox, L., Sun, H., Nealson, K. H. and Aguilar, C., 1999. Iron isotope biosignatures. *Science* **285**, 1889-1892.

Beard, B.L. and Johnson, C.M., 2004. Fe isotope variations in the modern and ancient earth and other planetary bodies. Rev. *Mineral. Geochem.* **55**, 319-357.

Beard, B.L., Johnson, C. M., Skulan, J. L., Nealson, K. H., Cox, L., and Sun, H. 2003. Application of Fe isotopes to tracing the geochemical and biological cycling of Fe. *Chemical geology* **195**, 87-117.

Biegler, T., and Swift, D.A., 1979. Anodic behavior of pyrite in acidic solution. *Electrochim Acta*, **24**, 415-420.

Blowes, D.W., Ptacek, C.J. and Jurjovec, J., 2003., Mill Tailings: Hydrogeology and geochemistry. *Environmental aspects of mine wastes. Editor J. L. Jambor, D. W. Blowes and A.I.M. Ritchie*. Short Course series 31, **95**-116.

Brett, J.B., Banfield, J., 2003. Microbial communities in acid mine drainage, *FEMS microbiology ecology* **44**, 139-152.

Brown A.D. and Jurinak J.J. 1989. Mechanisms of pyrite oxidation in aqueous mixtures, *J. Environ. Qual.*, **18**, 545.

Bullen, T. D., White, A., Childs, C. W., Vivit, D. V., and Schulz, M. 2001. Demonstration of significant abiotic iron isotope fractionation in nature. *Geology*, **29**, 699-702.

Chambers, L.A. and Trudinger, P.A., 1978. Microbiological fractionation of sulfur, *Geomicrobiology*, **1**, 249-293.

Chang, S.G, Littlejohn, D., Hu, K. Y.,1987. *Science*, **237**, 756-758.

Chiba, H., and Sakai, H., 1985. Oxygen isotope exchange rate between dissolved sulfate and water at hydrothermal temperatures, *Geochimica Cosmochimica Acta*, **49**, 993-1000.

Croal, L.R., Johnson, C. M., Beard, B.L., and Newman, D,K., 2004. Iron isotope fractionation by Fe[II]-oxidizing Photoautotrophic bacteria, *Geochim. et Cosmochim. Acta*, **68** **(6)**, 1227-1242.

Crundwell, F.K., 1987. Kinetics and mechanism of the oxidative dissolution of a zinc sulfide concentrate in ferric sulfate solution, *Hydrometallurgy* **19**, 227-242.

Crundwell, F.K., 1988. The influence of the electronic structure of solids on the anodic dissolution and leaching of semiconducting sulfide minerals, *Hydrometallurgy*, **21**, 155-190.

Curutchet, G., Tedesco, P., Donati, E., 1996. *Biotech. Lett.*, **18**, 1471-1476.

Descostes M., Mercier F., Beaucaire C., Zuddas P., and Trocellier P., 2001. Nature and distribution of chemical species on oxidized pyrite surface: Complementarity of XPS and nuclear microprobe analysis. *Nucl. Inst. Methods Phys. Res.*, B **181**, 603–609.

Donati, E., Pogliani, C., and Boiardi, J.L., 1997. Anaerobic leaching of covellite by Thiobacillus ferrooxidans. *Applied and environmental microbiology*, **47**, 636-639.

Ehrlich H.L,. 1982. *Geomicrobiology*, New York: Marcel Dekker. Inc. 393 .

Ehrlich H.L., 1981. *Geomicrobiology*, Dekker, New York

Elhrlich, H. L., 1990. *<u>Geomicrobiolgy.</u>* 2nd revised and expanded edition. Marcel Dekker, New York.

Evangelou, V.P and Zhang, Y.L., 1995. A review: pyrite oxidation mechanism and acid mine drainage . prevention. *Crit. Rev. Environ. Sci. Technol.*, **25**, 141-199.

Field, C.W., 1966. Sulfur isotope method for discriminating between sulfates of hypogene and supergene origin. *Econ. Geol.,* **61**, 1428-1435.

Fowler, T.A., and Crundwell, F.K. 1999. Leaching of zinc sulfide by *Thiobacillus ferrooxidans*: Bacterial oxidation of the sulfur product layer increases the rate of zinc sulfide dissolution at high concentrations of ferrous ions. *Applied and Environmental Microbiology* **65**, 5285-5292.

Fritz, P., Basharmal, G.M., Drimmie, R.J., Ibsen, J., Qureshi, R.M., 1973. Oxygen isotope exchange between sulfate and water during bacterial reduction of sulfate. *Chemical Geology (Isotope Geosciences section)* **79**, 99-105.

Fry, B., Cox, J., Gest, H. and Hayes, M., 1986. Discrimination between 34S and 32S during bacterial metabolism of inorganic sulfur compounds. *J. Bacteriol.*, **165**, 328-330.

Fry, B., Ruf, W., Gest, H., and Hayes, J.M., 1988. Sulfur isotope effects associated with the non-biological oxidation of sulfide in aqueous solution, *Chem. Geol.,* **73**, 205-210.

Fry, B., William, R., Gest, H., and Hayes, J. M., 1988. Sulfur isotope effects associated with oxidation of sulfide by O_2 in aqueous solution, *Chemical Geology (Isotope Geoscience Section)*, 73, 205-210.

Fry, I. V., Lazaroff, N., and Packer, L., 1986. Sulfate dependent iron oxidation by T. ferrooxidans: Characterization of a new EPR detectable electron transport component on the reducing side of rusticyanin. *Archives of biochemistry and biophysics*, **246 (2)**, 650-654.

Garcia, O., Jr, Bigham, J. M., and Tuvonien, O.H., 1995a. Oxidation of galena by Thiobacillus ferrooxidans and Thiobacillus thiooxidans. *Can. J. Microbial*, **41**, 508-514.

Garcia, O., Jr, Bigham, J. M., and Tuvonien, O.H., 1995b. Oxidation of sphalerite by Thiobacillus ferrooxidans and Thiobacillus thiooxidans. *Can. J. Microbial.*,, 578-584.

Garrels, R.M and Thompson, M.E 1960. Oxidation of pyrite by iron sulfate solution, *Am. J.Sci.* **258A,** 57-67.

Gavelin, S., Parwel, A. and Ryhage, R., 1960. Sulfur isotope fractionation in sulfide mineralization. Econ. Geol. 55, 510-530. *Geochim. Cosmochim. Acta* **51**, 3193 - 3199.

Ghiorse, W. C., 1984., Biology of iron and manganese-depositing bacteria. *Annual Review of Microbiology,* **38**, 515-550.

Glasauer, S., Weidle, P. G., Langley, S. and Beveridge, Terry J., 2003. Controls on Fe reduction and mineral formation by a subsurface bacterium. *Geochimica et Cosmochimica Act.,* **67, Issue** 7, 1277-1288.

Goldhaber M.B. 1983., Experimental study of metastable sulfur oxyanion formation during pyrite oxidation at pH 6–9 and 30oC. *Am. J. Sci.* 283, 193 - 217.

Guevremont J.M., Bebie J., Elsetinow A.R., Strongin D.R. and Schoonen M.A.A., 1998. Reactivity of the (100) plane of pyrite in oxidizing gaseous and aqueous environments:Effects of surface imperfections. *Environ. Sci. Technol.* **32**, 3743 - 3748.

Gussone, N., Eisenhauer, A., Heuser, A., Dietzel, M., Bock, B., Bohm, F., Spero, H., Lea, D., Buma, J., and Nagler, T.F., 2003. Model for kinetic effects on calcium isotope fractionation (δ^{44}Ca) in inorganic aragonite and cultured planktonic foraminifera, *Geochim. Cosmochim. Acta,* 67, 1375-1382.

Guy R.D., Fogel, M.F., Berry, J.A., and Hoering, T.C., 1987. Isotope fractionation during oxygen production and consumption by plants. *In progress in photosynthesis research* , 597-600

Harahuc, L., Lizama, Hector, M., and Suzuki, I., 2000. Selective Inhibition of the Oxidation of Ferrous Iron or Sulfur in *Thiobacillus ferrooxidans. Applied and Environmental Microbiology.* **66, 3,** 1031-1037.

Hazeu, W., W. H. Batenburg-van der Vegte, Bos, P., Van der Pas, and Kuenen, J. G., 1988. The production and utilization of intermediary elemental sulfur during the oxidation of reduced sulfur compounds by Thiobacillus ferrooxidans. *Arch. Microbiol.*, **150**, 574-579.

Hoering, T.C. and Kennedy, J.W., 1957. *Journal of American Chemical Society,* **79**, 56 60.

Holt, B.D., Kumar, R., Cunningham, P.T., 1981. *Atmos. Environ.* **15**, 557-566.

Jambor, J.L., 2003. Mine waste mineralogy and mineralogical perspective of acid-base counting, Environmental aspects of mine wastes, Editor J. L. Jambor, D. W. Blowes and A.I.M. Ritchie. *Short Course series*, **31**, 117-145.

Johnson, C. M., Skulan, J. L., Beard, B. L., Sun, H., Nealson, K. H., and Braterman, P. S., 2002. Isotopic fractionation between aqueous FeIII and FeII in aqueous solutions, *Earth and Planetary Science Letters,* **195**, 141-153.

Kaplan, I.R., and Rafter, T.A., 1958. Fractionation of stable isotopes of sulfur by thiobacilli, *Science* **127**, 517-518.

Kaplan, I.R., and Rittenberg, S.C., 1964. Microbiological fractionation of sulphur isotopes, *J. Gen. Microbiol,*. **34**, 195–212.

Kappler, A., Marcus, B., Schink, B., and Brune, A., 2004. Electron shuttling via humic acids in microbial iron(III) reduction in a freshwater sediment. *FEMS Microbiology Ecology*. **47**, Issue 1, 15 85-92.

Kelly, D., 2003. Microbial Inorganic Sulfur Oxidation: The APS Pathway, Biochemistry and Physiology of Anaerobic Bacteria, by Lars G. Ljungdahl (Editor), Michael W. Adams (Editor), Larry L. Barton (Editor), James G. Ferry (Editor), Michael K. Johnson (Editor)

Kelly, D.P., Shergill, J.K., Wei-Ping Lu and Wood, Ann P., 1997. Oxidative metabolism of inorganic sulfur compounds by bacteria. *Antonie van Leeuwenhoek*, **71**, 95-107.

Kelly,D.P., 1982. Biochemistry of the chemo-lithotrophic oxidation of inorganic sulphur. *Phil. Trans. Roy.Soc. London B,* **298**, 449-528.

Kelly,D.P, and Tuovinen O.H., 1975. Metabolism of inorganic sulphur compounds by Thiobacillus ferrooxidans and some comparative studies on Thiobacillus A2 and T. neopolitanus, *Plant and Soil* 43, 77-93.

Kroopnick, P. and Craig, H., 1976. Oxygen isotope fractionation in dissolved oxygen oxygen in deep sea, *Earth Planet. Sci. Lett.,* **32**, 375-388.

Krouse, H. R, Gould, W.D, McCready, R.G.L and Rajan, S., 1991. 18O incorporation into sulfate during the bacterial oxidation of sulfide minerals and the potential for oxygen isotope exchange between O2, H2O and oxidized sulfur intermediates, *Earth and Planetary Science Letters*, **107**, 90-94.

Kuenen, J.G., and Tuovinen, O.H., 1981. Ch. 81: The genera Thiobacillus and Thiomicrospira. In M.p.Starr. et al., eds. *The Prokaryotes. New York*, Springer-Verlag, 1023-1036.

Lane, G.A. and Dole, M., 1956. Fractionation of oxygen isotope during respiration, *Science,* 123, 574-576.

Lizama, H. M., and Suzuki, I., 1989. Bacterial leaching of a sulfide ore by *Thiobacillus ferrooxidans* and *Thiobacillus thiooxidans* part II: Column leaching studies. *Hydrometallurg,* **22, Issue** 3, 301-310.

Lloyd R.M., 1968. Oxygen isotope behavior in the sulfate water system, *J. Geophysical Res.,* **73**, 6099-6110.

Lovley, D. R., and E. J. P. Phillips., 1986b. Availability of ferric iron for microbial reduction in bottom sediments of the freshwater tidal Potomac River. *Appl. Environ. Microbiol.* **52**, 751-757.

Lovley, D. R., and E. J. P. Phillips., 1986a. Organic matter mineralization with reduction of ferric iron in anaerobic sediments. *Appl. Environ. Microbiol.* **51,** 683-689.

Lovley, D. R., and E. J. P. Phillips., 1987. Rapid assay for microbially reducible ferric iron in aquatic sediment. *Appl. Environ. Microbiol.* **53,** 1536-1540.

Lowson, R. T., 1982. Aqueous oxidation of pyrite by molecular oxygen. *Chem. Rev.,* 82, 461-497.

Lu, W.P and Kelly, D. P., 1988. Kinetic and energetic aspects of inorganic sulfur compound oxidation by Thiobacillus tepidarius, *J. Gen. Microbiol.,* **134,** 877-885.

Luther G.W. III., 1987. Pyrite oxidation and reduction: Molecular orbital theory considerations, *Geochim. Cosmochim. Acta* 51, 3193 - 3199.

M. Descostes, P. Vitorge, And C. Beaucaire Cea, Den., 2004. Pyrite dissolution in acidic media, *Geochimica et Cosmochimica Acta,* 68, No. 22, 4559-4569,

Mandernack, Kevin W., Marilyn L. Fogel, Bradley M. Tebo and Akira Usui., 1995. Oxygen isotope analyses of chemically and microbially produced manganese oxides and manganates, *Geochimica et Cosmochimica Acta,* 59, 4409-4425

Mandernack, K. W. Bazylinksi, D. A., Shanks, W. C., and Bullen, T. D., Oxygen and Iron isotope studies of magnetite produced by magnetotactic bacteria. *Science* 285, 1892-1896.

Mandernack, Kevin W., L. Lynch, H. R. Krouse and M. D. Morgan., 2000. Sulfur cycling in wetland peat of the New Jersey Pinelands and its effect on stream water chemistry. *Geochimica et Cosmochimica Acta.* 64, Issue 23, 949-3964.

Mariotti, A., Christiane, L., and Gilles, B., 1984. Natural isotopic composition of nitrogen as a tracer of origin for suspended organic matter in the Scheldt estuary. *Geochimica et Cosmochimica Acta.* 48, 549-555.

Matthews, A., Zhu, X. K., and O'nions, K., 2001. Kinetic iron stable isotope fractionation between iron (-II) and (-III) complexes in solution, *Earth and Planetary science letters,* 192, 81-92.

Matthews, S.F.and Depaolo, D. J., Iron isotopes in deep sea hydrothermal vents: The iron flux to the deep ocean and its importance to the global iron cycle **(source; internet).**

McCready, R.G.L., Krouse, H.R., 1982. Sulfur isotope fractionation during the oxidation of elemental sulfur by Thiobacilli in a Solonetzic soil, *Can. J. Soil Sci.,* **62**, 105– 110.

McGuirre M. M., Jallad K. N., Ben-Amotz D., and Hamers R. J., 2001. Chemical mapping of elemental sulfur on pyrite and arsenopyrite surfaces using near-infrared Raman imaging microscopy, *Appl. Surf. Sci.* **178,** 105–115.

McKibben M.A. and Barnes H.L., 1986. Oxidation of pyrite in low temperature acidic solutions:Rate laws and surface textures, *Geochim. Cosmochim. Acta,* **50**, 1509 - 1520.

Mcquire, M and Robert J. Hamers., 2000. Extraction and Quantitative analysis of elemental sulfur from sulfide mineral surfaces by high –performance liquid chromatography. *Environ. Sci. Technol.* **34**, 4651-4655.

Mizutani, Y and Rafter, T.A., 1969a. Oxygen isotope composition of sulfate. Part 3, oxygen isotope fractionation in the bisulfate ion water-system. *N.Z.J. Sci.*, **12,** 54-59.

Mizutani, Y., and Rafter, T. A., 1973. Isotopic behaviour of sulfate oxygen in the bacterial reduction of sulfate, *Geochemical Journal*, **6**, 183-191.

Morgan, J. J. **and Stumm, W.,** 1998. Water Properties, Kirk-Othmer Encyclopedia of Chemical Technology, Fourth Edition, **25**.

Moses, C.O., Herman, J.S., 1991. Pyrite oxidation at circumneutral pH, *Geochim. Cosmochim. Acta,* **55**, 471–482.

Moses, C.O., Nordstrom, D.K., Herman, J.S., Mills, A.L., 1987. Aqueous pyrite oxidation by dissolved oxygen and ferric iron, *Geochim. Cosmochim. Acta,* **51**, 1561– 1571.

Mycroft, J. R.; Bancroft, G.M., McIntyre, N. S., Lorimer, J. M., and Hill, I.R., 1990. Detection of sulfur and polysulfides on electrochemically oxidized pyrite surfaces by X-ray photoelectron spectroscopy and Raman spectroscopy, *J Electroanal. Chem.* **292**, 139-152.

Nakai, N. and Jensen, M. L., 1964. The kinetic isotope effect in the bacterial reduction and oxidation of sulfur, *Geochim. Cosmochim. Acta*, **28**, 1893-1912.

Nealson, K. H., Tebo, B. M., and Rosson, R. A., 1988. Occurrence and mechanisms of microbial oxidation of manganese, *Adv. Applied Microbiology,* **33**, 279-318.

Nesbitt H.W. and Muir I.J., 1994. X-ray photoelectron spectroscopic study of a pristine pyrite surface reacted with water vapor and air, *Geochim. Cosmochom. Acta* **58**, 4667 - 4679.

Nordstrom, D. and Southam, G., 1997. Geomicrobiology of sulfide mineral oxidation. In J.F. Banfield &K.H. Nealson (Eds.), Geomicrobiology : Interactions between microbes and minerals, *Mineralogical Society of America*, **35**, 361-390.

Nordstrom, D.K., 1982. Aqueous pyrite oxidation and the consequent formation of secondary iron minerals. In: Nordstrom, D.K. (Ed.), Acid Sulphate Weathering, *Soil Sci. Soc. Am., Spec. Publ.* **10**, 37– 56.

Nordstrom, D.K., Alpers, C.N., 1999. Geochemistry of acid mine waters. In: Plumlee, G.S., Logsdon, M.B. (Eds.), The Environmental Geochemistry of Mineral Deposits, 6. *Reviews in Economic Mineralogy,* Part A. Processes, Methods and Health Issues, **6**, 133–160.

Pearson, F. J and Rightmire, C.T., 1980. sulfur and oxygen isotopes in aqueous sulfur compounds. In Handbook of Environmental Isotope (eds. P. Fritz and J. CH. Fontes), 226-258, Elsevier.

Pronk, J.T, Meulenberg, R., Hazeu, W., Bos, P., and Kuenen, J. G., 1990. Oxidation of reduced inorganic sulphur compounds by acidophilic thiobacilli, *FEMS Microbiology Review,* **75**, 293-306.

Rimsdit and Vasguah., 2003. Pyrite oxidation: a state-of-the art assessment of the reaction mechanism, *Geochimica et Cosmochimica Acta,* 67, 873-880.

Roe, J. E., Anbar, A.D and Barling, J., 2003. Nonbiological fractionation of Fe isotopes: evidence of an equilibrium isotope effect, *Chemical geology* **195**: 69-85.

Roy and Trudinger., 1970. The biochemistry of inorganic compounds of sulfur. London: *Cambridge Univ. Press*, 400.

Rye, R.O., Bethke, P.M., and Wasserman, M.D., 1992. The stable isotope geochemistry of acid sulfate alteration, *Econ. Geol.* **87**, 225-262.

Sakai, H., 1957. Fractionation of sulfur isotopes in nature, *Geochim. Cosmochim. Acta,* **12**, 150-169.

Sampson, M.I., Phillips, C.V, and Ball, A.S., 2000. Investigation of the attachment of thiobacillus ferrooxidans to mineral sulfides using scanning electron microscopy analysis, *Minerals Engineering*, **13 (6)**: 643-656.

Sand, W, Gehrke, T., Jozsa, P. G., and Schippers, A., 2001. (Bio) chemistry of bacterial leaching-direct vs. indirect bioleaching, *Hydrometallurgy*, **59**, 159-175.

Sasaki K., 1994. Effect of grinding on the rate of oxidation of pyrite by oxygen in acid solutions, *Geochim. Cosmochim. Acta,* **58**, 4649 - 4655.

Sasaki K., Tsunekawa M., Ohysuku T. and Konno H., 1995. Confirmation of a sulfur-rich layer on pyrite after oxidative dissolution by Fe(III) ions around pH 2, *Geochim. Cosmochim.Acta,* **59**, 3155 - 3158.

Sasaki, K., 1997. Raman study of the microbially mediated dissolution of pyrite by Thiobacillus ferrooxidans, *Can. Mineral.,* **35**, 999-1008.

Sasaki, K., Tanaike, O., and Konno, H., 1995. Confirmation of a sulfur-rich layer on pyrite after oxidative dissolution by Fe(III) ions around pH 2, *Geochim. Cosmochim. Acta*, **59**, 3155-3158.

Sato M., 1992. Persistency-field Eh-pH diagrams for sulfides and their application to supergene oxidation and enrichment of sulfide ore bodies, *Geochim. Cosmochim Acta,* **56**, 3133 - 3156.

Savić, D. S., Veljković, V. B., Lazi, M. L., Vrvić, M. M., and Vučetić, J. I., 1998. Effects of the oxygen transfer rate on ferrous iron oxidation by *Thiobacillus ferrooxidans. Enzyme and Microbial Technolog.* **23,** 427-431.

Schauble, E. A., Rossman, G. R., and Taylor, H. P. Jr., 2001. Theoretical estimates of equilibrium Fe-isotope fractionations from vibrational spectroscopy, *Geochimica et Cosmochimica Acta*, **65**, 2487-2497.

Schippers A., Peter-Georg J. and Sand W., 1996. Sulfur chemistry in bacterial leaching of pyrite, *Appl. Environ. Microbiol.*, **62**, 3424 - 3431.

Schippers, A. and Sand, W., 1999. Bacterial Leaching of metal sulfides proceeds by two indirect mechanisms via thiosulfate or via polysulfides and sulfur, *App. Env. Micro.*, **3**, 319-321.

Schoen, R., and Rye, R.O., 1970. Sulfur isotope distribution in solfataras, Yellowstone National Park, *Science*, **170**, 1082-1084.

Schrenk, M., Edwards, K., Banfield, J.,1998. Distribution of T.ferrooxidans and Leptospirillum ferrooxidans: implication for generation of acid mine drainage, *Science*, **279**, 1519-1522.

Schwarcz, H.P. and Cortecci, G., 1974. Isotope analysis of spring and stream water sulfate from the Italian Alps and Apennines, *Chem. Geol.,* **13**, 285-294.

Seal, R II and Wandless, G.A., 1997. Stable isotope characteristics of waters draining massive sulfide deposits in the eastern United states, In Fourth international symposium on environmental *Geochemistry , proceedings* (RB Wanty, SP Marsh &L.P.Gough, eds.). U.S. Surv. Open file report, **97**-496.

Sharma, M., Polizzotto, M., and Anbar, A.D., 2001. Iron Isotopes in hot springs along the Juan de Fuca Ridge, *Earth and Planetary Science Letters,* **194**, 39-51.

Simms, P.K., Drake, A. A., Jr. Tooker, E. W., 1963. U.S. Geol. Survey prof. paper **359.**

Singer P.C. and Stumm W., 1968. Kinetics of the oxidation of ferrous iron. In: *2nd Symposiumon Coal Mine Drainage Research,* **12 – 34,** *National Coal Association/Bituminous CoalResearch.*

Singer P.C. and Stumm W., 1970. Acidic mine drainage: The rate-determining step. *Science* 167, 1121 - 1123.

Skulan, J.L., Beard, B.L., and Johnson, C. M., 2002. Kinetic and equilibrium Fe isotope fractionation between aqueous Fe[III] and hematite, *Geochimica et Cosmochimica Acta*, **66 (17)**: 2995-3015.

Steudel, R., *1996*. Mechanism for the formation of elemental sulfur from aqueous sulfide in chemical and microbiological desulfurization processes, *Ind. Eng. Chem. Res.,* **35**, 1417-1423.

Steudel, R., Hold, G., Gobel, T. and Hazeu, W., 1987. Chromatographic separation of higher polythionates S_nO_6 $^{2-}$ (n=3.....22). and their detection in cultures of T. ferrooxidans, Molecular composition of bacterial sulfur secreations, *Angew. Chem. Int. Ed. Engl.,* 26, 151-153.

Sugio, S., Domatsu, C., Munakat, O., Tano, T. and Imai, K., 1985. Role of a ferric iron reducing system in sulfur oxidation of Thiobacillus ferrooxidans, *Applied and Env. Micr.,* **49**, 1401-1406.

Suzuki I., Takeuchi T.L., Yuthasastrakosol T.D. and Oh J.K., 1990. Ferrous iron and sulfur oxidation and ferric iron reduction activities on *Thiobacillus ferrooxidans* are affected by growth on ferrous iron, sulfur, or a sulfide ore, *Appl. Environ. Microbiol*, **56**, 1620 - 1626.

Suzuki, I and Silver, M., 1966. The initial product and properties of the sulfur-oxidizing system of thiobacilli, *Biochim. Biophys. Acta*, **122**, 22-33.

Suzuki, I., 1965. Incorporation of atmospheric oxygen into thiosulfate by the sulfur oxidizing enzyme of T. thiooxidans, *Biochim. Biophys. Acta,* **110**, 97-101.

Suzuki, I., Chan, C. W. and Takeuchi, T. L., 1994. Oxidation of inorganic sulfur compounds by thiobacilli, *Environmental Geochemistry of Sulfide Oxidation,* C. N. Alpers and D. W. Blowes. Washington D.C., American Chemical Society, 61-67.

Suzuki, I., 1999**.** Oxidation of inorganic sulfur compounds:Chemical and enzymatic reactions. *Canadian Journal of Microbiology*. **45**, 97-105.

Taylor, B.E., and Wheeler, M.C., 1994. Sulfur and Oxygen-isotope geochemistry of Acid mine drainage in the Western United States, *Environmental Geochemistry of Sulfide Oxidation,* C. N. Alpers and D. W. Blowes. Washington D.C., American Chemical Society, 482-514.

Taylor, B.E., Wheeler, M.C., Nordstrom, D.K., 1984a. Isotope composition of sulphate in acid mine drainage as measure of bacterial oxidation, *Nature* **308**, 538–541.

Taylor, B.E., Wheeler, M.C., Nordstrom, D.K., 1984b. Stable isotope geochemistry of acid mine drainage: experimental oxidation of pyrite. Geochim. Cosmochim. Acta **48**, 2669– 2678.

Toran, L., and Harris, F., 1989. Interpretation of sulfur and oxygen isotopes in biological and abiological sulfide oxidation . Geochimica et Cosmochimica Acta, **53**, 2341-2348.

Tributsch, H., and Gerischer, H., 1981. Semiconductor – electrochemical aspects of bacterial leaching, 1. oxidation of metal sulfides with large energy gaps, *J. Chem. Technol. Biotechnol.*, **31**: 565-577.

Turcotte, S.B., Benner, R.E., Riley, A. M., Li, J., Wadsworth, M.E., and Bodily, D., M. Surface analysis of electrochemically oxidized metal sulfides using Raman spectroscopy, *J. Electroanal. Chem.*, 347, 195-205.

Van Everdingen, R. O. and Krouse, H. R., 1985. Isotope composition of sulphates generated by bacterial and abiological oxidation, *Nature,* **315**, 395-396.

Van Stempvoort, D. R. and Krouse, H. R., 1994. Controls of $\delta^{18}O$ in sulfate: Review of experimental data and application to specific environments. Environmental Geochemistry of Sulfide Oxidation, C. N. Alpers and D. W. Blowes. Washington D.C., *American Chemical Society,* 447-479.

Wakao, N., Mishina, M., Sakurai, Y., and Shiota, H., 1984. Bacterial pyrite oxidation. III Adsorption of T. ferrooxidans cell on solid surfaces and its effect on iron release from pyrite, *J. Gen. Appl. Microbiol.*, **28**, 331-343.

Watson, E. B., 2004. A conceptual model for near-surface kinetic controls on the trace-element and stable isotope composition of abiogenic calcite crystals. *Geochimica et Cosmochimica Acta*, **68**, 1473-1488

Welch, S.A., Beard, B.L., Johnson, C. M., and Braterman, P.S., 2003. Kinetic and equilibrium Fe isotope fractionation between aqueous Fe[II] and Fe[III], *Geochimica et Cosmochimica Acta*, **67 (22)**: 4231-4250.

Wentz, D, A., 1975. A review report for water and related land sources management study, metrapolitan Denver and South Platte River abd Tributaries, Colorado, Wyoming and Nebraska; *U. S. Army, Corp.*, **5**, 61.

Wiersma C.L. and Rimstidt J.D., 1984. Rates of reaction of pyrite and marcasite with ferric iron at pH 2, *Geochim. Cosmochim. Acta,* **48**, 85 - 92.

Williamson, M. A and Rimstidt, J.D., 1992. Correlation between structure and thermodynamics properties of aqueous sulfur species, *Geochim. Cosmochim Acta,* **56**, 3867-3880.

Xu, Y., and Schoonen M.A.A., 1995. The stability of thiosulfate in the presence of pyrite in low temperature aqueous solutions, *Geochim. Cosmochim Acta,* 59, 4605-4622.

Zak, I., Sakai, H., Kaplan, I. R., 1980. In Isotope Marine Geochemistry; *Miyake, Y., Ed.,* Uchida, Rokakuho, Tokyo, Japan., 339-373.

VITAE

Nurgul Celik Balci was born in Sivas, Divrigi in 1974. After the graduation from Divrigi High School, she entered Istanbul Technical University in 1990 , from where she received the BSc degree with honor in Geology Engineering in 1994. In the same year, Ms. Nurgul Celik Balci began her MSc study at Istanbul Technical University where she was awarded with MSc degree in 1997 from Ore deposits & Geochemistry Division. After graduating, she became a research assistant in the same division. She was accepted Istanbul Technical University for PhD. In 2001, she joined to the research group in the Department of Geochemistry &Chemistry at Colorodo School of Mines, USA. In the same year, she got NSF(National Science Foundation)-TUBITAK Fellowship for her doctoral research and continued her research in the Department of Geochemistry &Chemistry at Colorodo School of Mines, USA until 2004. During her doctoral research, she was awarded by Geobiology fellowship by University of Southern California Wrigley Institute for Environmental Studies and joined the geobiology summer course at University of Southern California, California, USA from June 11-July 23, 2004. She has been currently working as research assistant in the Department of Geology-Division of Ore deposits & Geochemistry at Istanbul Technical University.